University of Szeged

Faculty of Pharmacy

Institute of Pharmaceutical Technology and Regulatory Affairs

Head: *Prof. Dr. Ildikó Csóka*

Ph.D. Thesis

DEVELOPMENT OF NOVEL FORMULATED CIPROFLOXACIN HYDROCHLORIDE CONTAINING DRY POWDER INHALATION SYSTEM

By

Dr. Edit Benke

Doctor of Pharmacy, Pharmacist Specialized in Economics

Supervisor:

Dr. habil. Rita Ambrus

SZEGED

2023

PUBLICATIONS RELATED TO THE THESIS

1.) **Benke E.**, Szabóné Révész P., Hopp B., Ambrus R.: Hordozó alapú száraz porinhalációs rendszerek jellemzése és fejlesztési lehetőségei. Acta Pharmaceutica Hungarica, 87, 59-68 (2017).

Q4, IF_{2017}: -, Citations: 4 (Independent citations: -)

2.) **Benke, E.**, Szabóné Révész, P., Ambrus, R.: Innovatív technológiájú ciprofloxacin-hidroklorid tartalmú száraz porinhalációs rendszer fejlesztése. Acta Pharmaceutica Hungarica, 87, 49-58 (2017).

Q4, IF_{2017}: -, Citations: 3 (Independent citations: -)

3.) **Benke, E.**, Farkas, Á., Balásházy, I., Szabó-Révész, P., Ambrus, R.: Szárazporinhalációs készítmények bevitelére alkalmas eszközök és modern szerelékek aktualitásai I. Gyógyszerészet/Pharmacy, 62, 131-139 (2018).

Q: -, IF_{2018}: -, Citations: 2 (Independent citations: -)

4.) **Benke, E.**, Hopp, B., Farkas, Á., Balásházy, I., Szabó-Révész, P., Ambrus, R.: Szárazporinhalációs készítmények bevitelére alkalmas eszközök és modern szerelékek aktualitásai II. Gyógyszerészet/Pharmacy, 62, 195-201 (2018).

Q: -, IF_{2018}: -, Citations: -

5.) R. Ambrus, **E. Benke**, Á. Farkas, I. Balásházy, P. Szabó-Révész: Novel dry powder inhaler formulation containing antibiotic using combined technology to improve aerodynamic properties, European Journal of Pharmaceutical Sciences, 123, 20-27 (2018). (https://doi.org/10.1016/j.ejps.2018.07.030)

Q1, IF_{2018}: 3.532, Citations: 18 (Independent citations: 11)

6.) **E. Benke**, Á. Farkas, I. Balásházy, P. Szabó-Révész, R. Ambrus: Stability test of novel combined formulated dry powder inhalation system containing antibiotic: Physical characterization and *in vitro-in silico* lung deposition results, Drug Development and Industrial Pharmacy, 45, 1369-1378 (2019). (https://doi.org/10.1080/03639045.2019.1620268)

Q2, IF_{2019}: 2.365, Citations: 11 (Independent citations: 6)

7.) **E. Benke**, Á. Farkas, P. Szabó-Révész, R. Ambrus: Development of an Innovative, Carrier-Based Dry Powder Inhalation Formulation Containing Spray-Dried Meloxicam Potassium to Improve the *In Vitro* and *In Silico* Aerodynamic Properties. Pharmaceutics, 12, 535 (2020). (https://doi.org/10.3390/pharmaceutics12060535)

Q1, IF_{2020}: 6.321, Citations: 16 (Independent citations: 10)

8.) **E. Benke**, P. Varga, P. Szabó-Révész, R. Ambrus: Stability and *in vitro* aerodynamic studies of inhalation powders containing ciprofloxacin hydrochloride applying different DPI capsule types. Pharmaceutics, 13, 689 (2021).

Q1, IF_{2021}: 6.525, Citations: 3 (Independent citations: 3)

9.) **E. Benke**, C. Winter, P. Szabó-Révész, E. Roblegg, R. Ambrus: The effect of ethanol on the habit and *in vitro* aerodynamic results of dry powder inhalation formulations containing ciprofloxacin hydrochloride. Asian Journal of Pharmaceutical Sciences, 16, 471-482 (2021). (https://doi.org/10.1016/j.ajps.2021.04.003)

D1, IF_{2021}: 9.273, Citations: 5 (Independent citations: 4)

10.) **E. Benke**, P. Szabó-Révész, R. Ambrus: Development of meloxicam potassium-containing co-spray-dried inhalation powder with sodium stearate. Acta Pharmaceutica Hungarica, 91, 75-82 (2021). (https://doi.org/10.33892/aph.2021.91.75-82)

Q: -, IF_{2021}: -, Citations: -

Σ IF: 28.032

Σ Citations: 62 (Σ Independent citations: 34)

PUBLICATIONS NOT RELATED TO THE THESIS

1.) Chvatal, A., **Benke, E.**, Szabóné Révész, P., Ambrus, R.: Új formulálási stratégiák a porinhalációs készítmények előállításában. Gyógyszerészet/Pharmacy, 60, 197-206 (2016).

Q: -, IF_{2016}: -, Citations: 3 (Independent citations: -)

2.) T. Athamneh, A. Amin, **E. Benke**, R. Ambrus, C. S. Leopold, P. Gurikov, I. Smirnova: Alginate and hybrid alginate-hyaluronic acid aerogel microspheres as potential carrier for pulmonary drug delivery. The Journal of Supercritical Fluids, 150, 49-55 (2019). (https://doi.org/10.1016/j.supflu.2019.04.013)

Q1, IF_{2019}: 3.744, Citations: 61 (Independent citations: 57)

3.) M. Mukhtar, E. Pallagi, I. Csóka, **E. Benke**, Á. Farkas, M. Zeeshan, R. Ambrus: Aerodynamic properties and *in silico* deposition of isoniazid loaded chitosan/thiolated chitosan and hyaluronic acid hybrid nanoplex pulmonary powder as a potential TB treatment, International Journal of Biological Macromolecules, 165, 3007-3019 (2020). (https://doi.org/10.1016/j.ijbiomac.2020.10.192)

Q1, IF_{2020}: 6.953, Citations: 24 (Independent citations: 17)

4.) T. Athamneh, A . Amin, **E. Benke**, R. Ambrus, C. S. Leopold, P. Gurikov, I. Smirnova: Pulmonary drug delivery with aerogels: Engineering of alginate and alginate-hyaluronic acid microspheres. Pharmaceutical Development and Technology, 26, 509-521 (2021). (https://doi.org/10.1080/10837450.2021.1888979)

Q2, IF_{2020}: 3.133, Citations: 11 (Independent citations: 11)

Σ IF: 13.830

Σ Citations: 99 (Σ Independent citations: 85)

Cumulative IF: 41.862

Cumulative citations: 161 (Cumulative independent citations: 119)

PRESENTATIONS RELATED TO THE THESIS

Verbal presentations

1.) **Benke E**.: Meloxikám és meloxikám-kálium tartalmú hagyományos száraz porinhalációs készítmények fejlesztése. SZTE ÁOK-FOK-GYTK-ETSZK TDK Konferencia, Szeged, 2016. 10. 23-24.

2.) Ambrus R., **Benke E**., Farkas Á., Balásházy I., Szabóné Révész P.: Hagyományos és új generációs száraz porinhalációs rendszerek fejlesztése. XIII. Magyar Aeroszol Konferencia: Pécs, 2017. 04. 19-21.

3.) **Benke E.**: Új irányvonal a hagyományos száraz porinhalációs készítmények előállításában. XI. Kárpátaljai Tudományos Diákköri Konferencia, Beregszász, Ukrajna, 2017. 05.19.

4.) Ambrus R., **Benke E.**, Farkas Á., Balásházy I., Szabó-Révész P.: Development of a novel formulated, pulmonary microparticle (new generation DPI) containing antibiotic agent with improved aerosolization efficiency. 7th BBBB Conference on Pharmaceutical Sciences: Balatonfüred, 2017. 10. 05-07.

5.) **Benke E.**: Innovatív és tradicionális száraz porinhalációs rendszerek előállítása és vizsgálata krónikus tüdő megbetegedések antibiotikus és gyulladáscsökkentő kezelése céljából. Magyar Tudomány Ünnepe rendezvénysorozat, SZAB Gyógyszerésztudományi Szakbizottság előadőülés: Szeged, 2017. 11. 09.

6.) **Benke E.**: Cisztás fibrózis kezelésére alkalmas száraz porinhalációs rendszerek fejlesztése. Szegedi Tudományegyetem Sófi József A Szegedi Tehetségekért Alapítvány Ösztöndíj Konferencia, Biológia Doktori Iskola Kategória. Szeged, 2018. 03. 14.

7.) **Benke E.,** Szabóné Révész P., Ambrus R.: Szerkezeti stabilitás és a szerkezeti változás hatása az aerodinamikai eredményekre ciprofloxacin-hidroklorid tartalmú száraz porinhalációs termékek esetén. MKE Kristályosítási és Gyógyszerformulálási Szakosztálya Kerekasztal Konferenciája, Balatonszemes, 2018. 05. 04-05.

8.) **Benke E**.: Antibiotikum tartalmú száraz porinhalációs rendszerek fejlesztése mucoviscidosis kezelésére. EFOP 3.6.3-VEKOP-16-2017-00009 pályázat keretein belül megrendezett I. SZTE-ÁOK PhD Szimpózium, Szeged, 2018. 06. 22.

9.) **Benke E**.: Ko-porlasztással előállított, hordozómentes száraz porinhalációs készítmények vizsgálata. XIII. Clauder Ottó Emlékverseny, Budapest, 2018. 11. 22-23.

10.) **Benke E**.: Fluorokinolon antibiotikum tartalmú száraz porinhalációs termékek stabilitási vizsgálata és inhalációs kapszula típusok tanulmányozása. EFOP 3.6.3-VEKOP-16-2017-00009 pályázat keretein belül megrendezett II. SZTE-ÁOK PhD Szimpózium, Szeged, 2018.11.30.

11.) **Benke E**.: Új trendek a pulmonális gyógyszerformulálás területén. EFOP 3.6.3-VEKOP-16-2017-00009 pályázat keretein belül megrendezett II. SZTE-ÁOK PhD Szimpózium, Szeged, 2018.11.30.

12.) **Benke E**., Ambrus, R., Szabó-Révész, P.: Formulation and investigation of novel, carrier-based dry powder inhalation system. I. Symposium of Young Researchers on Pharmaceutical Technology, Biotechnology and Regulatory Science, Szeged, 2019.01. 31. DOI: https://doi.org/10.14232/syrptbrs.2019.op13

13.) **Benke E.**, Varga P., Kozma G., Szabó-Révész P., Ambrus R.: Investigation of capsule-based dry powder inhalation systems. 8th Interdisciplinary Doctoral Conference, Pécs, 2019.05.24-25.

14.) **Benke E.**, Szabó-Révész P., Ambrus R.: Characterization of dry powder inhalation systems using an organic solvent to reach special micrometric properties. II. Symposium of Young Researchers on Pharmaceutical Technology, Biotechnology and Regulatory Science, Szeged, 2020.01. 23-24. DOI: 10.14232/syrptbrs.2020.op20

15.) Varga P., **Benke E.**, Szabóné Révész P., Ambrus R.: Hordozómentes porinhalációs rendszerek előállítása és gyógyszerforma vizsgálata. XIV. Magyar Aeroszol Konferencia: Visegrád, 2019. 10. 02-04.

16.) Ambrus R., **Benke E**., Varga P., Szabó-Révész P.: Formulation and stability testing of inhalable powder preparation containing an antibiotic agent. Congressus Pharmaceuticus Hungaricus XVI. (online), 2020. 09. 10-12.

17.) **Benke E.**, Szabó-Révész P., Ambrus R.: Stability test of novel pulmonary formulation for further application in cystic fibrosis. Proceedings of the EFOP-3.6.2-16-2017-00006 (LIVE LONGER) project (online), 2020.10.16.

18.) **Benke E.**, Szabó-Révész P., Ambrus R.: Role of sodium stearate on co-spray-dried meloxicam potassium-containing dry powder inhalation systems. 9th Interdisciplinary Doctoral Conference (online), 2020. 11. 27-28.

19.) **Benke E.**, Szabó-Révész P., Ambrus R.: Development of NSAID containing dry powder inhalation formulation co-spray-dried with sodium stearate, Drug Delivery to the Lungs (online), 2020.12.09-11.

20.) **Benke E.**, Winter C., Szabó-Révész P., Roblegg E., Ambrus R.: Effect of solvent compositions on habits and *in vitro* aerodynamic results of spray-dried pulmonary formulations. III. Symposium of Young Researchers on Pharmaceutical Technology, Biotechnology and Regulatory Science, Szeged, 2021.01. 20-22. DOI: 10.14232/syrptbrs.2021.op17

21.) Révész P., **Benke E.**: Terápiaspecifikus gyógyszerfejlesztés, fókuszban a krónikus tüdőbetegségek: COPD és cisztás fibrózis a transzlációs medicina tükrében. Magyar Gyógyszerésztudományi Társaság: E-learning (online), 2021.08.31.

Poster presentations

1.) **Benke, E**., Chvatal A., Szabó-Révész, P., Ambrus, R.: Formulation of lactose-based dry powder inhalers by surface treatment containing different habit of active agent. 2nd European Conference on Pharmaceutics: Krakow, Poland, 2017.04.03-04.

2.) **Benke E**., Szabó-Révész P., Ambrus R.: The effect of sodium stearate on the aerosol performance of meloxicam potassium using a carrier-free procedure. 7th BBBB Conference on Pharmaceutical Sciences: Balatonfüred, Hungary, 2017. 10. 05-07

3.) **Benke, E**., Zsembery, Á., Szabó-Révész, P., Ambrus, R.: Development of novel formulated meloxicam potassium containing dry powder inhaler systems. 12th Central European Symposium on Pharmaceutical Technology and Regulatory Affairs. Szeged, Hungary, 2018. 09. 20-22.

4.) **Benke E**., Farkas, Á., Balásházy, I., Szabó-Révész P., Ambrus R.: New formulation approach for dry powder inhalers to improve CF/COPD inhalation therapy. 6th International Workshop on Lung Health. New approaches to respiratory diseases, Nice, France 2019.01.17-19.

5.) **Benke E**., Varga P., Szabóné Révész P., Ambrus R.: Antibiotikum tartalmú száraz porinhalációs készítmények kapszula alapú formulálása és stabilitási vizsgálata. Gyógyszertechnológiai és Ipari Gyógyszerészeti Konferencia. Siófok, 2019. 09. 26-28.

6.) **Benke E**., Szabó-Révész P., Ambrus R.: The effect of ethanol on aerosolization properties of spray-dried inhalation powders. Congressus Pharmaceuticus Hungaricus XVI. (online), 2020.09.10-12.

PRESENTATIONS NOT RELATED TO THE THESIS

Verbal presentations

1.) **Benke E.**: Cisztás fibrózis. EFOP-3.6.2-16-2017-00006 „LIVE LONGER - Modern orvostudományi diagnosztikus eljárások és terápiák fejlesztése transzlációs megközelítésben: a laboratóriumtól a betegágyig" Miniszimpózium és képzés. Budapest, 2017.11.17.

2.) Szabó-Révész P., **Benke E**.: Pulmonális gyógyszerbevitel, készítmény- és vizsgálati módszerfejlesztés. EFOP-3.6.2-16-2017-00006 „LIVE LONGER - Modern orvostudományi diagnosztikus eljárások és terápiák fejlesztése transzlációs megközelítésben: a laboratóriumtól a betegágyig" Miniszimpózium és képzés. Budapest, 2017.11.17.

3.) Ambrus, R., Chvatal, A., **Benke, E**., Bartos, Cs., Party, P., Szabóné Révész P.: Porlasztva-szárításos eljárás alkalmazása "nano in micro" száraz porinhalációs rendszerek fejlesztése céljából. Gyógyszerkémiai és Gyógyszertechnológiai Szimpózium, Szeged, 2018. 09. 06-07.

4.) **Benke E**.: Rheological properties of mucin – its pathophysiological role in cystic fibrosis. EFOP-3.6.2-16-2017-00006 Translational interactive hands-on training and conference on epithelial ion transport, Budapest, 2018. 11. 22-23.

5.) Party P., **Benke E.**, Szabóné, Révész P., Ambrus R.: Új szerkezet, új lehetőségek a száraz porinhalációs rendszerek fejlesztésében. "Nano in micro" formulációk. XIV. Magyar Aeroszol Konferencia: Visegrád, 2019. 10. 02-04.

Poster presentations

1.) Ambrus R., Chvatal A., **Benke E.**, Zsembery, Á., Szabó-Révész P.: Development of new generation-formulations containing different water-soluble model drugs for dry powder inhalation. 11th World Meeting on Pharmaceutics, Biopharmaceutics and Pharmaceutical Technology, Granada, Spain, 2018. 03. 19-22.

2.) Ambrus R., Party P., Chvatal A., **Benke E.**, Szabó-Révész P.: Nano-in-micro formulation for further pulmonary administration of meloxicam in lung diseases. 3rd European Conference on Pharmaceutics, Bologna, Italy 2019. 03. 25-26.

TABLE OF CONTENTS

ABBREVIATIONS

ACI	Andersen Cascade Impactor
AFM	Atomic Force Microscope
API	Active Pharmaceutical Ingredient
APSD	Aerodynamic particle size distribution
BH	Breath-hold time
CF	Cystic fibrosis
CFTR	Cystic fibrosis transmembrane conductance regulator
CIP	Ciprofloxacin hydrochloride
COPD	Chronic obstructive pulmonary disease
D [0.5]	Geometric diameter
DPI	Dry powder inhaler
EF	Emitted fraction
ET	Extrathoracic airways
EXH	Exhalation fraction
F_{adh}	Adhesion force
FPF	Fine particle fraction
GEL	Gelatine
GEL-PEG	Gelatine-polyethylene glycol
HPMC	Hydroxypropyl methylcellulose
ICH	The International Council for Harmonisation of Technical Requirements for Pharmaceuticals for Human Use
IH 70	Inhalac® 70
IUPAC	International Union of Pure and Applied Chemistry
LM	Light Microscope
LPP	Large porous particle
LPNP	Large porous nanoparticle
LUNG	Bronchial and acinar parts
MgSt	Magnesium stearate
MMAD	Mass median aerodynamic diameter
MXP	Meloxicam potassium
NaSt	Sodium stearate
NEM	Nano-embedded microparticle

NPMP	Nanoporous microparticle
PNAP	Porous Nanoparticle Aggregate Particle
PDD	Pulmonary drug delivery
pMDI	Pressurized metered-dose inhalers
RH	Relative humidity
R_{RMS}	Root means square roughness
RSC	Residual solvent content
SEM	Scanning Electron Microscope
SLM	Stochastic lung model
SMI	Soft Mist Inhaler
spd	spray dried/spray drying
SPP	Small porous particle
XRPD	X-ray powder diffraction
W_{adh}	Adhesion work
W_c	Cohesion work

1. INTRODUCTION

Inhalation therapy dates back a long time [1], but research and product development for pulmonary drug delivery (PDD) has been focused on the last two to three decades at least. Accordingly, several companies and research groups have specialized in this field. The products and research available on the market are still typically focused on local therapy (e.g. asthma, cystic fibrosis (CF), tuberculosis, etc.). In particular, the use of antibiotics [2] in inhalation therapy has a lot of potentials, as bacterial infections typical of many lung diseases can be treated locally with a remarkable reduction in systemic side effects compared to *oral* administration. There are not yet many inhaled products containing antibiotics on the market, but several promising formulations have been published. There is great potential for the inhaled use of ciprofloxacin hydrochloride (CIP) as a broad-spectrum fluoroquinolone antibiotic.

There are four main categories of PDD implementation: nebulizers, soft mist inhalers (SMIs), pressurized metered-dose inhalers (pMDIs), and dry powder inhalers (DPIs). Among these, the development of DPI systems has recently received the greatest focus due to its many advantageous features. On the one hand, in the case of DPIs, traditional carrier-based systems are distinguished, where micronized drug particles create an interactive physical mixture with large carrier particles. The micronized drug particles are then swept off from the surface of the large carrier during inhalation. The other group consists of carrier-free DPIs, where different manufacturing methods and applied excipients allow good aerodynamic properties. Both groups of DPIs mentioned above have advantageous properties and development potential, but the combination of their beneficial properties indicates a new development line that is still unexploited.

The efficiency of DPI products is influenced – in addition to the DPI formulation – by the applied DPI device, since the design and characteristics of the delivery system, the adhesion between the DPI formulation and the device also contributes to the achievement of the appropriate aerodynamic result. Nevertheless, the properties of DPI capsules can also influence the aerosolization, aerodynamics and stability of inhalation powders, and are therefore not only used for packaging of formulations. Patients also play a major role in the aerosolization and lung deposition outcome of DPI powders, for example in terms of breathing maneuver and breath-holding time. Overall, the development of DPI dosage forms is challenging, but there are many untapped opportunities.

2. AIMS OF THE WORK

The goal of the Ph.D. work was to develop and investigate a novel formulated DPI microcomposite containing CIP as an antibiotic agent, which combines the advantages of traditional, carrier-based, and carrier-free formulations and provides adequate stability. The ultimate aim was to create a well-adapted DPI drug formulation for the treatment of cystic fibrosis and chronic bronchitis. The main steps of the work were as follows:

I. Literature review of the benefits of PDD compared to the *oral* administration route. Exploration of the similar pathophysiological course of CF and chronic bronchitis and the potential for antibiotic therapy intervention in this progressive process. Identification of PDD options and collection of inhaled antibiotic formulations on the market. Furthermore, to collect factors influencing the effectiveness of the delivery of DPI systems and to explore their potential.

II. Development of a **carrier-based** CIP-containing DPI system where the carrier particles are surface-treated with magnesium stearate (MgSt) and the drug particles were blended on the surface of these particles are prepared by prior spray drying (spd). In this way, a sample with better *in vitro* lung deposition results than the traditional carrier-based DPI formulations on the market can be expected.

III. To study how different solvent proportions used in the stock solution during the preparation of CIP-containing **carrier-free** DPI samples, influences the habit of these powders and consequently their *in vitro* aerodynamic results. The purpose is to apply the results to select the optimal solvent composition for this drug. This segment seeks to shed a new perspective on published experience, using new numerical concepts, and contexts to provide new explanations and expand knowledge on the subject. In addition, preparation, physicochemical, and *in vitro* lung deposition studies of co-spd DPI formulations containing the active ingredient CIP and sodium stearate (NaSt) as an excipient in different concentrations using the optimal solvent mixture described above. Thereby further development of the carrier-free DPI direction.

IV. Development, physical / *in vitro* lung deposition / *in silico* lung simulation investigations, and short-term stability testing of **novel formulated** DPI microcomposite containing CIP, through the integration of the experience gained from the improvement of traditional carrier-based and carrier-free DPI formulations described above. Furthermore, the development of the final dosage form of this above-mentioned DPI sample, which involves testing in different DPI capsule types and a more extended 6-month stability study according to the ICH (The International Council for Harmonisation of Technical Requirements for Pharmaceuticals for Human Use) guideline.

3. LITERATURE BACKGROUND OF THE RESEARCH WORK

3.1. Importance of PDD in the therapies for lung diseases

The properties of the lungs - highly absorbable tissue, large surface area, thin adsorption membrane, and excellent blood supply - make them particularly suitable for use as drug delivery gates [3,4]. The pulmonary drug administration allows the medical treatment of local illnesses such as CF, chronic obstructive pulmonary disease (COPD), etc., and systemic diseases e.g. diabetes mellitus, agitation associated with schizophrenia, etc [5,6]. The advantages of this administration way of active pharmaceutical ingredient (API) delivery are that it is not an invasive treatment, and the applied drug can reach the C_{max} value in a few minutes [7]. Furthermore, a more favorable side effect profile is expected than with *oral* administration because approximately one-tenth of the *oral* dose is enough to trigger the identical therapeutic effect [8]. The reason is that the API bypasses the gastrointestinal tract, that is, so that not exposed to intestinal and hepatic first-pass metabolism [9]. Many APIs have thus been tested and several of them have been marketed from the edge of PDD [10–12].

CF is a slowly progressive – autosomal recessive – inherited disease, which is a pathophysiological process resulting from a mutation affecting the cystic fibrosis transmembrane conductance regulator (CFTR) gene [13]. Fundamentally, a molecular defect affecting a gene can be classified into 6 classes [14], so the severity of the disease can vary greatly from individual to individual [15]. The disorder affects the exocrine glands of the body, causing particularly severe problems in the lungs (lung infections, shortness of breath, decreased respiratory function, frequent cough, etc.) and pancreas (obstruction, poor nutrition, etc.) [16,17]. Since ion transport is regulated by CFTR protein through several mechanisms, so the pathophysiological process is very difficult and complex [18]. In terms of the lungs, the process is summarized as follows (Figure 1.), due to mutation in the CFTR gene, the influenced Na^+ and Cl^- transport (osmosis, dehydration) result in mucociliary dysfunction and airway mucus plugging [19,20], which lead to hypoxia followed by sterile inflammation and bacterial infection [21]. In turn, influencing HCO_3^- transport results in a decrease in HCO_3^- concentration on the apical side compared to physiology (decreased pH of the airway surface liquid), which also contributes to bacterial infection [22,23]. The presence of inflammation and bacterial infection induces a pathophysiological cycle since inflammation leads to mucin hypersecretion (obstruction), which favors bacterial growth and bacterial infection induces inflammation [24,25]. Respiratory failure is the end result of a process that leads to the death of patients [26]. According to the current state of science, this disease cannot be cured [27], but it can materially slow down the course of the disease with appropriate therapy [28].

COPD is a collective name applied to describing progressive pulmonary illnesses, which include chronic bronchitis, emphysema, refractory (irreversible) asthma, and various types of bronchiectasis [29]. Especially chronic bronchitis has similar pathological manifestations to CF [30]. More than 90% of people with this disease have a background of smoking [31]. Cigarette smoke has been found to degrade CFTR expression beyond the induction of inflammation, thereby causing an "acquired" dysfunction of CFTR [19]. This may lead to a similar process as shown in Figure 1. also in patients with chronic bronchitis and CF.

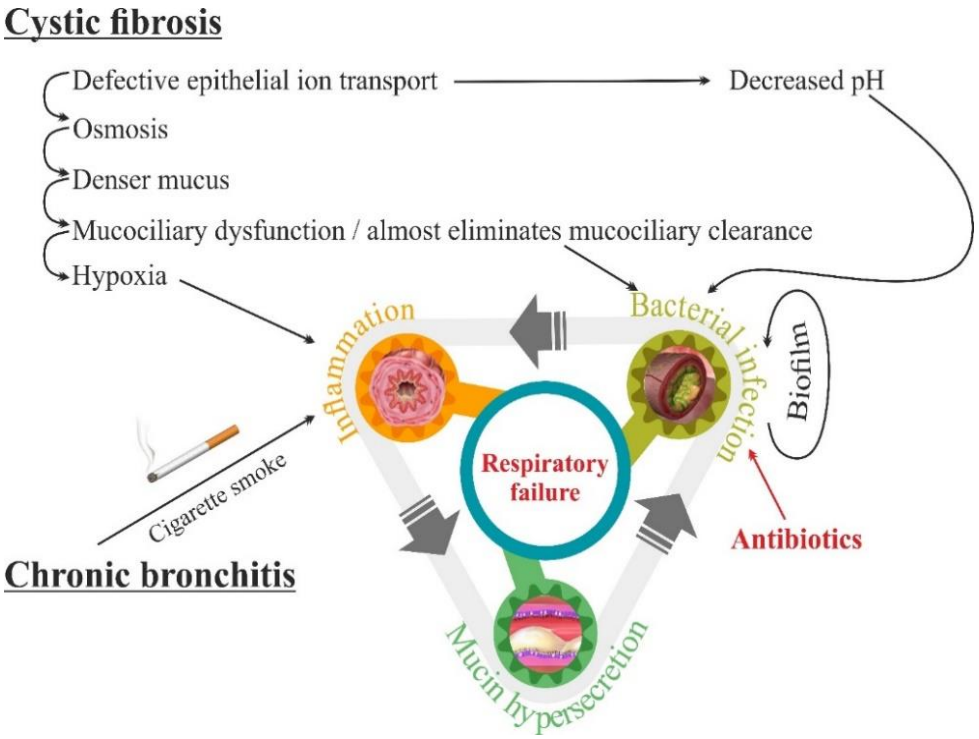

Figure 1. *A visualization of similar pathophysiological progression in CF and chronic bronchitis.*

The pathophysiological cycle mentioned above is characterized by polymicrobial infection, i.e. a patient is infected with several different organisms at a given time. For example, in CF, many studies support that *Haemophilus influenzae* and *Staphylococcus aureus* cause respiratory tract infections in younger CF patients, followed by *Pseudomonas aeruginosa* becoming the most important pathogen in adulthood, but with the presence of multiple pathogens [32]. In addition, the continuous presence of bacterial infection in small flare-ups also promotes biofilm formation, which further enhances disease progression. Therapy with antibiotics can slow down this pathophysiological progression [33]. On one side, by acting directly on the bacterial infection and biofilm formation, and on the other hand, by indirectly reducing inflammation and mucin hypersecretion. For these reasons, besides a large number of marketed *oral* antibiotic formulations for patients with these diseases, there is an increasing focus on the production of formulations for the inhalation administration of antibiotics, which is also becoming necessary as local therapy is beneficial for these patients.

3.2. Classification of inhalation products

Concerning PDD, four main categories of inhalation products can be distinguished. In the case of nebulizers, the inhalation device is an electrically powered machine that converts the liquid medicine (e.g. Berodual® Inhalation Solution – Boehringer Ingelheim, Ingelheim, Germany –) into a continuous nebulization mist so that it can be inhaled directly into the lungs through a face mask or mouthpiece [34]. Soft mist inhalers (SMIs) (e.g. Respimat® Soft Mist™ Inhaler – Boehringer Ingelheim, Ingelheim, Germany –) also produce mist, but they create a slow and prolonged aerosol mist that is induced by mechanical force via a spring. They have the advantage that inhalation can be easily matched to aerosol flow for patients, in addition to not having to reach a threshold for inhalation flow for the drug to be properly aerosolized and inhaled. They are a relatively new group and their application is not yet widespread on the market [35,36]. Pressurized metered-dose inhalers (pMDIs) (e.g. Ventolin – GlaxoSmithKline, Brentford, United Kingdom –) are also liquid-based systems, where inhalation products incorporating one or more propellants within a pressurized delivery device. Although this type has a long and considerable presence on the market, a major drawback is that among the four PDD solutions, it requires the greatest coordination between product activation and patient inhalation, and thus effective drug intake depends to a large extent on good inhalation technique. Most pMDI products have high oropharyngeal and low lung deposition. However, for pMDIs, it is challenging to administer high doses of APIs to the lungs [37]. The DPIs (e.g. Incruse Ellipta® – GlaxoSmithKline, Brentford, United Kingdom –) are breath-activated inhalation products that aerosolize a given dose of micronized API in a solid-state on the airflow. The DPIs offer advantages in terms of drug stability, ease of management, and the range of possible doses that can be administered. As the API is processed, dosed, and packaged in powder form, the risk of degradation, disintegration and microbiological contamination is minimized concerning wet formulations [38,39]. With regard to antibiotic drugs, a number of inhalation formulation developments have already taken place and several products containing antibiotic are already on the market (Table 1.), but there is no inhalation formulation containing CIP on the market yet.

Table 1. *Marketed inhalation products containing antibiotics [40–43].*

Product/ Company	Drug material	PDD option type	Indication
Arikayce® (Insmed Incorporated)	Amikacin	Nebulizer *(Liposome inhalation suspension)*	NTM lung infections caused by MAC in adults with limited treatment options who do not have CF
Cayston® (*Cayston Gilead Sciences Ireland UC)*	Aztreonam	DPI	Suppressive therapy of CPI due to *P.ae.* in patients with CF aged 6 years and older
Colobreathe® (*Forest Laboratories UK Ltd.)*	Colistimethate sodium	DPI	Management of CPI due to *P.ae.* in patients with CF aged 6 years and older
Promixin® (*Forest Laboratories UK Ltd.)*	Colistimethate sodium	Nebulizer *(Lyophilized powder for inhalation solution)*	Paediatric of CPI due to *P.ae.* in patients with CF
Quinsair® (Chiesi Farmaceutici S.p.A.)	Levofloxacin hemihydrate	Nebulizer *(Solution)*	CPI due to *P.ae.* in adult patients with CF
Bethkis® (Chiesi Farmaceutici S.p.A.)	Tobramycin	Nebulizer *(Solution)*	Management of CF patients with *P.ae.*
TOBI® (*Novartis International AG)*	Tobramycin	Nebulizer *(Solution)*	CF patients aged 6 years and older for long-term management of CPI due to *P.ae.*
TOBI® Podhaler® (*Novartis International AG)*	Tobramycin	DPI	Suppressive therapy of CPI due to *P.ae.* in adults and children aged 6 years and older with CF

Abbreviations in the table: *Cystic fibrosis (CF), Chronic pulmonary infections (CPI), Dry powder inhaler (DPI), Mycobacterium avium complex (MAC), Non-tuberculous mycobacterial (NTM), Pseudomonas aeruginosa (P.ae.), Pulmonary drug delivery (PDD)*

3.3. Optimal DPI product delivery

As our research team is exclusively dedicated to the development of DPIs due to the advantageous properties of this group [44]. For this reason, in the following sections, DPI systems will be discussed, whose efficiency is considerably influenced not only by the characteristics of the DPI formulations but also by the applied DPI devices used and the patients (Figure 2.). These influencing factors and their potential for improvement are discussed in detail below.

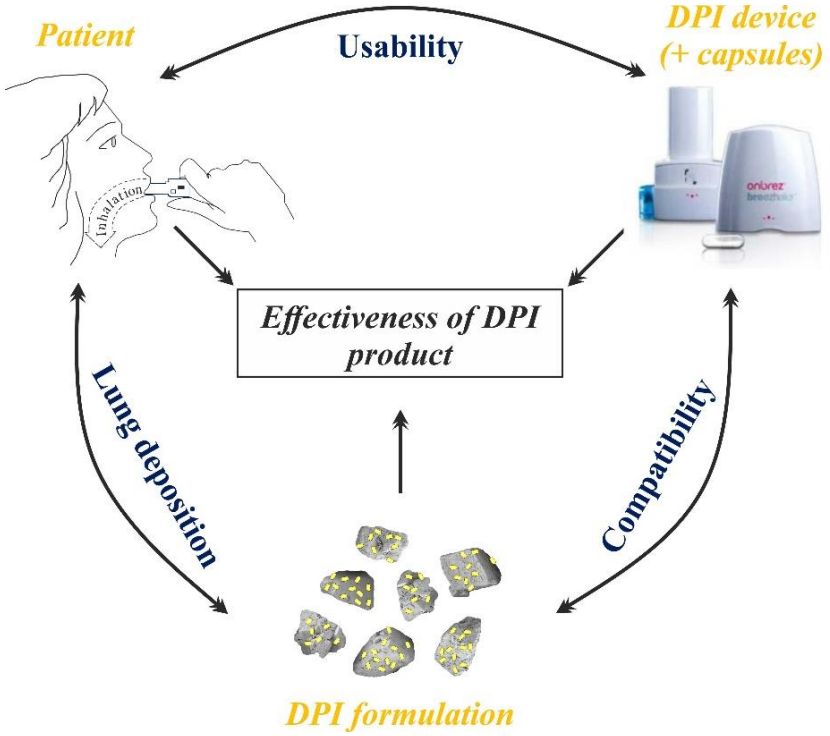

Figure 2. *Influencing factors of the efficiency of DPI product [45].*

3.3.1. DPI formulations

The effectiveness of DPI products is basically influenced by the properties of DPI formulations [45]. There is still a wide range of *in vitro* (and *in vivo*) lung deposition results of marketed and published DPI formulations, not to mention inhalers and patients as influencing factors. The manufacturing of DPI formulations has a lot of potentials, as the number of active ingredients, excipients, preparation methods, and parameters used is huge [46,47]. Basically, 2 main groups of formulations are distinguished in the literature for DPIs: traditional carrier-based and carrier-free composites. In the former, the micronized drug (usually by milling or sieving to an appropriate particle size range) by a top-down process is on large carrier particles from whose surface of which the API particles are swept off during inhalation. In the latter case, different manufacturing methods and applied excipients allow good aerodynamic properties (even without the use of large carrier particles) [48,49]. There are already a number of products on the market for the main groups, but both have advantages and disadvantages, which are summarized in Table 2. and their development possibilities are described in the following sections.

Table 2. *Advantages and disadvantages of carrier-based and carrier-free DPIs [50].*

	Traditional, carrier-based DPI formulations	**Carrier-free DPI formulations**
Advantages	• Sweet aftertaste during inhalation (most sugar-based compositions): confirms to the patient that inhalation was successful • Dispensing small amounts of API can be accurate • Improved aerosolization and dispersion due to carrier particles • Better moisture protection	• Production typically in a single step • A large number of excipients and processing options (production methods, nanoparticle engineering, etc.) can be used in the formulation • Favorable morphology • Improved aerodynamic behavior
Disadvantages	• Inhomogeneity • Relatively low FPF value (for marketed products) • High adhesion between the untreated carrier and drug particles	• Instability for amorphous particles • Risk of strong cohesion between drug particles • Electrostatic charging • Poor powder flow properties • High adhesion between the DPI capsule wall and drug particles

3.3.1.1. Development opportunities for carrier-based DPIs formulations

Traditional carrier-based DPI systems were the first to appear on the market for powder inhalation products. Representatives of this major group are still predominantly present on the market, typically commercially available formulations contain untreated carrier particles. There is great potential for the development of this main group, considering the advantages summarized in Table 2. On the one hand, those companies that produce carrier particles specifically for use in DPI formulations are rapidly expanding the number of carrier types available, e.g. MEGGLE's InhaLac® series [51], DFE Pharma's Respitose® and Lactohale® product lines [52], which differ most in their manufacturing method (milled, sieved) and particle size distribution. On the other hand, besides α-lactose monohydrate, which is currently the most dominant carrier for commercialized carrier-based DPIs, other carrier candidates have come to the fore due to their favorable properties and test results e.g. mannitol, glucose monohydrate, sorbitol, etc [46]. In addition, a number of developments have in recent years been made in the field of surface treatment of carrier particles, which are summarized in Figure 3.

One of these solutions is the recrystallization of carrier particles. Positive experiences have been described with the filtration of supersaturated aqueous solutions of α-lactose monohydrate and recrystallization using various antisolvents (ethanol (EtOH), butanol, acetone), antisolvent mixtures (EtOH-acetone, EtOH-butanol, acetone-butanol) or carbopol gels, as improved *in vitro* lung deposition values were measured for samples containing recrystallized carrier. The next effective surface treatment option is surface dissolution. The surface properties of α-lactose monohydrate are favorably altered when it is stirred in EtOH, methanol, or propanol for a short time (e.g. 5-20 min) and then filtered. The surface properties of the carriers are also beneficially modified (e.g. reduced roughness) by coating with fluidization (e.g. α-lactose monohydrate carrier hydroxypropyl methylcellulose (HPMC), distilled water, and lactose-containing coating fluid), which has been reported to lead to enhanced *in vitro* lung deposition results [46].

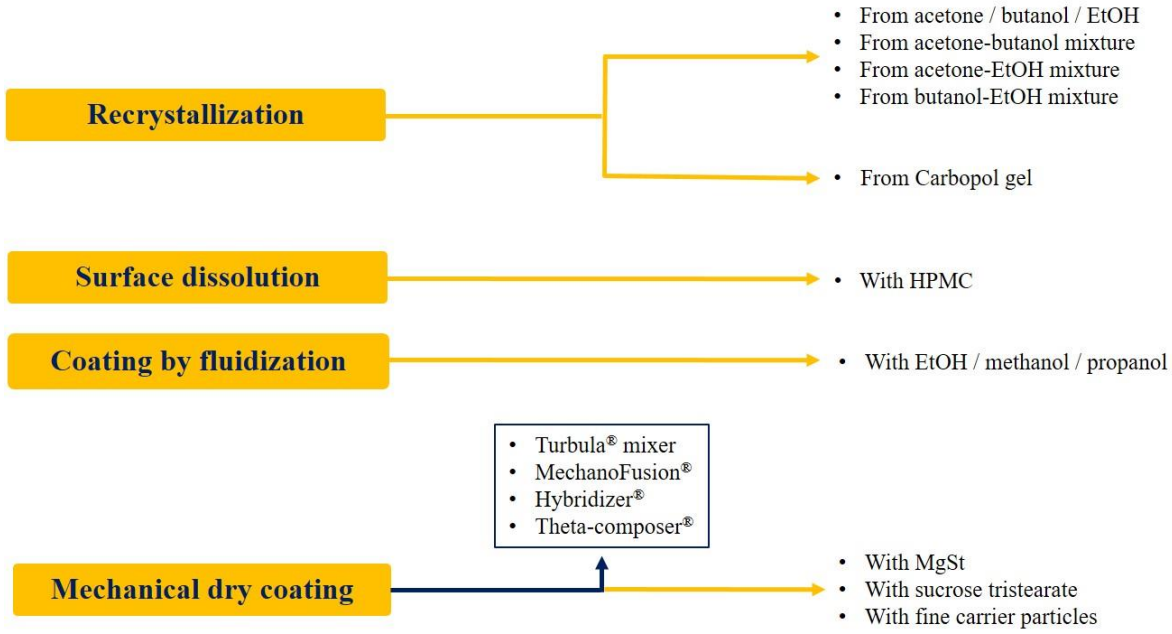

Figure 3. *Surface modification possibilities of traditional DPI carrier particles, with examples.*

Besides the wet surface modification methods described so far, the fourth option is the mechanical dry coating of the carrier particles, which is also aimed at improving lung deposition results. The coating particles are in close contact with the large carrier particles due to mechanical forces. The coating can be discontinuous or continuous (porous/single layer or film coating). It can be created with a Turbula mixer or intensive mechanical dry coating equipment such as MechanoFusion®, Hybridizer®, Theta-composer®, etc. Mechanical dry coating of classical large carriers is also possible with fine carrier particles, which are also called "secondary carriers". The average size of these particles is smaller compared to that of the classic large carriers, but their optimal diameter for DPI systems has not yet been agreed upon, with some studies suggesting a particle size of around 5-8 μm as an ideal range [46].

3.3.1.2. Development of carrier-free DPI formulations

The development of carrier-free DPI formulations came into focus later, when advanced bottom-up technologies (spd/nano spd, spray-freeze drying, supercritical-fluid technology) allowed to create drug particles with different morphologies compared to the previous top-down technologies [4]. In addition, by choosing the right excipients, favorable physicochemical properties can be achieved. The resulting composites alone gave good lung deposition results thus, the use of large carrier particles can be eliminated [47]. The most common bottom-up DPI production technology is spd, which based on its advantages and disadvantages, proves to be the most favorable method of production [53]. Formulations prepared by this technology are categorized in the literature according to their habit, with some overlap. Basically, two main groups of spd particles are distinguished: dense and non-dense particles (Figure 4.).

A common feature of the former group is that they typically have an average geometric diameter (D [0.5]) of 1-5 μm per particle and a denser structure than the other main group. In the case of conventional spd DPI microparticles, different morphologies are observed (spherical-smooth, spherical-dimpled). PulmoSol® formulations are a subtype of the group of dimpled particles, where a solution of human recombinant insulin is co-spd using excipients (mannitol, glycerol, sodium citrate) to give the characteristic shape. Coated particles with a layered structure also belong to the main group of dense particles (they can have both smooth and dimpled surfaces), which are most often manufactured using amino acids such as L-leucine [54,55], etc., which have a favorable effect on density, flow properties, and hygroscopicity, among other things. Spheroids, on the other hand, are formulations resulting from the aggregation of spd particles up to half a millimeter in size, of 1-5 μm with dense structure, which are broken down into individual microcomposites during inhalation. The large size favors interparticle interactions during the resting bed of particles. In the case of nano-embedded microparticles (NEMs), the nano-sized API particles are incorporated into a matrix (e.g. lactose, mannitol, maltodextrin, trehalose, etc.), making the particles in the sample micron-sized. They are also known as "nano-in-micro" formulations. This eliminates the problem that nano-sized particles are often exhaled. These composites then break down into nanoparticles in the lower airways after deposition, as the matrix dissolves in the lung lining fluid. The matrix material used may be present in a few percent or much larger amounts relative to the dry solids content of the formulation (Figure 4.) [47,56,57].

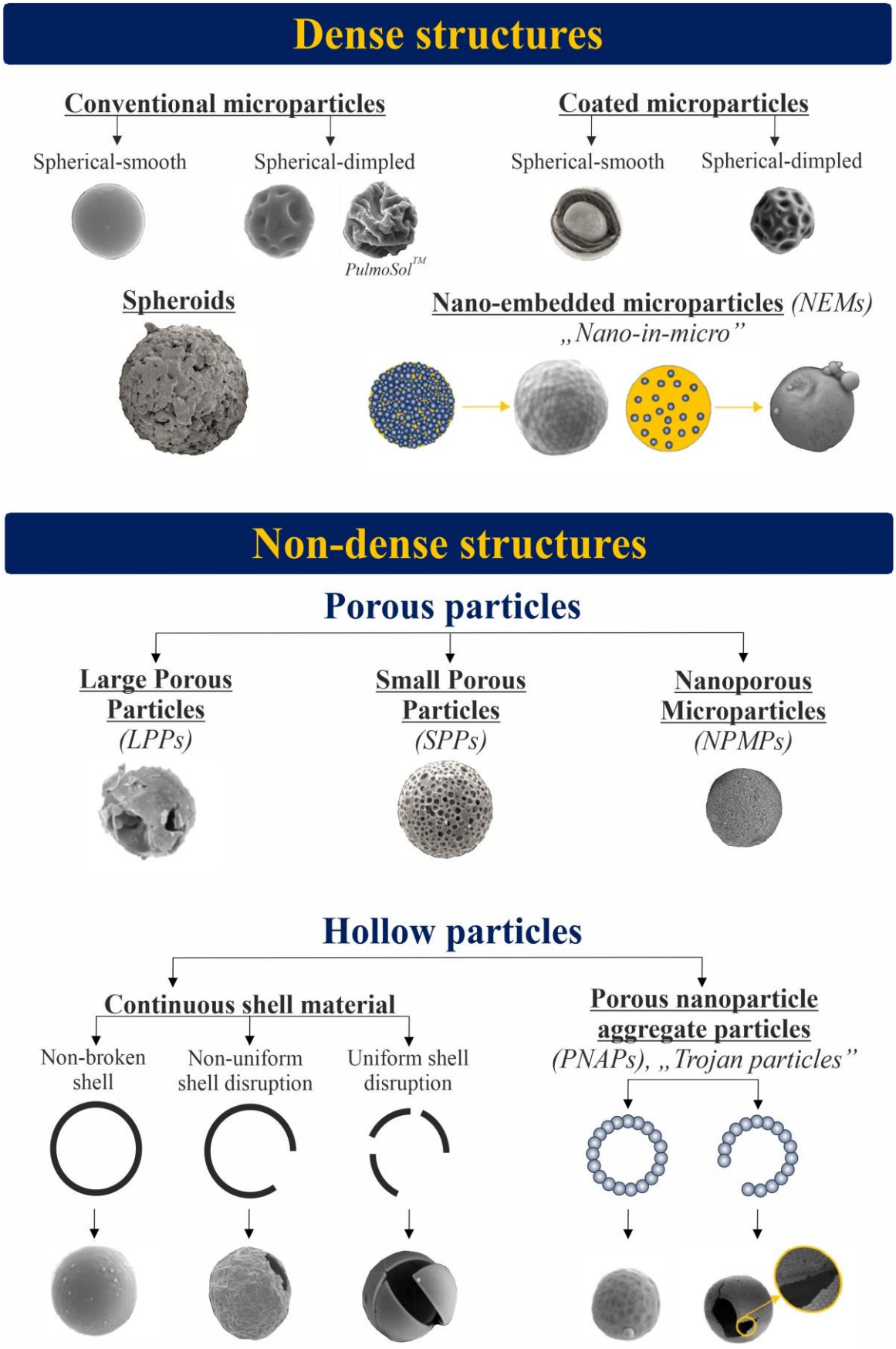

Figure 4. *Types of carrier-free (co-)spd DPI formulations.*

Types belonging to the non-dense main group are characterized by the presence of cavities, an average geometric particle size of 5-30 μm and a lower density compared to the dense main group. Within this major group, porous particles and hollow particles are distinguished. The porous particles contain a frame inside, and depending on the size of the pores specific to the particle, subgroups Large Porous Particles (LPPs), Small Porous Particles (SPPs) and Nanoporous Microparticles (NPMPs) are distinguished. LPPs are formulations prepared by spd complex emulsions, where often polymers (e.g. PLGA, PEG) are used to stabilize the remaining pores. The SPPs subgroup includes PulmoSphere® composites, which are made from O/W emulsions. In their case, the active ingredient and the emulsion-stabilizing excipient (e.g. phosphatidylcholine) are soluble in the aqueous phase. In the oily phase, a pore-forming perfluorocarbon derivative is used to form the characteristic shape of the particle. Different solvent mixtures are used in the production of NPNPs e.g. EtOH/water, methanol/water, water/methanol/butyl acetate, methanol/butyl acetate, etc. NPNPs can be prepared using solvent mixtures without the use of other excipients, but also by using, for example, ammonium carbonate, NPMP samples have been successfully generated. Typically, the resulting particles are 3 μm (D [0.5]) in size [57–59].

In the case of hollow composites, they no longer have an internal frame, a spongy structure, but only a shell. The shell can consist of continuous shell material, but depending on whether the shell is intact or disrupted, several subgroups can be distinguished: non-broken shell, non-uniform shell disruption and uniform shell disruption. There are also hollow micron-sized particles in which the shell is aggregated from nano-sized particles (even in several layers), which are also called Trojan particles because of their structure, in association with the Trojan wooden horse. Although they also belong to the group "Hollow particles", they are also referred to in the literature as PNAPs (Porous Nanoparticle Aggregate Particles), where the shell can be intact or cracked. This latter is also described in the literature as Large Porous Nanoparticles (LPNPs) [57,60,61].

Among the carrier-free DPI formulation types detailed above, several examples of successful development using antibiotics as active ingredients can be found (Table 3.). A number of these are already on the market or in the clinical phase. The preparation of dimpled particles for antibiotics is also very common.

Table 3. *Published examples of antiobiotic containing carrier-free (co-)spd DPI formulations.*

Carrier-free (co-)spd DPI formulation type			Drug material	Excipient	Ref.
Dense structures	*Conventional microparticles*	Spherical-smooth	Netilmicin	-	[62]
		Spherical-dimpled	CIP	-	[63]
			CIP monohydrate	-	[64]
			Aztreonam	-	[65]
			CIP, Doxycycline, CIP & Doxycycline	-	[66]
	Coated microparticles	Spherical-smooth	Tobramycin	Lipids: Cholesterol, Phospholipon 90H or Hydrogenated soy lecithin	[67]
		Spherical-dimpled	Netilmicin	L-leucine	[62]
			Gentamicin sulphate	L-leucine	[68]
			CIP	L-leucine	[63]
	Spheroids		N/A	N/A	N/A
	NEMs		Ciprofloxacin	D-Mannitol & L-Leucine matrix	[69]
			Ciprofloxacin	PEG-g-PHCs copolymer, sodium alginate solution	[70]
			Tobramycin	Chitosan-Alginate/ PVA-Alginate	[71]
Non-dense structures	*Porous particles*	*LPPs*	Capreomycin sulfate	L-leucine	[72]
		SPPs	Ciprofloxacin betaine	DSPC, Calcium chloride	[73]
			Tobramycin	Perflubron, DSPC, Calcium chloride, Sulphuric acid	[74]
			Gentamicin sulfate	Perflubron, Egg phosphatidylcholine, Sodium oleate	[75]
		NPMPs	N/A	N/A	N/A
	Hollow particles	*Continuous shell material*	Moxifloxacin HCl	-/L-leucine/DPPC	[76]
		PNAPs (Trojan particles)	Rifampicin	PLGA/L-leucine	[77]

Abbreviations in the table: *Ciprofloxacin hydrochloride (CIP), 1,2-dipalmitoyl-sn-glycero-3-phosphatidylcholine (DPPC), Distearoylphosphatidylcholine (DSPC), Large Porous Particles (LPPs), nano-embedded microparticles (NEMs), Nanoporous Microparticles (NPMPs), Phthaloyl chitosan (PHCs),Poly (lactide-co-glycolide) (PLGA), Porous Nanoparticle Aggregate Particles (PNAPs), poly(vinyl alcohol) (PVA), Reference (Ref.), Small Porous Particles (SPPs)*

3.3.1.3. Combining the advantageous features of traditional, carrier-based and carrier-free DPI systems

The development possibilities of traditional carrier-based and carrier-free DPI formulations have been categorically described above, however, there are countless possibilities for developers in terms of the number of excipients that can be used in the lungs and the preparation parameters, and it is not in vain that there have been plenty of publications on this subject. However, there are only a few examples in the literature of combined formulations that exploit the advantages of traditional carrier-based and carrier-free DPIs. In the beginning, Adi et al. [78] prepared a mixture of treatment-free carrier and spd API, Hazare et al [79] performed manual mixing as a surface treatment between lactose carrier and MgSt and then mixed them with spd API. Faulhammer et al. [80] blended decanted modified lactose and spd drug material, and Mönckedieck et al [81] applied spd API particles and mannitol to the surface of the larger spd mannitol (~ 60 μm), etc. Combined formulated DPIs hide even more possibilities that result in the emergence of a new category [48].

3.3.2. Inhalers

3.3.2.1. DPI devices

In addition to the role of DPI formulations, the second pillar (Figure 2.) that influences the efficiency of DPI systems is the DPI devices (structure, features of the dosing system). Compatibility is an important factor, i.e. the wide applicability of the devices for different API formulations and doses, furthermore, minimal adhesion between the DPI formulation and the device. The ideal DPI inhalers are cost-effective, easy to use, portable, aerodynamically favorable and adequately protect the microcomposites from moisture so that they remain sufficiently stable. They are required to have dose indicators for multiple-dose storage, as well as provide accurate and uniform dosing over a wide range of inspiratory flow rates and until the end of the indicated expiration date [45].

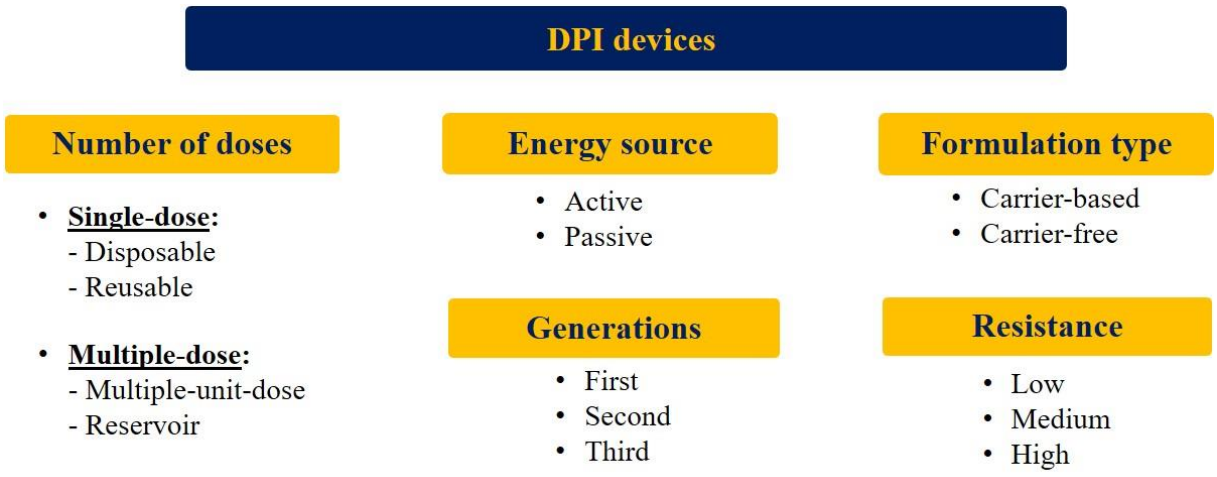

Figure 5. *Classification of DPI devices according to different aspects.*

For DPI devices, several groupings are known (Figure 5.). According to the number of doses, a distinction is made between single-dose (first generation) and multiple-dose (second generation) inhalers. In the former case, some devices are applied once, e.g. ICOone (Iconovo AB, Lund, Sweden), and those that involve patients placing a new capsule in the device each time they inhale, e.g. Breezhaler® (Novartis International AG, Basel, Switzerland). Two types of multiple-dose DPI inhalers are distinguished: multiple-unit-dose inhalers – the inhalers provided with factory-dosed and individually, usually using a blister disc or blister strip, sealed doses e.g. Diskus® (GSK, Brentford, United Kingdom) –, and reservoir DPI devices, which contain multiple doses in a single container, with a safe built-in mechanism to ensure unit dose delivery during inhalation e.g. NEXThaler® (Chiesi Farmaceutici S.p.A., Parma, Italy) c. DPI devices can also be classified as passive or active (third-generation) depending on whether they utilize the patient's inhalation airflow as an energy source during inhalation e.g. Ellipta® (GSK, Brentford, United Kingdom) or whether they also use another energy source e.g. Exubera® (Pfizer Inc., New York, United States), DPI inhalers may even be differentiated by the fact that they are developed or marketed for the application of a traditional carrier-based or carrier-free formulation [45].

Table 4. *Classification of DPI devices according to their internal resistance and pressure drop across the device [82].*

Grouping of DPI devices based on their resistance	Pressure drop through a DPI device	Example
Low resistance	<5 Mbar 1/2 L/min $^{-1}$	Breezhaler® (*Novartis International AG)*
Medium resistance	5-10 Mbar 1/2 L/min $^{-1}$	Turbohaler® *(AstraZeneca UK Ltd)*
High resistance	>10 Mbar 1/2 L/min $^{-1}$	Handihaler® *(Boehringer Ingelheim Ltd)*

The last grouping aspect can be based on the resistance of DPI devices to airflow, which is a key parameter for both API de-aggregation and lung deposition effectiveness, thus affecting the outcome of aerosol pharmacological therapy. The flow resistance of currently marketed devices is in the range of approximately 0.02-0.2 ($cmH_2O^{1/2}$/(L/min)) and the higher the resistance of a device, then the lower the flow rate will be for given patient inhalation, as the pressure drop across the device is high. The literature basically distinguishes between low, medium, and high resistance devices, but in other cases, their classification is related to the pressure drop through the DPI inhalers (Table 4.). High-resistance inhalers may produce more turbulence (aiding de-aggregation of the DPI formulation), but the patient will realize a lower volume flow rate on a high-resistance inhaler than on a low-resistance device. Each patient's case requires individual consideration by the doctor as to which inhaler is preferred in cases of respiratory difficulties so that a balance between inhaler resistance and flow rate is achieved to allow optimal de-aggregation and proper lung deposition [45].

Lately, several DPI inhalers with new structures have been commercialized or published, e.g. applying high-frequency piezoelectric vibrator, microstructured carrier tape, reverse cyclone technology, sublimation, etc. In particular, the proliferation of carrier-free DPI formulations and the use of high doses of antibiotics are the main triggers for these innovations. Nevertheless, they should remain simple enough to be used appropriately by patients. They also need to have low manufacturing overheads to reach a broad range of potential customers. Furthermore, e-Health is also gaining ground, thanks to the opportunities offered by fast-developing digital technology. The most recent advancements include so-called smart inhalers. Their use allows, for instance, clinical researchers to screen lifestyle and environmental factors that influence respiratory diseases [83].

3.3.2.2. DPI capsules

As mentioned earlier, capsule-based DPI products are very common in the market. However, in their case, in addition to inhaler structure, the DPI capsules also play an important role in the appropriate delivery of DPI microcomposites, thereby achieving the required therapeutic efficacy. While capsules applied for *per os* drug delivery are mainly used for packaging of formulations, in addition, they play a role in the liberation of the API, too. In the case of DPI capsules, it should be highlighted that the characteristics of the capsule wall (internal surface properties, staticity, residual solvent content – RSC) and its stability (appearance of fragility) can affect the aerosolization, aerodynamics, and stability of the inhalation powders. Furthermore, in the case of carrier-based systems, the dispersion of the API particles from large carrier particles may also be influenced. DPI capsules are separated by manufacturers as a specific portfolio because, on the one hand, they have to meet more stringent microbiological requirements than *oral* capsules and, on the other hand, developments are ongoing to optimize the previously mentioned properties of the capsule walls for inhalation applications [84].

Three types of capsules are currently marketed as DPI capsules. Gelatine (GEL) capsules were the earliest to appear and are still used in a considerable part of capsule-based DPI products on the market. It should be noted that this type is incompatible with certain drug materials, e.g. hydrolysis agents and that the capsule wall becomes brittle after losing 10% of its RSC. Gelatine-polyethylene glycol (GEL-PEG) capsules have a favorable capsule wall property because they are less susceptible to fragmentation, but their use in inhaled pharmaceutical products has not become as widespread as that of the GEL type. HPMC DPI capsules are the third category, which are incompatible with fewer materials and have a relatively low optimum RSC (3-7%) so they are even less prone to fragmentation than the two types discussed above. This type is gaining ground on the market. The characteristics of the two main DPI capsule types (GEL, HPMC) are summarized in Table 5. The impact of DPI capsules on formulations has only recently come into focus, which has been extensively discussed in a few publications. However, it is still an area for

further development, as there is potential for improving the properties of capsule types for inhalation use as well as in the case of DPI formulations, there should be an increasing focus on the selection of the ideal DPI capsule [84,85].

Table 5. *Characteristics of GEL and HPMC DPI capsule types.*

DPI capsule types	**GEL**	**HPMC**
Origin	Animal	Plant
Structure	Protein	Cellulose
RSC	13-16 %	3-8 %
Becoming fragile	< 10 %	< 1 %
Brittleness at low RH*	Yes	Barely characteristic
Glass transition temperature	50-60 °C	170-180 °C
Deformation	> 60 °C	> 80 °C
Static charge	Large	Small
Example	Coni-Snap® Gelatin *(Capsugel®)*	Vcaps® *(Capsugel®)*
Applied in the marketed product	Onbrez® Breezhaler®	TOBI™ Podhaler™

***RH:** Relative humidity*

3.3.3. Role of the patients

The third pillar (Figure 2.) that influences the effectiveness of DPI systems is the patient. On the one hand, in the case of respiratory disease, the type (e.g. CF), phase, severity, age and socioeconomic status of the patient all influence the success of inhalation therapy. However, it is essential that patients accept inhalation therapy, use the device correctly and inhale the formulation as desired, i.e. for the right duration, preferably as evenly as possible, and hold their breath for the required time to ensure proper efficacy. Unfortunately, in many cases, patients do not use inhalers correctly and the inhalation technique is not always carried out properly. To improve these, they should be trained to perform the correct exercise. It is also important because the correct inhalation flow can vary due to the different resistances of DPI devices. For this reason, there are inhaler-specific training devices, e.g. for those using Turbuhaler® (AstraZeneca UK Ltd., Cambridge, United Kingdom), and also devices for teaching the use of several inhalers, e.g. In-Check DIAL G16 (Clement Clarke International Ltd., Harlow, United Kingdom), where the patient selects the resistance of the inhaler they are using based on a scale and sets the training device to the appropriate pictogram. This allows the patient to learn the correct inhalation flow specific to the DPI device. Monitoring patient adherence is also very important for the effectiveness of DPI systems, as the correct timing and number of daily applications of the API is essential for the success of therapy [45,86].

4. MATERIALS AND METHODS

4.1. Materials

4.1.1. Active Pharmaceutical Ingredient

CIP (D [0.5]: 10.51 μm) is the hydrochloride salt form of ciprofloxacin, which was received by TEVA Pharmaceutical Industries Ltd. (Debrecen, Hungary). This API is a second-generation fluoroquinolone antibiotic, whose primary mechanism of action is the inhibition of bacterial DNA gyrase – topoisomerase II – and topoisomerase IV enzymes, thereby blocking the uncoiling and duplication of bacterial DNA, which leads to cell death. It possesses strong and effective activity towards a wide range of Gram-positive bacteria (e.g. *Staphylococcus*, *Bacillus* species) and most Gram-negative microorganisms (e.g. *Pseudomonas* species), often used in the treatment of lung infections [63]. It can also be a good therapeutic solution for CF and chronic bronchitis against the bacteria that occur during the course of the disease [87–91]. Further information on the API is given in Table 6.

Table 6. *Information about CIP [92,93].*

Drug material	**CIP**
Chemical structure	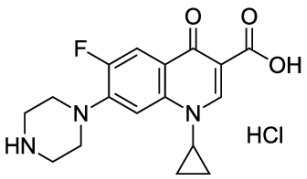
IUPAC* Name	1-cyclopropyl-6-fluoro-4-oxo-7-(piperazin-1-yl)-1,4-dihydroquinoline-3-carboxylic acid hydrochloride
Physical characteristics	Crystalline substance, Colour: from pale yellow to light yellow
Dose	$Oral_{tablets}$: 100 – 750 mg

**IUPAC: International Union of Pure and Applied Chemistry*

4.1.2. Excipients

For the carrier-based samples, α-lactose monohydrate was used as the carrier particle, which is included in most commercial carrier-based DPI products. Its usefulness is supported by its long history of use as an excipient in *oral* formulations, so it has a safe and adequate stability profile [94–96]. When administered by inhalation, it is deposited in the oral cavity and throat in the highest percentage due to its large carrier nature. It is hydrolyzed by bacterial enzymes present in normal saliva or metabolized by intestinal enzymes when ingested. Lactose particles that reach the lungs are rapidly absorbed, then metabolized, and finally excreted in the urine [97]. There are many types of α-lactose monohydrate available for inhalation [51,52]. For the formulations detailed below, InhaLac® 70 (IH70) (D [0.5]: 215.00 μm; Meggle Group GmbH., Wasserburg am Inn, Germany) has been used, which is the lactose type for inhalation with the best flowability value in the manufacturer's portfolio [51].

Magnesium stearate (MgSt) (D [0.5]: 6.92 μm; Sigma Aldrich, Budapest, Hungary) was applied for the surface treatment of the aforementioned carrier particles. In carrier-based DPI products, it contributes to improved powder flow, favors interparticle interactions, and promotes the sweeping and dispersion of API particles from the surface of the large carrier. Furthermore, it has also been shown to improve the moisture resistance of the DPI formulation in high humidity conditions [98]. Only negligible amounts of MgSt are deposited in the deeper segments of the lung, with no adverse effects [99]. Due to the above-mentioned favorable properties, the use of MgSt as an excipient has been approved for use in inhalation [100]. Among the commercially available DPI products, e.g. Foster® NEXThaler® (Chiesi Farmaceutici, Parma, Italy), Seebri® and Ultibro® Breezhaler® (Novartis International AG, Basel, Switzerland), etc. also contain MgSt [101].

Sodium stearate (NaSt) (Alfa Aesar, Heysham, United Kingdom) was used in the co-spd of the CIP drug material. NaSt is the sodium salt of stearic acid [102] and its role has been investigated for a few APIs [103,104] in carrier-free DPI development by spd. For formulations prepared with its application, changes in particle habit have been reported. It may change depending on its concentration, where it is located in the particles for a given spd formulation. It may also influence the morphology of the particles in a sample and the level of interparticle (cohesive) interaction between the particles. In the presence of NaSt, a decrease in cohesive interactions was typically reported. The beneficial change in particle habit for the published samples also had a positive effect on *in vitro* aerodynamic properties. The optimal NaSt concentration for a given API requires individual assessment. For example, Zhu et al. for theophylline [103] and Parlati et al. for tobramycin [104] both found the use of 1.0% (w/w%) NaSt to be ideal for aerodynamic results. Concerning the toxicity of NaSt, Parlati et al. found that its effect on A549 lines (tested at up to 2 w/w%) did not affect cell viability to a greater degree than pure tobramycin [104]. The development with NaSt has not been published before for DPIs containing CIP, so in our study, we used the range of 0-2 w/w% NaSt concentrations tested for other APIs.

The 96% ethanol (EtOH, AppliChem GmbH, Darmstadt, Germany) was used to modify the physical properties of the produced microcomposites. In most publications, it has been applied as a classical co-solvent in the preparation of DPI powders in starting solutions. Its applied concentration in the stock solution prepared prior to spd (similar to other organic solvents) is often reported without explanation. Its effect on the habit of DPI formulations has been poorly studied and reported to have a major influence on the micrometric properties of DPI formulations. The residual EtOH content must not exceed 0.5% in the final DPI formulation according to ICH Q3C (R6) [105].

4.2. Methods

4.2.1. Preparation of the samples

The following describes how traditional carrier-based, carrier-free and novel formulated DPI samples were produced. Since the carrier-free samples are in many cases also components of carrier-based formulations, their preparation is presented earlier.

4.2.1.1. Formulation of carrier-free composites

The DPI samples were made up from aqueous solutions of CIP. The CIP concentration in the stock solutions was 0.015 g/mL in all cases. In one of the samples, the stock solution did not include EtOH, in the other cases EtOH was used as a liquid excipient at various concentrations (5%, 10%, 20% and 30%) near distilled water and the used temperature was 65 °C. Samples containing NaSt were also applied with the same amount of API as described above, which was first solubilized in distilled water. In parallel, the corresponding amount of NaSt – Table 7. – was solved in EtOH. Then, the two above-mentioned solutions were mixed in a ratio of 7:3 (for NaSt-containing samples, in the stock solution 30% EtOH concentration was used in all cases). The solubility of CIP was studied in the used solvent/solvent mixtures before the fabrication of the formulations. The solubility values of CIP were 0.094 g/mL in distilled water and 0.072 g/mL in a 7:3 mixture of distilled water and EtOH at 65 °C with stirring at 200 rpm for 2 hours [53].

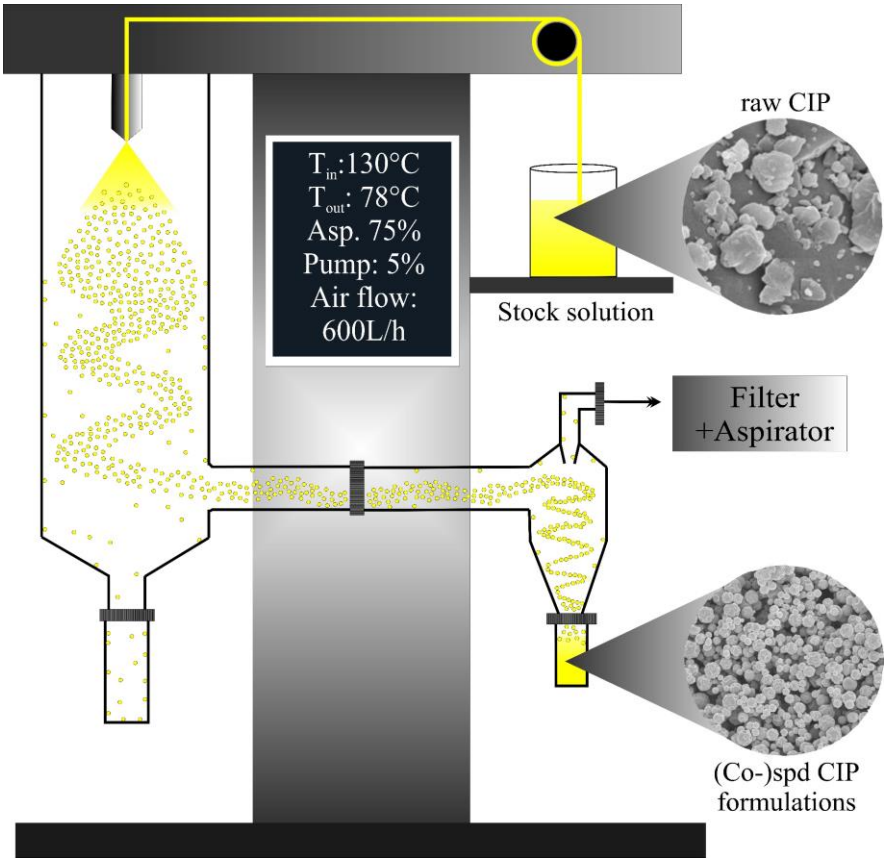

Figure 6. *Schematic illustration of the spd equipment and the process of the (co-)spd.*

The (co-)spd process was carried out using a Büchi B-191 (Mini Spray Dryer, Büchi, Switzerland) and the parameters were as follows: inlet heating temperature 130 °C, outlet temperature about 80 °C, drying air flow rate 75%, sample pump speed 5% and compressed air flow rate 600 L/h (Figure 6.) [106]. The spd yields were between 70 and 80 % for each DPI composite, which can be considered satisfactory with this technique [107–109]. The formulations were named according to the applied EtOH and NaSt concentrations in the stock solutions.

Table 7. *Samples for carrier-free formulation development with CIP content.*

Samples	CIP (g)	NaSt (g)	EtOH (g)	H_2O (g)
$CIP_{spd}EtOH^{0}$	3.0	-	-	ad 200
$CIP_{spd}EtOH^{5}$	3.0	-	10.0	ad 200
$CIP_{spd}EtOH^{10}$	3.0	-	20.0	ad 200
$CIP_{spd}EtOH^{20}$	3.0	-	40.0	ad 200
$CIP_{spd}EtOH^{30}$	3.0	-	60.0	ad 200
$CIP_{spd}EtOH^{30}NaSt^{0.5}$	3.0	0.0151	60.0	ad 200
$CIP_{spd}EtOH^{30}NaSt^{1.0}$	3.0	0.0303	60.0	ad 200
$CIP_{spd}EtOH^{30}NaSt^{2.0}$	3.0	0.0606	60.0	ad 200

4.2.1.2. Preparation of the carrier-based formulations

The raw CIP (D [0.5]: 10.51 μm) particle size was reduced by sieving (mesh size: 25μm) to allow the production of traditional carrier-based formulations as a reference, by reducing the applied API particles to a size range relevant for inhalation therapy. The carrier-based DPI formulations were prepared using CIP_{sieved} or CIP_{spd} particles and carrier/surface-modified carrier, blended in a 1:10 [110] mass ratio by Turbula mixing (T2F Turbula System Schatz; Willy A. Bachofen AG Maschinenfabrik, Basel, Switzerland) with a 30 min mixing time at 60 rpm [98]. The powder mixtures were prepared according to the rules of powder blending before Turbula mixing. The surface modification of the carrier (IH70) was completed by using 2.0 w/w% of MgSt relative to the final formulations [84,111–113] – Table 8. – with Turbula blending for 4 h [114]. Thus, MgSt can form a thin film coating the surface of the IH, which can modify its surface properties [112]. Basically, all freshly prepared samples were stored in a desiccator containing lumps of silica gel until the tests, but for the stability studies, the storage of the formulations was as described in subsubsection 4.2.3.

Table 8. *Samples for carrier-based DPI development with CIP content.*

Samples	**CIP_{sieved}** (w/w %)	**$CIP_{spd}EtOH^{10}$** (w/w %)	**$CIP_{spd}EtOH^{30}NaSt^{0.5}$**(w/w %)	**IH 70** (w/w %)	**MgSt** (w/w %)
CIP_{sieved}+IH70	9.09	-	-	90.91	-
CIP_{sieved}+IH70_MgSt	9.09	-	-	88.91	2.00
$CIP_{spd}EtOH^{10}$+IH70	-	9.09	-	90.91	-
$CIP_{spd}EtOH^{10}$+IH70_MgSt	-	9.09	-	88.91	2.00
$CIP_{spd}EtOH^{30}NaSt^{0.5}$+IH70_MgSt (*novel formulated DPI)*	-	-	9.09	88.91	2.00

4.2.2. Determination of blend uniformity and real API content

After the preparation of the carrier-based DPI formulations, homogeneity and real API content tests were carried out due to the implementation of mixing procedures. The real API content was also investigated for carrier-free DPI microcomposites. The United States Pharmacopeia (USP) prescribed that testing must be performed with DPI unit dose volumes [115] collected from ten random sites [116]. These were dissolved in distilled water and the CIP content was calculated using a UV/VIS spectrophotometer (ATIUNICAM UV/VIS spectrophotometer, Cambridge, United Kingdom) at a wavelength of 276 nm. The linearity of the CIP in this medium at the above-mentioned wavelengths was determined in advance. The linearity of the calibration curve was y = 0.0736x. The unit of the slope was mL/μg. In all cases, samples were loaded into DPI capsules (prior to stability and *in vitro* aerodynamic testing) in a mass per sample that contained the amount of API corresponding to the applied inhalation dose for CIP (10 mg), knowing the real API content of the formulations.

4.2.3. Stability tests

Stability experiments were carried out in a Binder KBF 240 device (Binder GmbH, Tuttlingen, Germany) with a constant climate chamber. An electronically operated APT.line™ line preheating chamber and cooling system provided temperature precision and repeatability of results over a temperature range of 10 to 70 °C and an RH range of 10 to 80 %. Two types of stability tests were performed (Table 9.) [84,113].

In the case of the short-term stability study, CIP_{sieved}+IH70, $CIP_{spd}EtOH^{30}NaSt^{0.5}$, and $CIP_{spd}EtOH^{30}NaSt^{0.5}$+IH70_MgSt samples were loaded after preparation into Coni-Snap® hard GEL (Capsugel®/Lonza Pharma & Biotech, Basel, Switzerland) capsules (size 3) and stored in open containers; the duration of storage was 1 month, under room conditions at 25 ± 2 °C, 50 ± 5% RH. Investigations of the samples were performed after production, 10 days, and 1 month [113].

A long-term stability study was performed according to ICH guideline at 40 ± 2 °C with 75 ± 5 % RH for 6 months also using the formulations $CIP_{spd}EtOH^{30}NaSt^{0.5}$ and $CIP_{spd}EtOH^{30}NaSt^{0.5}$+IH70_MgSt. To perform this stability study, the above-mentioned formulations were filled into 3 different DPI capsule types after their preparation. The Coni-Snap® hard GEL capsule mentioned in the previous stability test, as well as Ezeefit™ GEL-PEG (ACG-Associated Capsules Pvt. Ltd., Mumbai, India) and Ezeeflo™ HPMC (ACG-Associated Capsules Pvt. Ltd., Mumbai, India) capsules were utilized to store DPI microcomposites throughout the stability assay, thus yielding 6 samples. Hereafter, these capsule types will be referred to as GEL, GEL-PEG, HPMC. The samples were blistered before starting the stability test. Sampling took place after 1 month, 3 months and 6 months. In the same environment, the capsule types used were stored empty and blistered for 6 months for the study [84].

Table 9. *Details of the stability tests.*

Conditions for the stability test	Duration of the stability test	Investigated formulations	Applied DPI capsule types
T: 25 ± 2 °C RH: 50 ± 5%	1 month (short-term)	CIP_{sieved}+IH70	GEL
		$CIP_{spd}EtOH^{30}NaSt^{0.5}$	
		$CIP_{spd}EtOH^{30}NaSt^{0.5}$ +IH70_MgSt	
T: 40 ± 2 °C RH: 75 ± 5 %	6 months (long-term)	$CIP_{spd}EtOH^{30}NaSt^{0.5}$	GEL, GEL-PEG, HPMC
		$CIP_{spd}EtOH^{30}NaSt^{0.5}$ +IH70_MgSt	

4.2.4. Characterization using Light Microscope (LM)

The holes created by punching the capsules were recorded in shape and area using a Leica image analyzer (Leica Q500MC, LEICA Cambridge Ltd., Cambridge, United Kingdom) at 4x magnification. For each capsule type, ten repeats were carried out in all cases.

4.2.5. Thermogravimetry measurements

The Mettler Toledo STARe (Mettler Inc., Schwerzenbach, Switzerland) was applied to determine the RSC of DPI capsule types and DPI formulations. Regarding thermogravimetric tests, 3-5 mg of sample per capsule was weighed into 40 µl aluminum crucibles, and the temperature dependence of the mass change of the samples was observed between 25-350 °C at a heating rate of 10 °C / min under nitrogen gas flow. The weight loss up to 110 °C was due to the water leaving the sample.

4.2.6. X-ray powder diffraction (XRPD)

The structural identification of the samples was detected with a BRUKER D8 Advance X-ray powder diffractometer (Bruker AXS GmbH, Karlsruhe, Germany). Cu K λI radiation (λ = 1.5406 Å) was the radiation source. The investigated solid-state samples were monitored at 40 kV and 40 mA, with an angular range of 3°-40° 2-Theta, a step time of 0.1 s/step, and a step size of 0.01°. X-ray scattering was carried out with a silicon disc. The DIFFRACT plus EVA software (Bruker, Brussels, Belgium) was utilized to assess the results. The diffractograms were corrected by Kα2, smoothed, and analyzed after the elimination of the background.

4.2.7. Particle size distribution

For the determination of the particle size distribution of the samples, laser diffraction was applied (Malvern Mastersizer Scirocco 2000, Malvern Instruments Ltd., Worcestershire, United Kingdom). About 0.5 g of the samples were filled into a measuring pan. A dry analytical test method was applied and the air was the dispersion medium for the particles under study. The dispersion air pressure was adjusted to 2.0 bar to establish whether particle attrition had taken place. Three measurements were carried out in repetition. The particle size distribution was characterized by the values D [0.1], D [0.5], and D [0.9].

4.2.8. Morphology by Scanning Electron Microscope (SEM)

The shape, surface features and estimated size of the raw materials/formulations were studied by SEM (Scanning Electron Microscope – Hitachi S4700, Hitachi Scientific Ltd., Tokyo, Japan). A sputter coating machine (Bio-Rad SC 502, VG Microtech, Uckfield, United Kingdom) was utilized to induce electrical conductivity on the surface of the composites. The range of air pressure used was 1.3-13.0 MPa. Samples were coated with gold-palladium (90 s) in an argon atmosphere with the use of a gold sputtering module within a high vacuum evaporator.

4.2.9. Topology by Atomic Force Microscope (AFM), and the expressed values

Before AFM mapping, particles were spread out carefully on a two-sided adhesive strip so that they were fixed during the analysis. The imaging was performed with a FLexAFM atomic force microscope supported by C3000 control software (Nanosurf AG, Liestal, Switzerland). To extend the dynamic force measurement mode, uncoated TAP-300-Al-G cantilevers (BudgetSensors, Sofia, Bulgaria) with a nominal resonance frequency of 300 kHz were applied in phase-contrast mode. Data were processed and interpreted via Gwyddion 2.55 software (Czech Metrology Institute, Brno, Czech Republic). Root means square roughness (R_{RMS}) was determined according to Equation 1. by running the Gwyddion software. In the case of each sample, at least five particles and an area of 0.5 μm x 0.5 μm per individual particle were analyzed at least at three separate locations.

$$R_{RMS} = \sqrt{\frac{1}{n}\sum_{i=1}^{n} y_i^2} \quad (1)$$

In this equation, 'n' is the number of data points in the topographic profile and 'y_i' is the distance of the asperities (i) from the midline.

The roughness (%) value for the particle size was obtained from the average R_{RMS} ($R_{RMS\ (average)}$) and the average diameter (d) – the average of 10 diameters in various orientations – for a given particle, using the following equation:

$$\text{Roughness } \% = \frac{R_{RMS\ (average)}}{d} \times 100 \quad (2)$$

Moreover, the above-mentioned software makes it possible to measure only the single depressions/dimples of the particle surface. In the case of each particle, a minimum of three dimples was used as the basis for determining the average values (depth and width of the dimples (average)). By obtaining these values, and also knowing the value of d for the particle as discussed above, the depth and width of the dimples relative to the particle size were calculated (Equations 3 and 4). For each sample, analyses were carried out for at least five particles.

$$\text{Depth of the dimples } \% = \frac{Depth\ of\ the\ dimples_{(average)}}{d} \times 100 \quad (3)$$

$$\text{Width of the dimples } \% = \frac{Width\ of\ the\ dimples_{(average)}}{d} \times 100 \quad (4)$$

4.2.10. Studying the interparticle interactions

To investigate the interparticle interactions between the components of the samples, pastilles were created using 100 mg of each substance and 1 tonne of compressive force (Perkin Elmer hydraulic press, Waltham, United States). The contact angle (Θ) was established using a Dataphysics OCA 20 instrument (Dataphysics Inc. GmbH, Germany). Three pastilles per sample were dropped with a polar liquid medium (distilled water) and the other three pastilles were dropped with a dispersion liquid medium (diiodomethane) to perform parallel measurements. Simultaneously with the dripping, the instrument was set to record at a time interval of 1-25 s; this allowed the change in contact angle to be detected and determined. In this way, the contact angle of the two different applied liquids was obtained, determined always in relation to the same second. Surface free energy (γ_s) of the components, which is made up of two parts: a disperse (γ_s^d) and a polar part (γ_s^p), that is ($\gamma_s = \gamma_s^d + \gamma_s^p$), was calculated using the Wu formula. The surface tensions of the applied fluids are given in the literature ($\gamma_l = \gamma_l^d + \gamma_l^p$): distilled water γ^p= 50.2 mN/m, γ^d= 22.6 mN/m; and diiodomethane γ^p= 1.8 mN/m, γ^d= 49 mN/m [117]. In Wu's formula (equation

5) [118], only the disperse (γ_s^d) and the polar component (γ_s^p) of the investigated substances are unknowns, which can be expressed from the equation:

$$(1 + \cos\Theta)\gamma_l = \frac{4(\gamma_s^d \gamma_l^d)}{\gamma_s^d + \gamma_l^d} + \frac{4(\gamma_s^p \gamma_l^p)}{\gamma_s^p + \gamma_l^p} \quad (5)$$

where Θ = contact angle; γ = surface free energy; s = solid phase; l = liquid phase; d = dispersion component; and p = polar component

The cohesion work (W_c) is defined as twice the surface free energy [119]:

$$W_c = 2 \times \gamma_s \quad (6)$$

The adhesion work (W_{adh}) can be established between two different substances (denoted by the numbers 1 and 2) and is obtained from the value of the disperse (γ_s^d) and the polar component (γ_s^p) of the substance, in this formula γ^d and γ^p. The W_{adh} can be calculated in the following way [119]:

$$W_{adh} = 4\left[\frac{\gamma_1^d \gamma_2^d}{\gamma_1^d + \gamma_2^d} + \frac{\gamma_1^p \gamma_2^p}{\gamma_1^p + \gamma_2^p}\right] \quad (7)$$

The Derjaguin approach was used to determine the adhesion force (F_{adh}) [118]:

$$F_{adh} = 2\pi\left(\frac{R_A R_B}{R_A + R_B}\right) W_{adh} \quad (8)$$

where R_A and R_B are the radii of the particles A and B, respectively, between which the adhesion interaction is studied. The size R is defined as half of the value D [0.5] determined in the particle size analysis for each applied substance.

The spreading coefficient (S_{12}) – a dimensionless value – shows the probability of one material (1) on the surface of the second component (2). It is used to characterize the distribution in binary systems. The spread is favorable if it has a positive value and a high number. In this case, the API particle spreading over the surface of either a carrier or a surface-modified carrier is investigated. The spreading coefficient or the inverse case can be given by the following expressions [118,119]:

$$S_{12} = 4\left[\frac{\gamma_1^d \gamma_2^d}{\gamma_1^d + \gamma_2^d} + \frac{\gamma_1^p \gamma_2^p}{\gamma_1^p + \gamma_2^p} - \frac{\gamma_1}{2}\right] \quad (9)$$

$$S_{21} = 4\left[\frac{\gamma_1^d \gamma_2^d}{\gamma_1^d + \gamma_2^d} + \frac{\gamma_1^p \gamma_2^p}{\gamma_1^p + \gamma_2^p} - \frac{\gamma_2}{2}\right] \quad (10)$$

where γ^d is the disperse part of surface-free energy, γ^p is the polar part of surface free energy, and γ is the total surface free energy of the components spread on the other component [119]. In our work, equation (10) was used for all relevant cases.

4.2.11. *In vitro* aerodynamic test

The Andersen Cascade Impactor (ACI) (Copley Scientific Ltd., Nottingham, United Kingdom) was used as an *in vitro* testing tool to characterize the aerodynamic particle size distribution (APSD) of the formulations (Figure 7.). This instrument is approved for testing APSD by the United States Pharmacopeia /Test Chapter <601>/, the European Pharmacopoeia 2.9.18 /Method Chapter/ and by the Chinese Pharmacopoeia /Chapter <0951>/ [120]. Discs of the impactor were coated with a mixture of Span® 80 and cyclohexane (1:99) and left to dry. The applied flow rate (28.3 ± 1 L/min or 60 ± 1 L/min) for the measurements was generated using a vacuum pump (High-capacity Pump Model HCP5, Critical Flow Controller Model TPK, Copley Scientific Ltd., Nottingham, United Kingdom), and monitored with a mass flow meter (Flow Meter Model DFM 2000, Copley Scientific Ltd., Nottingham, United Kingdom) [84]. Fresh formulations were basically filled into GEL capsules prior to the study, however, already encapsulated samples were stored as detailed in subsubsection 4.2.3. were used in the ACI inhalation studies. In the *in vitro* assay, three capsules [121] from a studied sample were applied in a single measurement, using the Breezhaler® (Novartis, Basel, Switzerland) as a low-resistance inhaler, which may thus benefit patients with lung diseases due to the aerosolization and deaggregation of particles and their aerodynamic properties. For each single used capsule, the inhalation time was set as related to the flow rate (28.3 L/min or 60 L/min) so that the inhaled volume was always 4 L [120].

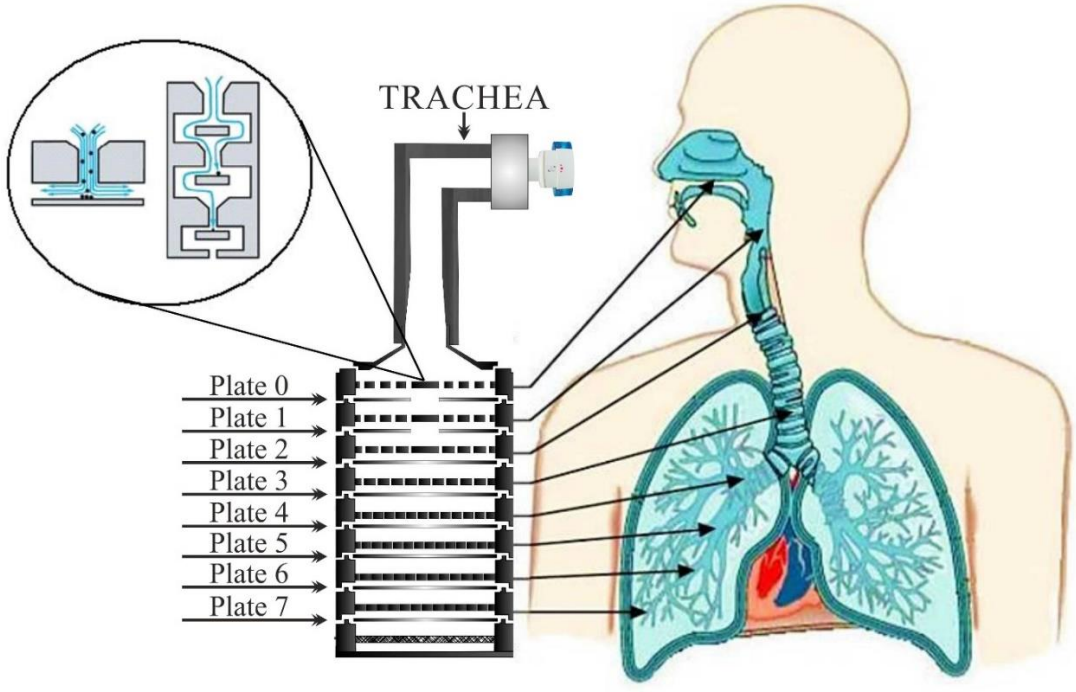

Figure 7. *Structure of ACI and illustration of the flow.*

After each *in vitro* examination, the inhaler, the applied DPI capsules, and the components of the impactor (mouthpiece, throat, eight disks, the used filter) were rinsed with distilled water. The quantity of API deposited on these objects was detected using an ultraviolet-visible spectrophotometer (ATI-UNICAM UV/VIS spectrophotometer, Cambridge, United Kingdom)

with a 276 nm wavelength. The linearity of the CIP calibration curve in distilled water was y = 0,0736x at 276 nm (unit of slope: mL/μg). From the above data, the terms describing the *in vitro* aerodynamic behavior of the samples can be calculated: emitted fraction (EF), fine particle fraction (FPF), and mass median aerodynamic diameter (MMAD). The EF is the percentage of the amount of API detected from the impactor (mouthpiece to filter), which is essentially the same mass as the emitted dose, compared to the total amount of API recovered [84]. The cumulative percentage less than the size range versus the effective cut-off diameter [120] was plotted in the KaleidaGraph 4.0 program (Synergy Software, Reading, PA, United States) on the log probability scale. If the abscissa value of the 5 μm ordinate value is known, mass less than 5 μm in diameter can be specified. The percentage of this mass relative to the ED gives the FPF. The MMAD is defined as the diameter at which 50% of the aerosol particles are larger by mass and 50% are smaller [122]. This is expressed as the ordinate value for the 50% abscissa value. It should be noted that the calculations must also consider the number of DPI capsules applied per *in vitro* test [84].

4.2.12. *In silico* assessment

Quantification of inhaled API deposition in the airways was carried out with the help of the stochastic lung model (SLM). The SLM is a full airway particle deposition model that was first developed in 1990 by Koblinger and Hofmann [123], which has been under continuous development since then. In this study, the most recent version of the model was used and it was validated for medical aerosols. The efficiency of particle deposition in the upper airways (oral cavity, pharynx and larynx) was evaluated using empirical deposition formulas derived by Cheng [124] and embedded in the SLM model. Bronchial and bronchiolar geometries are constructed from distributions based on a random selection of branching tube morphometric parameters (length, branching diameter and angle of gravity) and taken from measurements on airway castings (Raabe et al. 1976) [125]. The digitized reproduction of the acinar airways is inspired by a detailed anatomical description from Haefeli-Bleuer and Weibel [126]. Particles are monitored in this stochastic intrathoracic airway structure until they are either deposited or exhaled. Determination of the deposition of particles is performed from analytical deposition equations inferred for this part of the respiratory tract on straight and curved tubes and hemispheres. Inertial impaction and gravitational settling are the two dominant deposition mechanisms. The Brownian diffusion does not substantially affect the deposition of aerosol APIs on account of their size distribution. Patients' respiratory data and the APSD values of the studied formulations were the key inputs to the deposition model. Parameters typical of patient breathing during DPI formulation inhalation were taken from the work of Colthorpe and colleagues [127]. The respiratory profile of patients inhaling via Breezhaler® inhaler was recorded by them. The APSD was determined by applying an impactor technique.

4.2.13. Statistical analyses

Statistical analysis was performed using t-test computations with a significance level of 0.05 and one-tailed hypothesis using Social Science Statistics [128] available online. All reported data represent the ± standard deviation of three replicate tests (n = 3).

5. RESULTS

5.1. Development of CIP containing traditional carrier-based DPI samples

The first line of improvement was the development of traditional carrier-based systems. For the experimental series, a CIP_{sieved} with a particle size suitable for inhalation and the spd CIP ($CIP_{spd}EtOH^{10}$), which was previously manufactured by our research group [63], were used as API particles. These particles have a relatively high W_c value, on the one hand, the CIP_{sieved} particles are not spherical and thus have a large surface area in contact, on the other hand, the $CIP_{spd}EtOH^{10}$ sample particles, although spherical, promote strong cohesion due to the interlocking of the approximately identical dimpled particle shapes (Table 10.). In the case of the carrier-based samples, the SEM images show that the CIP_{sieved} and $CIP_{spd}EtOH^{10}$ particles are uniformly distributed on the surface of the untreated carrier IH70 (CIP_{sieved}+IH70; $CIP_{spd}EtOH^{10}$+IH70). However, in the case of the MgSt surface-treated carrier, the API particles were not uniformly embedded in the carrier and were present in higher concentrations in some places (CIP_{sieved}+IH70_MgSt; $CIP_{spd}EtOH^{10}$+IH70_MgSt) (Table 11.). It can be concluded that MgSt, by occupying the active sites of the carrier, modifies the spreading of the API on the surface of the large carrier particles. Without surface modification, the surface of the carrier used is presumably microporous (pore diameter 1-10 μm), in the case of surface treatment, it is macroporous (pore diameter above 10 μm). This also explains the different API-spreading phenomena observed [46,111].

Table 10. *The specificities of sieved and spd API particles.*

API samples	**CIP_{sieved}**	**$CIP_{spd}EtOH^{10}$**
SEM	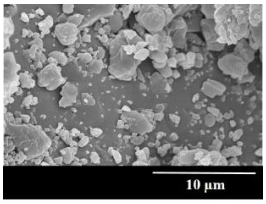	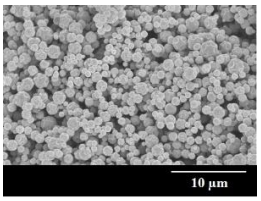
Schematic pictures		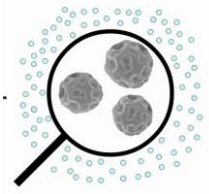
D [0.5] (μm)	5.09 ± 0.23	3.52 ± 0.04
W_c (mN/m)	161.60	155.40

The W_{adh} and F_{adh} of the carrier-based samples and their specific spreading coefficient – S_{21} – values were determined (Table 11.). It is observed that the F_{adsh} of the samples containing spd API ($CIP_{spd}EtOH^{10}$) is substantially lower, approximately one-third than that of the samples containing CIP_{sieved}. It can be concluded that MgSt reduced the W_{adh} and F_{adh} values (antiadhesive excipient). Furthermore, the negative numerical value results – S_{21} – in a more unfavorable spreading of the drug material on the carrier surface, which was confirmed by SEM images of $CIP_{sieved}EtOH^{10}$+IH70_MgSt and $CIP_{spd}EtOH^{10}$+IH70_ MgSt [111].

Table 11. *The SEM recording and interparticle interactions of carrier-based DPI samples.*

Carrier-based samples	**CIP_{sieved} +IH70**	**CIP_{sieved} +IH70_MgSt**	**$CIP_{spd}EtOH^{10}$ +IH70**	**$CIP_{spd}EtOH^{10}$ +IH70_MgSt**
SEM	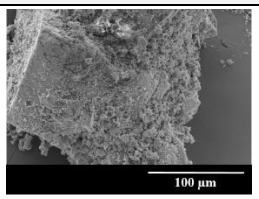	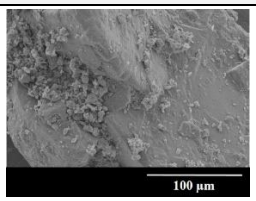	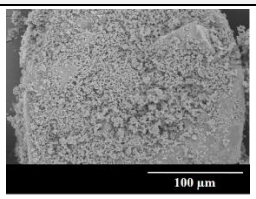	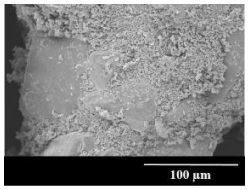
Schematic pictures		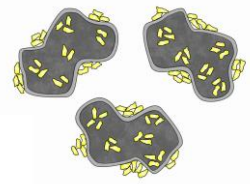	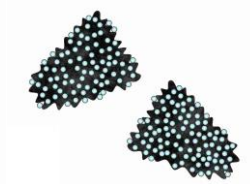	
W_{adh} (mN/m)	108.26	78.27	98.72	73.23
F_{adh} (mN)	$1.690*10^{-3}$	$1.216*10^{-3}$	$0.596*10^{-3}$	$0.440*10^{-3}$
S_{21}	1.64	-45.59	16.67	-18.36

In terms of pulmonary deposition (FPF), formulations containing spd API ($CIP_{spd}EtOH^{10}$) performed remarkably better than those containing sieved drug particles (CIP_{sieved}). This was due to the aerodynamically favorable properties of the former API particles, and the formulation of the carrier, especially the MgSt surface treated carrier particles ($CIP_{spd}EtOH^{10}$+IH70_MgSt), further improved the FPF result. In contrast, in the case of CIP_{sieved}, the presence of IH70/IH70_MgSt did not result in the improvement predicted by the large adhesion values (most of the factory formulations are similar to these samples, i.e. particle size optimized but not containing spd API particles on large carrier/surface treated carrier particles). Concerning MMAD, it can be noted that an inverse proportionality between the *in vitro* aerodynamic size of the drug particles and the deposition efficiency is observed. For EF, it can be seen that for carrier-based systems, less drug is retained in the capsule during inhalation (Table 12.). Thus, the conclusions based on the physical studies and their anticipated trends in lung deposition were confirmed by the results of the ACI measurements [111].

Table 12. *In vitro aerodynamic results of samples of the carrier-based development line measured at 60 L/min flow rate.*

Formulations	FPF (%)	MMAD (μm)	EF (%)
CIP_{sieved}	32.19 ± 0.45	6.93 ± 0.02	99.38 ± 0.14
CIP_{sieved}+IH70	33.00 ± 0.12	5.66 ± 0.08	99.99 ± 0.01
CIP_{sieved}+IH70_MgSt	32.87 ± 0.09	4.91 ± 0.05	99.75 ± 0.03
$CIP_{spd}EtOH^{10}$	58.96 ± 0.81	3.47 ± 0.11	97.39 ± 0.26
$CIP_{spd}EtOH^{10}$+IH70	62.42 ± 0.28	3.23 ± 0.07	99.87 ± 0.09
$CIP_{spd}EtOH^{10}$+IH70_MgSt	74.40 ± 0.33	2.45 ± 0.08	99.41 ± 0.34

Beyond the previous experiments described in section 3.3.1 of the literature background, an innovative formulation sample with improved *in vitro* aerodynamic (FPF) performance has been prepared, to our knowledge not yet reported, which already contains a mechanical dry coated carrier with MgSt and spd API on its surface ($CIP_{spd}EtOH^{10}$+IH70_MgSt). This is the initial improvement of the development line described in this thesis, which can be considered as the starting point for the combination of the two systems in our case, which still belongs to the development of traditional carrier-based DPI systems. Moreover, through the study of interparticle interactions, a correlation was found between the physical properties and *in vitro* lung deposition results of interactive physical mixtures [111]. In the case of meloxicam potassium (MXP), this development was similarly carried out (only the API was changed in the manufacturing process, and the production and testing methods were the same), and the *in vitro* aerodynamic results of the samples showed the same trend, which is described in a separate publication [48].

5.2. Development of CIP containing carrier-free DPI formulations

5.2.1. EtOH concentration optimization in the stock solution

While for carrier-based development the EtOH concentration in the spd starting solution was 10% based on preliminary experience [63], the first step in carrier-free development was to optimize the EtOH concentration in the starting solution for CIP. The effect of varying the EtOH concentration in the stock solution on the habit and *in vitro* aerodynamic results of the prepared samples was studied. According to the XRPD patterns (Figure 8.), the distinctive peaks of raw CIP were observed at 8.23, 9.25, 19.22, 26.39 and 29.16 2-Theta degree, which indicates a crystalline structure. In the spd samples, it can be noticed that the characteristic peaks are found with very low intensity, indicating that the amorphous feature dominates in these spd formulations. The structure of the samples influences their morphology, which can modify, for example, the interactions between particles [53].

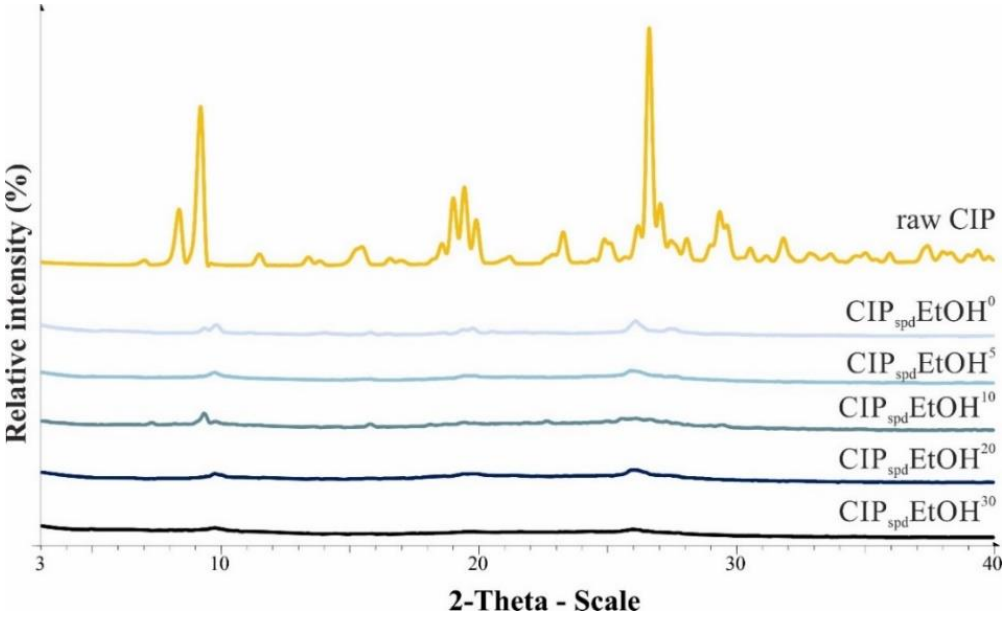

Figure 8. *XRPD pattern of the raw CIP and the spd samples prepared in the presence of various EtOH concentrations in stock solutions.*

In terms of the W_c values of the composites, it can be observed that the value for the case of $CIP_{spd}EtOH^0$ is comparatively high, which can be due to the spherical nature of the particles and the almost devoid of depressions on their surface – spherical-smooth/spherical-dimpled particles – (Table 13.). In the case of $CIP_{spd}EtOH^5$ and $CIP_{spd}EtOH^{10}$, the W_c is even higher, with almost equal values. This can be best understood from schematic figures, since the particles may contact over a larger surface area because of their dimpled nature and nearly similar surface morphology (inc. roughness, depth, and width of the dimples) (Table 13.). This context has been previously referred to in Lechanteur et al [129] publication [53]. Nevertheless, for $CIP_{spd}EtOH^{20}$ and $CIP_{spd}EtOH^{30}$ samples, a notable decrease in W_c is observed, which can be explained as morphological differences of individual particles shown in the SEM records, as also indicated by the larger variation in the AFM-detected dimples. As a consequence, the particles are more difficult to bond together and resulting in a reduction in the W_c values. However, the literature generally describes the occurrence of dimples as a positive factor for aerodynamic results [78], but they provide higher connectivity for particles with similar morphology. Hence, it is assumed that the larger (wide and deep) dimples, the somewhat variable morphology of particles, and thus the more beneficial W_c values imply comparatively improved *in vitro* aerodynamic results for $CIP_{spd}EtOH^{20}$ and $CIP_{spd}EtOH^{30}$ formulations [53]. The different morphologies and D [0.5] values of the samples are due to the different evaporation rates of water and EtOH. The EtOH diffuses from the droplet first, bringing dissolved CIP to the surface, which immediately solidifies and forms a shell on the surface, followed by the water. 30 % EtOH brings more CIP to the surface, hardens the crust and can leave a large cavity (hollow particles). At higher EtOH concentrations, the higher internal pressure may cause the particles to swell and crack more [130]. Thus, mixtures

of these solvents in different proportions in the stock solution will lead to different morphologies during the spd process under the same conditions [53].

Table 13. *Characteristics of samples with different EtOH concentrations in the stock solution.*

	$CIP_{spd}EtOH^{0}$	**$CIP_{spd}EtOH^{5}$**	**$CIP_{spd}EtOH^{10}$**	**$CIP_{spd}EtOH^{20}$**	**$CIP_{spd}EtOH^{30}$**
D [0.5] (μm)	3.168 ± 0.06	4.197 ± 0.08	3.521 ± 0.04	3.753 ± 0.09	4.317 ± 0.11
SEM	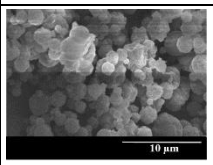	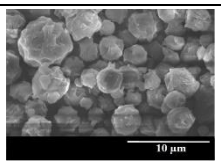	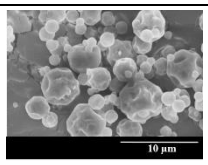	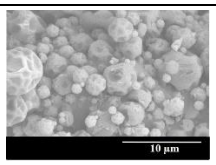	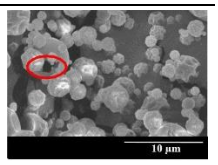
AFM	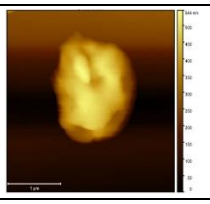	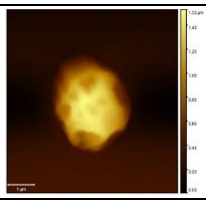	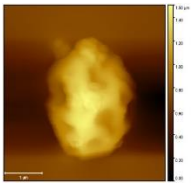	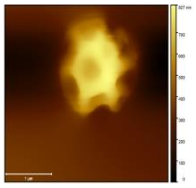	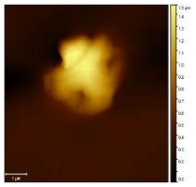
Roughness (%)	0.85 ± 0.09	2.37 ± 0.11	2.66 ± 0.16	4.10 ± 0.18	4.46 ± 0.36
Depth of the dimples (%)	0.83 ± 0.04	2.81 ± 0.19	2.93 ± 0.21	5.73 ± 0.51	8.36 ± 0.71
Width of the dimples (%)	4.04 ± 0.17	22.56 ± 1.52	22.85 ± 1.54	25.94 ± 2.08	28.34 ± 2.32
W_c (mN/m)	149.68	156.64	155.40	135.72	128.34
Schematic pictures	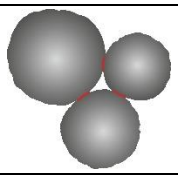	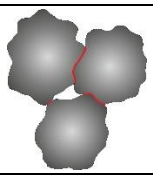	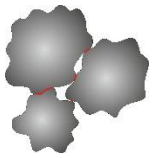	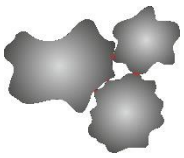	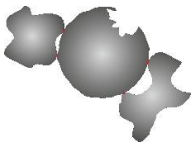

Concerning the performance of *in vitro* aerodynamic tests, it became possible from this sub-point to carry out measurements of samples already at 28.3 L/min flow rate instead of 60 L/min (flow rate corresponding to healthy lungs). That is, to determine the APSD of samples by modeling reduced airflow in lung diseases. Basically, a flow rate of 28.3 L/min is considered a standard measurement based on the pharmacopeia, although both 60 L/min (healthy lung) and 90 L/min (forced expiratory modeling) are also applied and accepted [120,131]. In the case of antibiotics intended for local use, thereby the aerodynamic properties and lung deposition of the samples can be more accurately characterized, therefore *in vitro* aerodynamic results obtained using a flow rate of 28.3 L/min are presented below.

The FPF results changed inversely with the MMAD values. For the $CIP_{spd}EtOH^{5}$ and $CIP_{spd}EtOH^{10}$ formulations, the FPF values were notably lower, about half of the values of the $CIP_{spd}EtOH^{0}$ sample. In comparison, considerable enhancement in *in vitro* lung deposition results is shown for $CIP_{spd}EtOH^{20}$ and $CIP_{spd}EtOH^{30}$. The latter reached the highest FPF result (34.39%). The EF value must be between 85% and 115% for *in vitro* APSD tests [132]. Among the tested samples, $CIP_{spd}EtOH^{0}$, $CIP_{spd}EtOH^{5}$ and $CIP_{spd}EtOH^{30}$ fulfilled this requirement (Table 14.) [53].

Table 14. *In vitro aerodynamic properties of the formulations at 28.3 L/min flow rate.*

Samples	FPF (%)	MMAD (µm)	EF (%)
$CIP_{spd}EtOH^{0}$	23.58 ± 0.73	7.62 ± 0.13	86.26 ± 0.44
$CIP_{spd}EtOH^{5}$	11.96 ± 0.16	12.03 ± 0.08	89.57 ± 0.31
$CIP_{spd}EtOH^{10}$	13.05 ± 0.25	10.18 ± 0.16	78.13 ± 0.83
$CIP_{spd}EtOH^{20}$	28.51 ± 0.43	5.83 ± 0.03	75.80 ± 0.65
$CIP_{spd}EtOH^{30}$	34.39 ± 0.54	5.21 ± 0.11	87.12 ± 0.39

A more detailed explanation of the *in vitro* aerodynamic results is shown in Figure 9. The analysis of the particle habit has already discussed how different EtOH concentrations affect the D [0.5] values and lead to morphological changes. The morphology of the particles of the samples has a major impact on the W_c results. Fig. 9. illustrates the relationship between W_c and MMAD/D [0.5] trends [53].

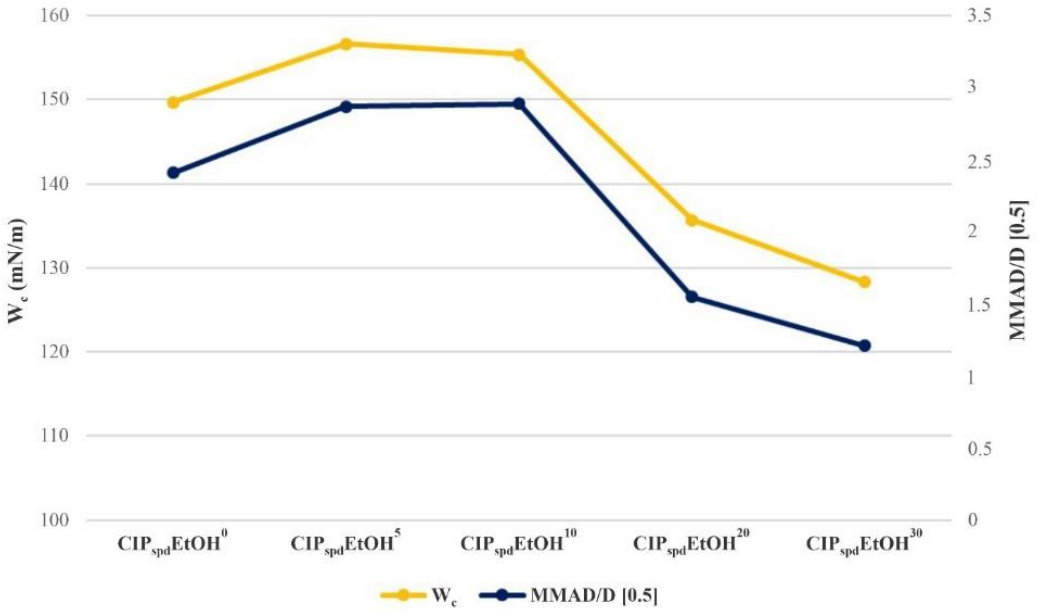

Figure 9. *Relationship between the trends of W_c and MMAD/D [0.5] values.*

This confirmed how many times per formula the MMAD value of the D [0.5] result became a function of the W_c values. Consequently, it is understandable that D [0.5] values were not directly correlated with FPF results, however, for example, the relatively low D [0.5] value (3.168 µm) and the high W_c value (149. 68 mN/m) for $CIP_{spd}EtOH^{0}$ resulted in an MMAD value of 7.62 µm (2.41 times the D [0.5] value), and for $CIP_{spd}EtOH^{5}$ the higher D [0.5] value (4.197 µm) and also high W_c value (156.64 mN/m) were reflected in the higher MMAD result (12.03 µm). Furthermore, for $CIP_{spd}EtOH^{30}$, although it has the highest D [0.5] value (4.317 µm) of all the formulations tested, the substantially lower W_c value (128.34 mN/m) gives the most favorable MMAD result (only 1.21 times the D [0.5] value) [53].

This work introduces new expressions for particle size-related roughness, depth and width of dimples, and correlation of MMAD/D [0.5] ratio with W_c, which to the best of our knowledge have not been published before, resulting in gap-filling findings. As a result, different ratios of solvent mixtures can be put into a new perspective as different EtOH concentrations affect the habit of the DPI formulations and therefore their *in vitro* aerodynamic performance. Based on these findings, it became clear why the stock solution of the tested DPI formulation containing 30% EtOH ($CIP_{spd}EtOH^{30}$) achieved the best FPF result [53].

5.2.2. Optimization of NaSt concentration

However, the results are presented in subsection 5.2.1. are very remarkable in terms of both development and observed correlations, but in the modeling of the diseased lung, a very low lung deposition – FPF – value was measured (Table 14.). For NaSt, it is described in subsection 4.1.2 that its beneficial effect on DPIs has already been demonstrated for several drug materials. Thus, samples were prepared to contain different concentrations of Nast (0.5%, 1.0%, 2.0% on the dry weight basis) and a 30% EtOH concentration in the stock solution during co-spd ($CIP_{spd}EtOH^{30}NaSt^{0.5}$, $CIP_{spd}EtOH^{30}NaSt^{1.0}$, $CIP_{spd}EtOH^{30}NaSt^{2.0}$) to be compared with the results of $CIP_{spd}EtOH^{30}$ sample – containing optimized EtOH concentration in the stock solution, reported in 5.2.1. subsubsection – for habit and *in vitro* aerodynamic performance. XRPD measurements of samples and raw materials were performed. NaSt was characterized by the following peaks: 4.0 and 6.0 2-Theta degree. NaSt has a semicrystalline structure. For the (co-)spd samples, it can be clearly seen that the characteristic peaks for CIP and NaSt are present with very low intensity, indicating that the amorphous property is dominant in these samples (Figure 10.).

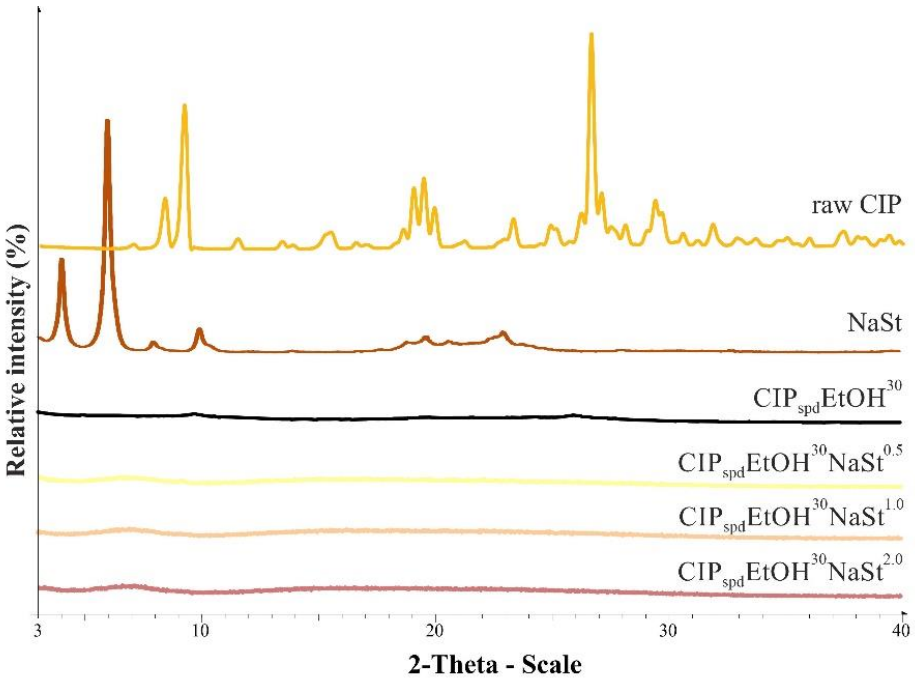

Figure 10. *XRPD patterns of raw CIP, NaSt and (co-)spd samples with different NaSt concentrations.*

In terms of habit, the use of NaSt resulted in a considerably smaller particle size D [0.5] compared to the $CIP_{spd}EtOH^{30}$ sample (and indeed compared to all samples described in subsubsection 5.2.1). Nevertheless, the effect of EtOH on the morphology is well observed in the case of $CIP_{spd}EtOH^{30}NaSt^{0.5}$, i.e. particles with typically different particle shapes are produced, and the somewhat larger deviation in particle size also means that the particles do not typically interlock. With increasing NaSt concentration, the W_c decreased for the tested samples, which is due to the material property of NaSt, but for $CIP_{spd}EtOH^{30}NaSt^{1.0}$ and $CIP_{spd}EtOH^{30}NaSt^{2.0}$, the D [0.5] values are slightly larger and with smaller variance than for $CIP_{spd}EtOH^{30}NaSt^{0.5}$, as well as the surface of the individual particles is quite similar, which can thus be more easily interconnected (Table 15.).

Table 15. *The habit of (co-)spd DPI formulations with different NaSt concentrations.*

	$CIP_{spd}EtOH^{30}$	**$CIP_{spd}EtOH^{30}$ $NaSt^{0.5}$**	**$CIP_{spd}EtOH^{30}$ $NaSt^{1.0}$**	**$CIP_{spd}EtOH^{30}$ $NaSt^{2.0}$**
D [0.5] (μm)	4.317 ± 0.11	2.364 ± 0.11	2.432 ± 0.04	2.550 ± 0.07
SEM	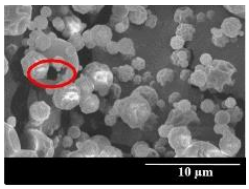	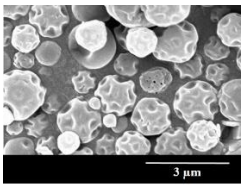	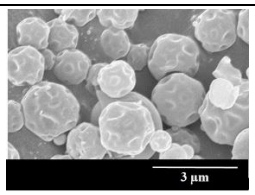	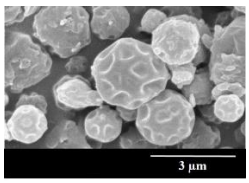
Schematic pictures	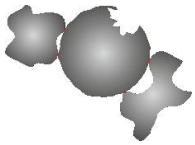		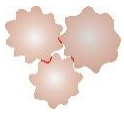	
W_c (mN/m)	128.34	123.26	121.67	118.98

The best *in vitro* aerodynamic result (FPF) among the samples discussed in this subsection was obtained by $CIP_{spd}EtOH^{30}NaSt^{0.5}$ (Table 16.), which is in agreement with the statements made about the habit of the samples. Although $CIP_{spd}EtOH^{30}NaSt^{2.0}$ has the lowest W_c value, but the aerosolization (FPF, MMAD, and EF values) is less good due to presumably similar particle shapes than for $CIP_{spd}EtOH^{30}NaSt^{0.5}$, where the effect of NaSt (cohesion and particle size) is already present, but the different particle shape is more supportive for aerosolization. Although it is a requirement for DPIs that the EF value should be between 85 and 115% for APSD testing [132], it can be considered as a successful carrier-free development. Remarkably, the FPF result of $CIP_{spd}EtOH^{30}NaSt^{0.5}$ is more than four times better than the FPF result of $CIP_{spd}EtOH^{10}$ (measured at a flow rate of 28.3 L/min).

Table 16. *Aerodynamic properties of (co-)spd samples with different NaSt concentrations measured at 28.3 L/min flow rate.*

Samples	FPF (%)	MMAD (μm)	EF (%)
$CIP_{spd}EtOH^{30}$	34.39 ± 0.54	5.21 ± 0.11	87.12 ± 0.39
$CIP_{spd}EtOH^{30}NaSt^{0.5}$	54.27 ± 2.75	4.14 ± 0.18	76.99 ± 3.32
$CIP_{spd}EtOH^{30}NaSt^{1.0}$	45.94 ± 1.12	4.62 ± 0.07	77.82 ± 0.71
$CIP_{spd}EtOH^{30}NaSt^{2.0}$	40.23 ± 1.44	4.93 ± 0.17	80.64 ± 0.36

For meloxicam potassium (MXP), this development was similarly carried out (only the API was changed in the preparation, the manufacturing and testing methods were the same), where the *in vitro* aerodynamic results of the samples were also improved by the use of NaSt, but in the case of the above mentioned API, the best *in vitro* aerodynamic results were obtained by using 2.0% NaSt. The findings are presented in a separate publication [133].

In conclusion, the use of NaSt in co-spd manufacturing of DPIs affects the size and shape of the particles, thereby having a positive effect on the *in vitro* aerodynamic results. This has been confirmed for two drug materials (CIP and MXP) in our cases, however, it depends on the API in which NaSt concentration is applied to achieve the best *in vitro* aerodynamic results. In the case of CIP, the use of 0.5% NaSt ($CIP_{spd}EtOH^{30}NaSt^{0.5}$ sample) is optimal based on the investigations of our studies.

5.3. Development of a pulmonary dosage form of the novel formulated DPI microcomposite

5.3.1. Comparison of a novel formulated DPI formulation with traditional carrier-based and developed carrier-free DPI samples

Already the traditional carrier-based and carrier-free DPI developments discussed earlier are very remarkable, both in terms of product development and the correlations explored. However, a novel formulated DPI sample ($CIP_{spd}EtOH^{30}NaSt^{0.5}$+IH70_MgSt) combining our previous developments has been developed. That is, an interactive physical mixture of MgSt surface-treated carrier particles and $CIP_{spd}EtOH^{30}NaSt^{0.5}$ was prepared. The physical properties and *in vitro* aerodynamic results of this sample were compared with the sample CIP_{sieved}+IH70, which is suitable for most commercial DPI products (micronized but not spd API on the surface of the untreated DPI carrier), as discussed earlier in section 5.1, and with the $CIP_{spd}EtOH^{30}NaSt^{0.5}$ formulation, which achieved the best FPF results in the carrier-free development line (Table 17.) [112].

It was found that also in the case of the novel formulated DPI, the application of surface-treated carrier considerably reduced W_{adh} and F_{adh} values compared to CIP_{sieved}+IH70. The negative value of the spreading coefficient – S_{21} – indicates that the spreading of the API on the carrier surface is unfavorable, which is confirmed by the SEM recording of the $CIP_{spd}EtOH^{30}NaSt^{0.5}$+IH70_MgSt sample. Regarding the *in vitro* aerodynamic results (Table 17.), it can be concluded that the novel formulated DPI also has the best FPF result (measured at a flow rate of 28.3 L/min) compared to the samples described in the previous sections, which combined the advantageous features of our traditional carrier-based and carrier-free developments. That is, the use of a surface-treated carrier enhances aerosolization, which is also related to the EF value, as the sample is more easily swept out of the DPI capsule (less API adherence to the capsule wall). Furthermore, the development of the drug particle $CIP_{spd}EtOH^{30}NaSt^{0.5}$ allowed for achieving an outstanding FPF result [112].

Table 17. *Characterization of the CIPsieved+IH70, $CIP_{spd}EtOH^{30}NaSt^{0.5}$ and $CIP_{spd}EtOH^{30}NaSt^{0.5}$+IH70_MgSt formulations.*

	CIP_{sieved}+IH70	**$CIP_{spd}EtOH^{30}NaSt^{0.5}$**	**$CIP_{spd}EtOH^{30}NaSt^{0.5}$ +IH70_MgSt**
D [0.5] (μm)	156.03 ± 1.85	2.240 ± 0.18	128.76 ± 0.78
SEM	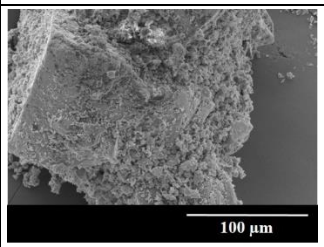	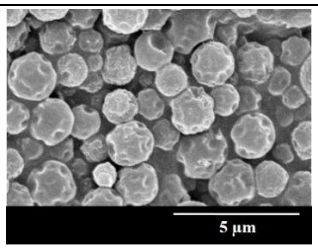	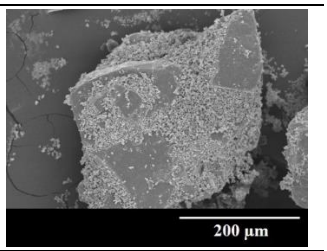
Schematic pictures		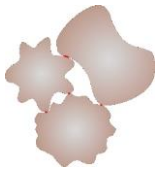	
W_c (mN/m)	-	123.26	-
W_{adh} (mN/m)	108.26	-	72.57
F_{adh} (mN)	$1.690 * 10^{-3}$	-	$0.504 * 10^{-3}$
S_{21}	1.64	-	−19.06
FPF (%)	23.30 ± 0.23	54.27 ± 2.75	63.75 ± 1.21
MMAD (μm)	7.98 ± 0.10	4.14 ± 0.18	3.47 ± 0.02
EF (%)	96.92 ± 0.11	76.99 ± 3.32	90.45 ± 1.80

For the three samples mentioned above, *in silico* simulations were also performed with the following parameter values: inhaled volume – 1.7 L, inhalation time – 3.2 s, and breath-hold time – 5, 10 s. These values correspond to an average inspiratory flow rate of 31.9 L/min. The results of the *in silico* deposition simulations are illustrated in Figure 11. For the carrier-free ($CIP_{spd}EtOH^{30}NaSt^{0.5}$) sample, the deposition in the lungs was already much more favorable

(~48%), as in the case of CIP_{sieved}+IH70. However, the *in silico* modeling also showed even higher deposition in the lungs (~55%) for the novel formulated DPI ($CIP_{spd}EtOH^{30}NaSt^{0.5}$+IH70_MgSt). To evaluate the duration of breath-holding after inhalation of the samples, regionally deposited dose fractions were also calculated for 10 s breath-hold time. Figure 11. shows that longer breath-hold time results in higher lung deposition and lower exhaled doses for all samples. This implies that the specific inhalation technique can further improve API exposure and keep exhaled API volumes to a minimum, especially for $CIP_{spd}EtOH^{30}NaSt^{0.5}$ and $CIP_{spd}EtOH^{30}NaSt^{0.5}$+IH70_MgSt samples [112].

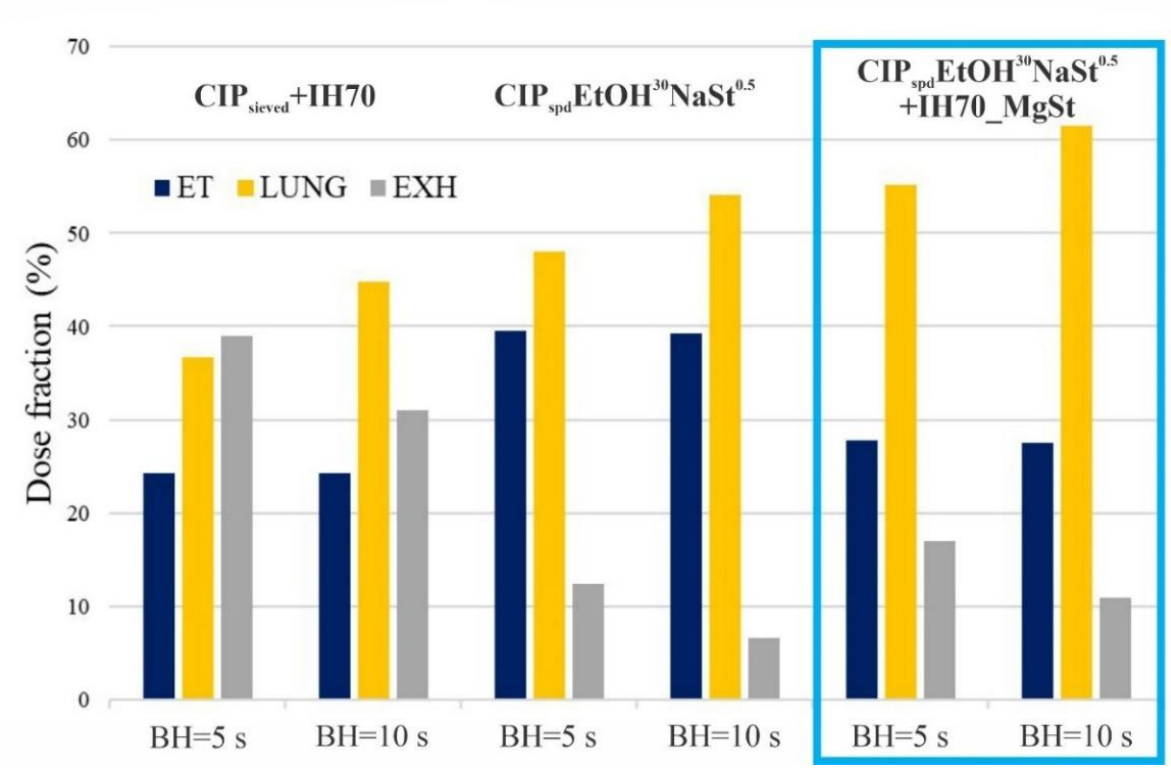

Figure 11. *Comparison of three formulation methods by in silico simulation using different breath-hold times (BHs) (ET: extrathoracic airways, LUNG: bronchial and acinar parts, EXH: exhalation fraction).*

To summarize, by combining the advantages of traditional carrier-based and carrier-free DPI improvements, the novel formulated DPI ($CIP_{spd}EtOH^{30}NaSt^{0.5}$+IH70_MgSt) was a successful development, since the cohesive-adhesive balance can be attained by particle engineering of the API and applied of excipients, and therefore has the best *in vitro* aerodynamic performance of all our developments, further confirmed by *in silico* simulation. In addition, this formulation embodies a new/third category of DPIs besides the traditional carrier-based and carrier-free formulations, which is a novelty in the literature. Moreover, *in silico* simulation has shown that the patient can further improve lung deposition results with appropriate inhalation technique [112].

5.3.2. Short-term stability results of the novel formulated DPI sample

For the three samples described in the previous section, i.e. a traditional carrier-based (CIP_{sieved}+IH70), the best *in vitro* lung deposition performance carrier-free ($CIP_{spd}EtOH^{30}NaSt^{0.5}$) and a novel formulated DPI ($CIP_{spd}EtOH^{30}NaSt^{0.5}$+IH70_MgSt), short term stability testing was performed at room temperature under the conditions detailed in section 4.2.3. As before, Coni-Snap® hard GEL capsules were also used to store these formulations. After storage, the novel formulated DPI had the best MMAD and FPF results after 1 month, followed by $CIP_{spd}EtOH^{30}NaSt^{0.5}$, and the worst results were achieved by CIP_{sieved}+IH70. This is consistent with the findings presented in section 5.3.1. Based on the results of physical studies, it can be concluded that the novel formulated DPI formulation does not show any remarkable crystal structure changes on XRPD. In terms of interparticle interactions, the W_{adh} of CIP_{sieved}+IH70 remained high during the stability study, while the W_c of $CIP_{spd}EtOH^{30}NaSt^{0.5}$ increased considerably, suggesting that the latter formulation aggregates more easily (as confirmed by SEM images, recrystallization is visible). The results show that $CIP_{spd}EtOH^{30}NaSt^{0.5}$+IH70_MgSt has better stability than the carrier-free formulation (although the used API particles were produced in the same way), so the use of a carrier surface-treated with MgSt improved not only the lung deposition results but also the stability compared to $CIP_{spd}EtOH^{30}NaSt^{0.5}$ (Table 18.) [113].

Table 18. *SEM records and in vitro aerodynamic results at 28.3 L/min flow rate of the carrier-free ($CIP_{spd}EtOH^{30}NaSt^{0.5}$) and novel formulated ($CIP_{spd}EtOH^{30}NaSt^{0.5}$+ IH70_MgSt) DPI formulations before storage and after 1-month short-term stability test.*

	$CIP_{spd}EtOH^{30}NaSt^{0.5}$		**$CIP_{spd}EtOH^{30}NaSt^{0.5}$+IH70_MgSt**	
	Before storage	1 month	Before storage	1 month
SEM	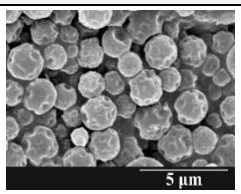	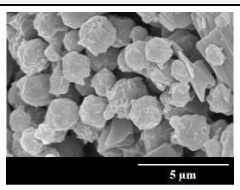	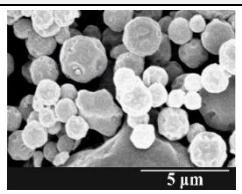	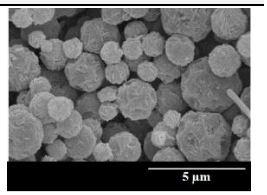
FPF (%)	54.27 ± 2.75	30.22 ± 1.82	63.75 ± 1.21	47.12 ± 0.78
MMAD (µm)	4.14 ± 0.18	6.54 ± 0.05	3.47 ± 0.02	5.47 ± 0.35
EF (%)	76.99 ± 3.32	92.32 ± 0.19	90.45 ± 1.80	89.46 ± 1.12

In silico lung modeling was performed for the novel formulated DPI, which correlated with the *in vitro* aerodynamic results. It should be highlighted that the ET dose fraction value of this sample was still below 30% after one month, while the other two samples showed worse results when freshly prepared. Finally, it can be concluded that the novel formulated DPI achieved better *in vitro-in silico* aerodynamic results than the traditional carrier-based CIP_{sieved}+IH70 and carrier-free $CIP_{spd}EtOH^{30}NaSt^{0.5}$ formulations even after 1 month of storage due to its favorable properties [113].

5.3.3. Long-term stability results of the novel formulated DPI sample in different capsule types

As a follow-up to the stability study described in section 5.3.2, and as the final step in the development of the dosage form, $CIP_{spd}EtOH^{30}NaSt^{0.5}$ and $CIP_{spd}EtOH^{30}NaSt^{0.5}$+IH70_MgSt (for further formulation designations: 1 and 2), a 6-month stability study was performed according to the ICH guideline at 40 ± 2 °C, 75 ± 5 % RH, and for all formulations also in GEL, GEL-PEG, HPMC DPI capsules to analyze the effect of DPI capsule types on their stability. The stability of the applied DPI capsules was also separately investigated under the above-mentioned conditions (Table 19., Figure 12.) [84].

Table 19. *LM recordings of different DPI capsule types during the stability test period.*

Capsule type	GEL	GEL-PEG	HPMC
LM imagines *Before storage*	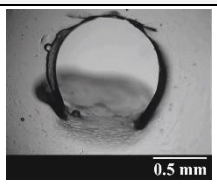	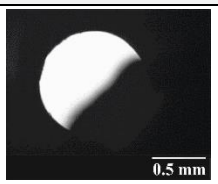	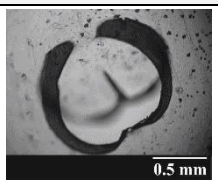
Area of capsule puncture (mm^2) *Before storage*	0.60 ± 0.28	0.54 ± 0.10	0.79 ± 0.05
LM imagines *1 month*	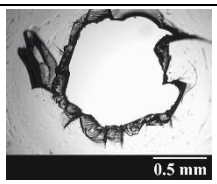	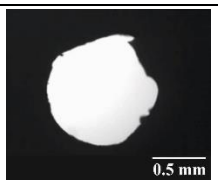	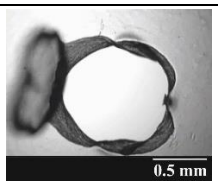
Area of capsule puncture (mm^2) *1 month*	0.74 ± 0.11	0.84 ± 0.12	0.79 ± 0.05
LM imagines *3 month*	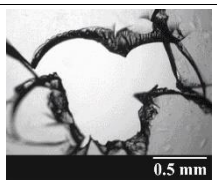	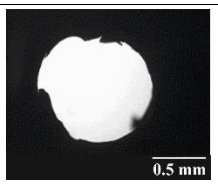	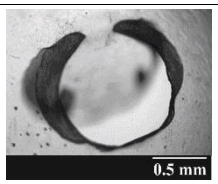
Area of capsule puncture (mm^2) *3 month*	1.01 ± 0.16	0.89 ± 0.14	0.88 ± 0.08
LM imagines *6 month*	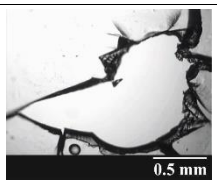	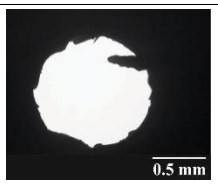	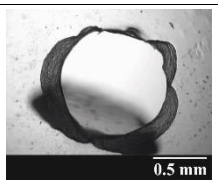
Area of capsule puncture (mm^2) 6 month	1.14 ± 0.38	0.92 ± 0.07	0.88 ± 0.03

Table 19. shows that GEL and GEL-PEG capsules started to fragment after 1 month, especially the GEL capsules, where irregularly shaped holes were formed. For HPMC capsules, no significant change in the shape of the perforated area was observed and their shape remained approximately regular even after 6 months. Capsule perforated area and the rate of fragmentation during perforation increased the most for GEL and GEL-PEG capsules during the stability study. The initial values of the perforated area for these DPI capsules increased more than one and a half times after 6 months. The increase in area was smaller for HPMC capsules. The RSC of the capsule walls was also determined after 1, 3 and 6 months of storage (Figure 12.). It can be observed that the RSC of GEL capsules fell below the optimal range (13-16%) after the first month, and the 3-month results showed that this was also the case for GEL-PEG capsules (optimal range: 10-12%), while the measured values for HPMC capsules remained within the optimal range of 3-8% after 6 months [84].

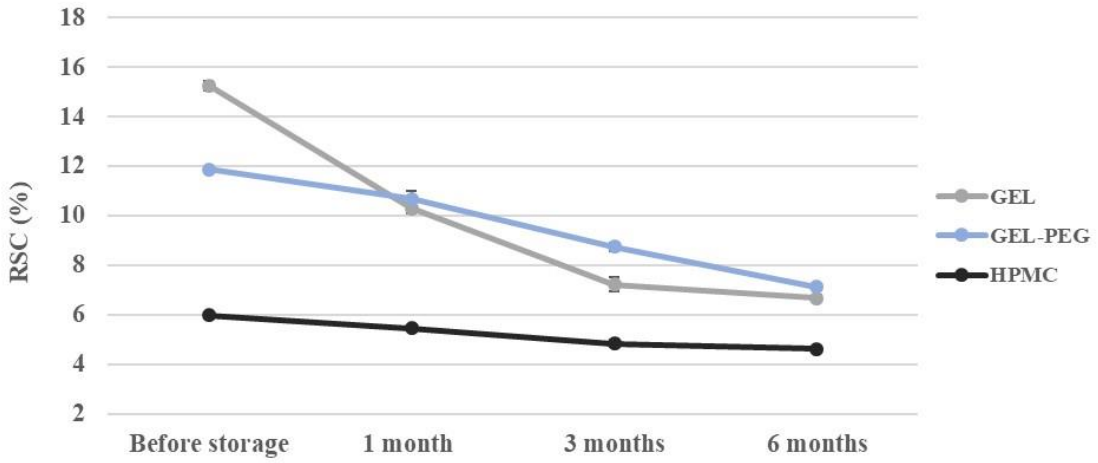

Figure 12. *RSC values of the capsule walls during the long term stability test.*

The RSC value of the samples play an important role in the stability since at increasing values, recrystallization of the amorphous drug particles and thus structural and morphological changes are expected. Furthermore, it may contribute to adverse changes in the interactions between particles and therefore affect the aerosolization and dispersion of particles and hence the lung deposition results. Based on the RSC results of the samples determined during the stability study (Figure 13.), it can be concluded that the values of formulation (1) increased more than formulation (2) in all three DPI capsules. In the latter case, the initial RSC value of around 5% corresponds to that already published for α-lactose monohydrate [134], as it is present in approximately 90% of the formulation; however, the values also reflect the effect of MgSt moisture resistance [135]. Furthermore, for both microcomposites, it was observed that the HPMC capsule had the lowest RSC value measured after 6 months, which is consistent with the values described for the capsules. It was found that the HPMC DPI capsule had the lowest decrease in RSC value during the stability test, thus less moisture could be transferred from the capsule to the DPI powders [84].

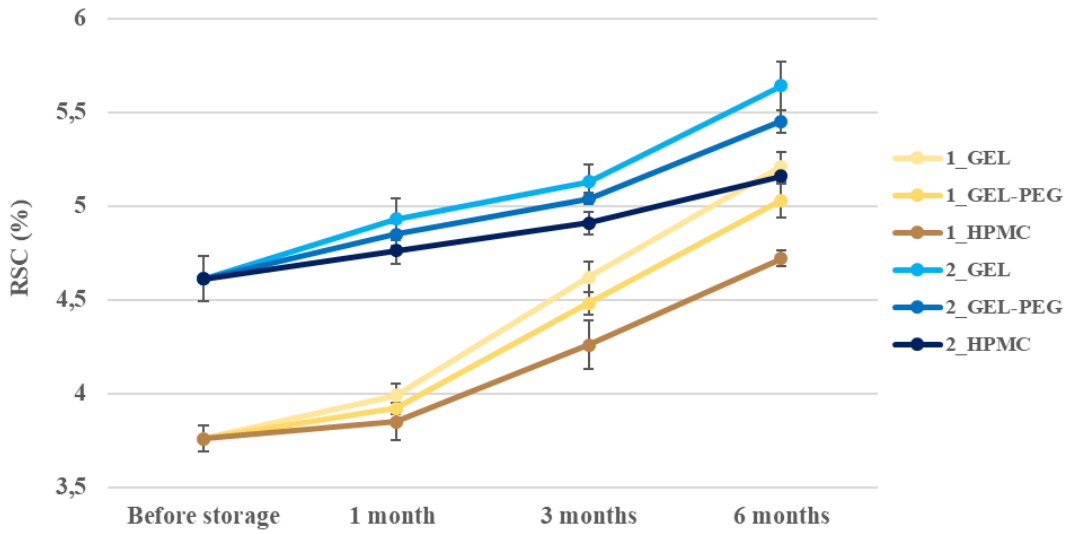

Figure 13. *RSC values of formulation (1) and (2) during the long term stability test, stored in different DPI capsule types.*

The SEM images were also correlated with the laser diffraction results. Regarding the morphology, it can be observed that there is a remarkable difference between the samples stored in different capsule types (Table 20.). In the case of $CIP_{spd}EtOH^{30}NaSt^{0.5}$ (1), recrystallization is visible in GEL capsules after 1 month, which correlates well with the results of the short-term stability study detailed in section 5.3.2. [113]. This formulation in this capsule type agglomerated most with the progress of the stability study. For the GEL-PEG capsule type, recrystallization started later, so the sample remained more stable in this one. In the HPMC capsules, the particles remained the most stable after 6 months [84].

Table 20. *SEM records and D [0.5] values of the carrier-free $CIP_{spd}EtOH^{30}NaSt^{0.5}$ formulation (1) before storage and after 6 months long-term stability test in different DPI capsule types.*

	Before storage	**6 months**		
		1_GEL	**1_GEL-PEG**	**1_HPMC**
SEM records	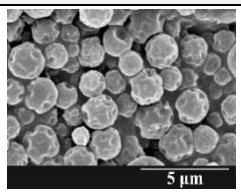	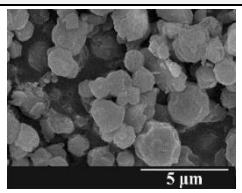	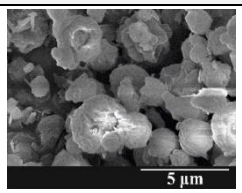	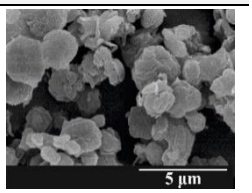
D [0.5] (µm)	2.167 ± 0.10	3.615 ± 0.17	3.452 ± 0.05	3.460 ± 0.15

For the novel formulated formulation (2), 6-months stability study demonstrated, based on morphological data and particle size analysis (Table 21.), that the composite stored in HPMC capsules remained the most stable and the least aggregated or recrystallized. For a more accurate analysis, since the samples contained formulation (1) on the IH70_MgSt surface-treated carrier particles, the values of D [0.5] were determined for both the API particles and the surface-treated carrier particles using bimodal distribution curves. Based on these results, the D [0.5] value of the API particle increased from 2.280 µm before storage to 6.129 µm in GEL capsules, 3.004 µm in PEG-GEL capsules, and 2.712 µm in HPMC capsules after 6 months. For the surface-treated

carrier, the following values were obtained after 6 months: 189.313 µm in GEL, 176.520 µm in PEG-GEL, and 171.635 µm in HPMC capsule. Thus, if we refine the values for each component, the same trends can be observed. Also shown in Table 21. are the D [0.5] values for the whole formulation (2) in the stability study [84].

Table 21. *SEM records and D [0.5] values of the novel formulated DPI $CIP_{spd}EtOH^{30}NaSt^{0.5}$+IH70_MgSt formulation (2) before storage and after 6 months long-term stability test in different DPI capsule types.*

	Before storage	**6 months**		
		2_GEL	**2_GEL-PEG**	**2_HPMC**
SEM records	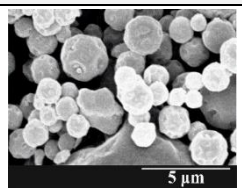	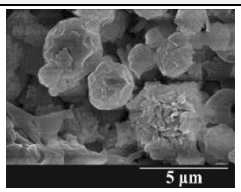	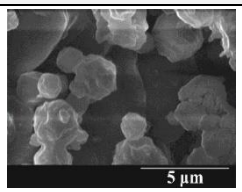	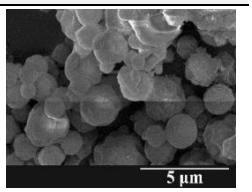
D [0.5] (µm)	130.459 ± 0.18	172.772 ± 0.36	170.503 ± 0.37	168.635 ± 0.89

Comparing formulation (1) and formulation (2) containing the same drug particles, it can be seen that the change in D [0.5] was smaller in the novel formulated DPI composite than in the carrier-free sample. The results detailed in this subsection are closely related to the changes in RSC during stability testing of DPI capsules and powders [84].

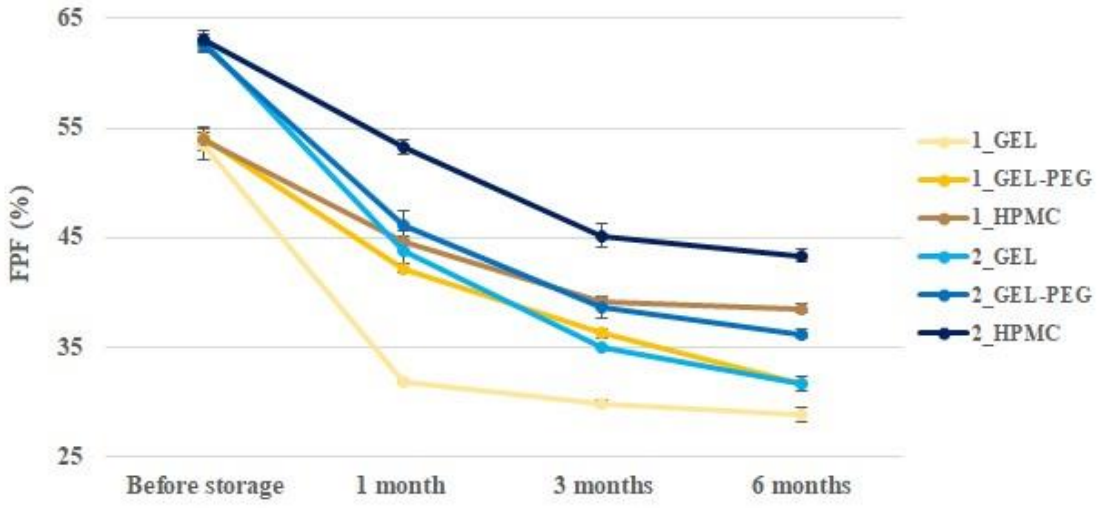

Figure 14. *FPF results at 28.3 L/min flow rate of formulation (1) and (2) during the long term stability test, stored in different DPI capsule types.*

Based on RSC, structure and particle size analysis and SEM records, the composites (1, 2) stored in HPMC capsules remained the most stable in terms of physical properties. For both formulations, *in vitro* aerodynamic studies carried out before storage show that the FPF values were not affected by the DPI capsule types, in both cases, the initial FPF values of samples 3-3 were almost identical (Figure 14.). After 6 months, for both composites tested, in GEL capsules had the lowest FPF results, followed by GEL-PEG capsules and FPF values decreased the least when formulations were stored in HPMC capsules. MMAD values at each measurement point correlated with FPF values throughout the study period. For EF, the initial values showed that in

case (1), the API was more easily swept out of the HPMC capsules, and in case (2), it was easily swept out of all capsule types due to the nature of the formulation (Table 22.). EF values were also most favorable when using HPMC capsules after 6 months, and in case (1), using only HPMC capsules, the composite met the required range of 85-115% at all measurement times [84].

Table 22. *MMAD and EF results at 28.3 L/min flow rate of formulation (1) and (2) during the long term stability test, stored in different capsule types.*

		MMAD (µm)		
Samples	**Before storage**	**1 month**	**3 months**	**6 months**
1_GEL	3.98 ± 0.15	4.43 ± 0.14	4.86 ± 0.17	5.02 ± 0.22
1_GEL-PEG	3.81 ± 0.06	4.31 ± 0.21	4.62 ± 0.15	4.93 ± 0.12
1_HPMC	3.78 ± 0.26	4.16 ± 0.14	4.32 ± 0.08	4.40 ± 0.11
2_GEL	3.51 ± 0.09	3.84 ± 0.13	3.93 ± 0.07	4.10 ± 0.16
2_GEL-PEG	3.45 ± 0.12	3.72 ± 0.05	3.87 ± 0.09	4.03 ± 0.13
2_HPMC	3.47 ± 0.08	3.68 ± 0.21	3.84 ± 0.04	3.91 ± 0.15
		EF (%)		
Samples	**Before storage**	**1 month**	**3 months**	**6 months**
1_GEL	77.04 ± 1.03	85.75 ± 0.16	86.14 ± 0.81	87.70 ± 0.64
1_GEL-PEG	72.72 ± 0.76	86.54 ± 0.54	86.85 ± 0.85	87.80 ± 0.73
1_HPMC	86.44 ± 0.99	86.96 ± 0.36	87.55 ± 0.49	90.16 ± 0.34
2_GEL	90.31 ± 0.95	91.15 ± 0.12	91.27 ± 0.36	92.89 ± 0.41
2_GEL-PEG	90.21 ± 0.83	89.75 ± 0.45	91.39 ± 0.21	92.56 ± 0.66
2_HPMC	89.55 ± 0.26	91.42 ± 0.52	94.39 ± 0.74	96.98 ± 0.63

In subsection 5.3.3, the importance of final dosage form development was demonstrated by studying the impact of DPI capsule types on the stability and aerodynamic properties of the formulations. The same composite has different stability and thus aerodynamic properties in different DPI capsule types. The RSC and LM results for DPI capsules supported the claim that GEL and GEL-PEG capsules start to break when the RSC value falls below the optimum range. Due to their fragmentation, the resulting holes became irregularly shaped and large, but the deaggregation of the particles was less efficient, which in turn reduced the FPF values. The HPMC capsules, however, retained their flexibility and after 6 months, the capsule wall fragments did not break off during punching and the holes remained regular in shape. RSC and XRPD analysis and SEM images also confirmed that the particles of DPI powders stored in GEL and GEL-PEG capsules became irregularly shaped during stability testing due to recrystallization (it is assumed that moisture was transferred to the DPI powders). The change in habit was least observed in composites stored in HPMC capsules, and therefore FPF values decreased to a lower extent. Overall, the initial, almost identical FPF values after 6 months for HPMC capsules were the most favorable for both tested DPI formulations. The results of the novel formulated DPI after stability testing were more favorable than the carrier-free composite for all DPI capsule types. Thus, it may be worthwhile to focus on the investigation of DPI formulations in different capsules for

pulmonary/DPI development, as the same formulations have different stability and thus aerodynamic properties in different DPI capsule types [84].

Nowadays, the study of the role of DPI capsules has been highly emphasized internationally, this work has highlighted the importance of this topic, which has already inspired other research groups to research and publish papers on this field [136–138]. The presented novel formulated DPI applying CIP described may represent a new option for the therapy of lung diseases (treatment of direct and indirect pathophysiological processes in the case of CF and chronic bronchitis) instead of *per os* antibiotic products.

6. SUMMARY

In summary, the following observations can be drawn in line with the objectives of the dissertation:

I. In the literature review, we found that **CF and chronic bronchitis diseases have a similar pathophysiological process**, **which can be alleviated/slowed down by antibiotic treatment, both directly and indirectly. PDD** provides the opportunity for the antibiotic administered to act locally in lung disease, thereby **achieving a smaller dose and quick effect compared to *oral* drug administration**. Several inhaled antibiotic-containing formulations are already available on the market, typically nebulizers and DPIs, but many additional inhaled antibiotic-containing DPI formulations have been published recently. **Among the four PDD implementation options, we consider the development of DPIs to be the most promising based on their specificities**, and this was the focus of the following. The effectiveness of an inhalation powder depends on several factors:

- On the one hand, it is very important to develop a **DPI formulation** with excellent physicochemical and stability properties. We have found that there is great potential in the development of both traditional carrier-based and carrier-free DPI formulations, but formulations combining the advantageous properties of these two approaches have been published previously at a rather rudimentary, testing level.
- The second factor is the properties of the **inhalers**, including their frame design – the DPI device – and the DPI capsules used, as people with lung disease may benefit from a low-resistance inhaler due to the aerosolization and deaggregation of the particles and their aerodynamic properties, and the DPI capsules marketed may also affect the properties of the particles differently, which should be tested.
- The third influencing factor is the **patient**'s compliance/adherence and specifically how the patient uses the inhalation technique.

Based on all this literature background knowledge and previous research group experience, the **development of traditional, carrier-based and carrier-free DPI formulations containing ciprofloxacin hydrochloride** (CIP) as fluoroquinolone antibiotic **was carried out**. **From these developments, the novel formulated DPI was created as the top formulation of the Ph.D. work. For this formulation, physical investigations, *in vitro - in silico* testing, stability studies, and pharmaceutical dosage form development have been performed in comparison with traditional carrier-based and carrier-free formulations. The results achieved at each stage of development are detailed in the following sections.**

II. **The traditional carrier-based DPI direction has been improved** by an innovative formulation, i.e. **the application of spd CIP on MgSt surface-treated large IH carrier** ($CIP_{spd}EtOH^{10}$+IH70_MgSt). The development resulted in better *in vitro* lung deposition results than traditional carrier-based (formulated by the commercialized formulation principle) DPIs or alone, for the spd samples used in the above formulation. This development was supported by *in vitro* APSD test results for CIP and even for another API (meloxicam potassium – MXP). In fact, in both cases, **interparticle interactions** were found to correlate the physical properties of the interactive physical mixtures with *in vitro* lung deposition outcomes.

III. As a first step in the **development of carrier-free inhalation powders**, **it was studied how changing the solvent composition in the starting solution used for spd of CIP**, specifically increasing the EtOH concentration (0-30%) in addition to distilled water, affects the habit of the samples produced and thus the *in vitro* aerodynamic results. **EtOH has a major effect on the habit of the samples** due to the different evaporation rates of water and EtOH**,** mainly on the morphological properties, which also has a considerable impact on the interparticle interactions **and the *in vitro* aerodynamic behavior**. We found that the application of **30% EtOH concentration in the starting solution gave the best results** ($CIP_{spd}EtOH^{30}$). **For the first time in the literature, the terms roughness, depth and width of the dimples for particle size values were used in relation to AFM measurements, and the relationship between the trends of W_c and MMAD/D [0.5] values was also found to be novel,** which can provide new insights to explain the inhalation behavior of the samples.

As a next step in the development of **carrier-free** formulations, **co-spd CIP formulations were prepared using different concentrations of NaSt** (0-2 %). In the sample preparations, 30% EtOH was already used in the starting solutions for spd in addition to distilled water as described above. Based on the physical and *in vitro* aerodynamic results of the samples, the **co-spd formulation containing 0.5% NaSt ($CIP_{spd}EtOH^{30}NaSt^{0.5}$) was found to be optimal**.

IV. **By combining the traditional carrier-based and carrier-free development results (points II-III), a novel formulated DPI formulation ($CIP_{spd}EtOH^{30}NaSt^{0.5}$+IH70_MgSt) was developed**, which thus contained CIP particles co-spd with NaSt (with 30% EtOH in the starting aqueous solution) on the surface of a large IH carrier, which has been surface pre-treated with MgSt. **This composite embodies a new/third category in the preparation of DPIs besides the traditional carrier-based and carrier-free formulations, which is still new in the literature.** In line with preliminary expectations, this formulation had excellent *in vitro* aerodynamic performance of all the samples presented in the Ph.D. thesis, underlining that both carrier-based and carrier-free developments are remarkable and can be considered successful developments in their own right. ***In silico*** **testing of the novel formulated DPI sample as a top formulation was also performed**, concluding that the patient can further improve lung deposition results by using the appropriate inhalation technique (10 s breath-hold time). Furthermore, **short-term room temperature stability testing** showed that after 1 month, this formulation still has favorable stability and better lung deposition results than the traditional carrier-based reference sample (CIP_{sieved}+IH70) and the carrier-free development ($CIP_{spd}EtOH^{30}NaSt^{0.5}$).

V. In the case of the **novel formulated DPI sample, a 6-month stability study was performed according to ICH guideline, testing in three different DPI capsule types**, thus developing the final dosage form of the formulation. For comparison, similar tests were also performed on the $CIP_{spd}EtOH^{30}NaSt^{0.5}$ sample. The novel formulated DPI sample also showed better lung deposition results than the carrier-free microcomposite after 6 months. Furthermore, the use of HPMC DPI capsules provided the best stability for both composites.

New findings/practical relevance of the work:

- The literature review showed that there is great potential for the development of inhalation formulations containing **antibiotics** because they **can slow down the similar pathophysiological progression in CF and chronic bronchitis in both direct and indirect ways**. Based on their advantageous specificities, we have targeted the development of DPIs for ciprofloxacin hydrochloride (CIP). **In the context of DPI systems**, it has become clear that **three pillars** (DPI formulations, DPI device and capsules, role of the patient) **need to be taken into account to maximize their effectiveness. Our development is already moving towards a therapeutic approach.**
- Within the scope of the Ph.D. work, an innovative carrier-based formulation was developed, which contains an spd CIP on the surface of a large IH carrier surface treated with MgSt by turbula mixing, whose justification for the development has been confirmed by other API (meloxicam potassium – MXP). It is a solution that goes beyond the

traditional carrier-based system and exceeds the lung deposition performance of spd API, thus **providing a stepping stone for the development of other carrier-based surface treatment solutions**. The work also highlights the **importance of studying the interparticle interactions** between carrier-API and API-API particles, both to aid development and to provide an explanation for the behavior of specific formulations during inhalation.

- For drug particles developed for PDD by spd, it has been found that the starting solvent ratios used in spd can have a remarkable impact on *in vitro* lung deposition results. In the present case, using CIP, **varying the amount of EtOH** used in addition to distilled water **in the starting solution markedly affected the habit of the prepared particles, which also influenced the *in vitro* aerodynamic properties**. **The result of our work was CIP coupled solvent composition optimization. Furthermore, the Ph.D. work highlights the role of pre-experiments with initial solvent mixtures used in spd in DPI development.**
- **During the Ph.D. work, new expressions have also been created concerning AFM measurements** (roughness, depth and width of the dimples for particle size values), **which, to our knowledge, have not yet been reported in the literature.**
- **A new correlation** has been found for CIP-containing DPI samples, **MMAD/D [0.5] ratio correlates with W_c results**, which is also not yet reported in the literature. The correlation provides an explanation for the *in vitro* lung deposition results from a novel approach.
- **In the case of CIP and MXP, the preparation of NaSt co-spd carrier-free DPI formulations was carried out for the first time on an international level and resulted in successful development.**
- **The development of a novel formulated DPI** combining carrier-based and carrier-free development results / CIP containing drug particles co-spd with NaSt (with 30% EtOH in the starting aqueous solution) on the surface of a large IH carrier surface treated with MgSt /, **will launch a new category of inhalation powders. Therefore, in the future, the effective combination of traditional carrier-based and carrier-free formulations could give a new impulse to the development of DPI systems at the international level.**
- **The development of a novel formulated DPI composite dosage form has shed light on how different DPI capsule types can affect the habit, stability and *in vitro* aerodynamic performance of the formulations.**

7. REFERENCES

1. Magramane, S.; Pápay, Z.; Turbucz, B.; Antal, I. Formulation and Characterization of Pulmonary Drug Delivery Systems. *Acta Pharmaceutica Hungarica* **2019**, *89*, 63–83, doi:10.33892/aph.2019.89.63-83.
2. Csóka, I.; Karimi, K.; Mukhtar, M.; Ambrus, R. Pulmonary Drug Delivery Systems of Antibiotics for the Treatment of Respiratory Tract Infections. *Acta Pharmaceutica Hungarica* **2019**, *89*, 43–62, doi:10.33892/aph.2019.89.43-62.
3. Labiris, N.R.; Dolovich, M.B. Pulmonary Drug Delivery. Part I: Physiological Factors Affecting Therapeutic Effectiveness of Aerosolized Medications: Physiological Factors Affecting the Effectiveness of Inhaled Drugs. *British Journal of Clinical Pharmacology* **2003**, *56*, 588–599, doi:10.1046/j.1365-2125.2003.01892.x.
4. Chaurasiya, B.; Zhao, Y.-Y. Dry Powder for Pulmonary Delivery: A Comprehensive Review. *Pharmaceutics* **2020**, *13*, 31, doi:10.3390/pharmaceutics13010031.
5. Ye, Y.; Ma, Y.; Zhu, J. The Future of Dry Powder Inhaled Therapy: Promising or Discouraging for Systemic Disorders? *International Journal of Pharmaceutics* **2022**, *614*, 121457, doi:10.1016/j.ijpharm.2022.121457.
6. Citrome, L. Aerosolised Antipsychotic Assuages Agitation: Inhaled Loxapine for Agitation Associated with Schizophrenia or Bipolar Disorder: Inhaled Loxapine for Agitation. *International Journal of Clinical Practice* **2011**, *65*, 330–340, doi:10.1111/j.1742-1241.2010.02615.x.
7. Ganderton, D.; Main, M.J.; Morgan, F.G. Compositions for Treating Parkinson's Disease 2009.
8. Momin, M.-N.; Hedayati, A.; Nokhodchi, A. Investigation into Alternative Sugars as Potential Carriers for Dry Powder Formulation of Budesonide. *BioImpacts; ISSN 2228-5660* **2011**, doi:10.5681/BI.2011.014.
9. Mukherjee, B.; Paul, P.; Dutta, L.; Chakraborty, S.; Dhara, M.; Mondal, L.; Sengupta, S. Pulmonary Administration of Biodegradable Drug Nanocarriers for More Efficacious Treatment of Fungal Infections in Lungs: Insights Based on Recent Findings. In *Multifunctional Systems for Combined Delivery, Biosensing and Diagnostics*; Elsevier, 2017; pp. 261–280 ISBN 978-0-323-52725-5.
10. Price, D.N.; Kunda, N.K.; Muttil, P. Challenges Associated with the Pulmonary Delivery of Therapeutic Dry Powders for Preclinical Testing. *KONA* **2019**, *36*, 129–144, doi:10.14356/kona.2019008.
11. Hou, S.; Wu, J.; Li, X.; Shu, H. Practical, Regulatory and Clinical Considerations for Development of Inhalation Drug Products. *Asian Journal of Pharmaceutical Sciences* **2015**, *10*, 490–500, doi:10.1016/j.ajps.2015.08.008.
12. Muralidharan, P.; Hayes, D.; Mansour, H.M. Dry Powder Inhalers in COPD, Lung Inflammation and Pulmonary Infections. *Expert Opinion on Drug Delivery* **2015**, *12*, 947–962, doi:10.1517/17425247.2015.977783.
13. Chen, Q.; Shen, Y.; Zheng, J. A Review of Cystic Fibrosis: Basic and Clinical Aspects. *Anim Models Exp Med* **2021**, *4*, 220–232, doi:10.1002/ame2.12180.
14. Wiencek, J.R.; Lo, S.F. Advances in the Diagnosis and Management of Cystic Fibrosis in the Genomic Era. *Clinical Chemistry* **2018**, *64*, 898–908, doi:10.1373/clinchem.2017.274670.
15. Weiler, C.A.; Drumm, M.L. Genetic Influences on Cystic Fibrosis Lung Disease Severity. *Front. Pharmacol.* **2013**, *4*, doi:10.3389/fphar.2013.00040.
16. Naehrig, S.; Chao, C.-M.; Naehrlich, L. Cystic Fibrosis. *Deutsches Ärzteblatt international* **2017**, doi:10.3238/arztebl.2017.0564.
17. Dickinson, K.M.; Collaco, J.M. Cystic Fibrosis. *Pediatrics In Review* **2021**, *42*, 55–67, doi:10.1542/pir.2019-0212.
18. Saint-Criq, V.; Gray, M.A. Role of CFTR in Epithelial Physiology. *Cell. Mol. Life Sci.* **2017**, *74*, 93–115, doi:10.1007/s00018-016-2391-y.
19. Mall, M.A.; Hartl, D. CFTR: Cystic Fibrosis and Beyond. *European Respiratory Journal* **2014**, *44*, 1042–1054, doi:10.1183/09031936.00228013.
20. Budai-Szűcs, M.; Berkó, S.; Kovács, A.; Jaikumpun, P.; Ambrus, R.; Halász, A.; Szabó-Révész, P.; Csányi, E.; Zsembery, Á. Rheological Effects of Hypertonic Saline and Sodium Bicarbonate Solutions on Cystic Fibrosis Sputum in Vitro. *BMC Pulm Med* **2021**, *21*, 225, doi:10.1186/s12890-021-01599-z.
21. Montgomery, S.T.; Mall, M.A.; Kicic, A.; Stick, S.M. Hypoxia and Sterile Inflammation in Cystic Fibrosis Airways: Mechanisms and Potential Therapies. *European Respiratory Journal* **2017**, *49*, 1600903, doi:10.1183/13993003.00903-2016.
22. Pezzulo, A.A.; Tang, X.X.; Hoegger, M.J.; Abou Alaiwa, M.H.; Ramachandran, S.; Moninger, T.O.; Karp, P.H.; Wohlford-Lenane, C.L.; Haagsman, H.P.; van Eijk, M.; et al. Reduced Airway Surface PH Impairs Bacterial Killing in the Porcine Cystic Fibrosis Lung. *Nature* **2012**, *487*, 109–113, doi:10.1038/nature11130.
23. Berkebile, A.R.; McCray, P.B. Effects of Airway Surface Liquid PH on Host Defense in Cystic Fibrosis. *The International Journal of Biochemistry & Cell Biology* **2014**, *52*, 124–129, doi:10.1016/j.biocel.2014.02.009.
24. Lubamba, B.; Dhooghe, B.; Noel, S.; Leal, T. Cystic Fibrosis: Insight into CFTR Pathophysiology and Pharmacotherapy. *Clinical Biochemistry* **2012**, *45*, 1132–1144, doi:10.1016/j.clinbiochem.2012.05.034.
25. Bilton, D. Cystic Fibrosis. *Medicine* **2008**, *36*, 273–278, doi:10.1016/j.mpmed.2008.03.014.
26. Turcios, N.L. Cystic Fibrosis Lung Disease: An Overview. *Respir Care* **2020**, *65*, 233–251, doi:10.4187/respcare.06697.
27. About Cystic Fibrosis | Cystic Fibrosis Foundation Available online: https://www.cff.org/intro-cf/about-cystic-fibrosis (accessed on 18 February 2023).
28. Staying Healthy Available online: https://rwjms.rutgers.edu/departments/pediatrics/divisions/cystic-fibrosis-center/staying-healthy/tips-for-staying-healthy (accessed on 19 February 2023).

29. COPD Available online: https://acil.med.harvard.edu/copd (accessed on 1 May 2021).
30. Raju, S.V.; Solomon, G.M.; Dransfield, M.T.; Rowe, S.M. Acquired Cystic Fibrosis Transmembrane Conductance Regulator Dysfunction in Chronic Bronchitis and Other Diseases of Mucus Clearance. *Clinics in Chest Medicine* **2016**, *37*, 147–158, doi:10.1016/j.ccm.2015.11.003.
31. Chronic Bronchitis Available online: https://www.ucsfhealth.org/Conditions/Chronic Bronchitis (accessed on 30 April 2023).
32. Malhotra, S.; Hayes, D.; Wozniak, D.J. Cystic Fibrosis and Pseudomonas Aeruginosa: The Host-Microbe Interface. *Clin Microbiol Rev* **2019**, *32*, e00138-18, doi:10.1128/CMR.00138-18.
33. Bouvier, N.M. Cystic Fibrosis and the War for Iron at the Host–Pathogen Battlefront. *Proc Natl Acad Sci USA* **2016**, *113*, 1480–1482, doi:10.1073/pnas.1525101113.
34. Carvalho, T.C.; McConville, J.T. The Function and Performance of Aqueous Aerosol Devices for Inhalation Therapy. *Journal of Pharmacy and Pharmacology* **2016**, *68*, 556–578, doi:10.1111/jphp.12541.
35. Zhang, W.; Xu, L.; Gao, S.; Ding, N.; Shu, P.; Wang, Z.; Li, Y. Technical Evaluation of Soft Mist Inhaler Use in Patients with Chronic Obstructive Pulmonary Disease: A Cross-Sectional Study. *COPD* **2020**, *Volume 15*, 1471–1479, doi:10.2147/COPD.S253338.
36. Iwanaga, T.; Tohda, Y.; Nakamura, S.; Suga, Y. The Respimat® Soft Mist Inhaler: Implications of Drug Delivery Characteristics for Patients. *Clin Drug Investig* **2019**, *39*, 1021–1030, doi:10.1007/s40261-019-00835-z.
37. Newman, S.P. Principles of Metered-Dose Inhaler Design. *Respir Care* **2005**, *50*, 1177–1190.
38. Ali, M. Pulmonary Drug Delivery. In *Handbook of Non-Invasive Drug Delivery Systems*; Elsevier, 2010; pp. 209–246 ISBN 978-0-8155-2025-2.
39. Party, P.; Kókai, D.; Burián, K.; Nagy, A.; Hopp, B.; Ambrus, R. Development of Extra-Fine Particles Containing Nanosized Meloxicam for Deep Pulmonary Delivery: In Vitro Aerodynamic and Cell Line Measurements. *European Journal of Pharmaceutical Sciences* **2022**, *176*, 106247, doi:10.1016/j.ejps.2022.106247.
40. Hamed, K.; Debonnett, L. Tobramycin Inhalation Powder for the Treatment of Pulmonary Pseudomonas Aeruginosa Infection in Patients with Cystic Fibrosis: A Review Based on Clinical Evidence. *Ther Adv Respir Dis* **2017**, *11*, 193–209, doi:10.1177/1753465817691239.
41. Taccetti, G.; Francalanci, M.; Pizzamiglio, G.; Messore, B.; Carnovale, V.; Cimino, G.; Cipolli, M. Cystic Fibrosis: Recent Insights into Inhaled Antibiotic Treatment and Future Perspectives. *Antibiotics* **2021**, *10*, 338, doi:10.3390/antibiotics10030338.
42. Prajapati, S.; Saha, S.; Kumar, C.D.; Sahoo, B. NEBULIZED DRUG DELIVERY: AN OVERVIEW. *IJPSR* **2019**, *10*, 3575–3582, doi:10.13040/IJPSR.0975-8232.10(8).3575-82.
43. Vazquez Espinosa, E.; Giron Moreno, R.M.; Gomez Punter, R.M.; Garcia Castillo, E.; Valenzuela, C.; Cisneros Serrano, C.; Zamora Garcia, E.; Garcia Perez, J.; Ancochea Bermudez, J. Long-Term Safety and Efficacy of Tobramycin in The Management of Cystic Fibrosis. *TCRM* **2015**, 407, doi:10.2147/TCRM.S75208.
44. University of Szeged, Interdisciplinary Centre Od Excellence, Nanotechnological Research Group: Particle Engineering for Formulation of Dry Powder Inhalation Systems Applicable in Lung Diseases Available online: http://www.med.u-szeged.hu/ice/drug-development/nanotechnology/projects/particle-engineering-dpi (accessed on 20 February 2023).
45. Benke, E.; Farkas, Á.; Balásházy, I.; Szabó-Révész, P.; Ambrus, R. Szárazporinhalációs készítmények bevitelére alkalmas eszközök és modern szerelékek aktualitásai I. *Gyógyszerészet/Pharmacy* **2018**, *62*, 131–139.
46. Benke, E.; Szabó-Révész, P.; Hopp, B.; Ambrus, R. Characterization and Development Opportunities of Carrier-Based Dry Powder Inhaler Systems. *Acta Pharmaceutica Hungarica* **2017**, *87*, 59–68.
47. Chvatal, A.; Benke, E.; Szabó-Révész, P.; Ambrus, R. New Strategies of DPI Formulations. *Gyógyszerészet/Pharmacy* **2016**, *60*, 197–206.
48. Benke, E.; Farkas, Á.; Szabó-Révész, P.; Ambrus, R. Development of an Innovative, Carrier-Based Dry Powder Inhalation Formulation Containing Spray-Dried Meloxicam Potassium to Improve the In Vitro and In Silico Aerodynamic Properties. *Pharmaceutics* **2020**, *12*, 535, doi:10.3390/pharmaceutics12060535.
49. Shetty, N.; Cipolla, D.; Park, H.; Zhou, Q.T. Physical Stability of Dry Powder Inhaler Formulations. *Expert Opinion on Drug Delivery* **2020**, *17*, 77–96, doi:10.1080/17425247.2020.1702643.
50. Costa, E.; Neves, F.; Andrade, G.; Winters, C. Scale-up & QBD Approaches for Spray-dried Inhalation Formulations. *ONdrugDelivery Magazine* **2014**, *50*, 3–8.
51. Products - MEGGLE Pharma - Excipients & Technology Available online: https://www.meggle-pharma.com/en/productConfigurator.html (accessed on 16 October 2022).
52. DFE Excipients Available online: https://dfepharma.com/excipients/ (accessed on 16 October 2022).
53. Benke, E.; Winter, C.; Szabó-Révész, P.; Roblegg, E.; Ambrus, R. The Effect of Ethanol on the Habit and in Vitro Aerodynamic Results of Dry Powder Inhalation Formulations Containing Ciprofloxacin Hydrochloride. *Asian Journal of Pharmaceutical Sciences* **2021**, *16*, 471–482, doi:10.1016/j.ajps.2021.04.003.
54. Raula, J.; Thielmann, F.; Kansikas, J.; Hietala, S.; Annala, M.; Seppälä, J.; Lähde, A.; Kauppinen, E.I. Investigations on the Humidity-Induced Transformations of Salbutamol Sulphate Particles Coated with l-Leucine. *Pharm Res* **2008**, *25*, 2250–2261, doi:10.1007/s11095-008-9613-4.

55. Alhajj, N.; O'Reilly, N.J.; Cathcart, H. Leucine as an Excipient in Spray Dried Powder for Inhalation. *Drug Discovery Today* **2021**, *26*, 2384–2396, doi:10.1016/j.drudis.2021.04.009.
56. Miranda, M.S.; Rodrigues, M.T.; Domingues, R.M.A.; Torrado, E.; Reis, R.L.; Pedrosa, J.; Gomes, M.E. Exploring Inhalable Polymeric Dry Powders for Anti-Tuberculosis Drug Delivery. *Materials Science and Engineering: C* **2018**, *93*, 1090–1103, doi:10.1016/j.msec.2018.09.004.
57. Healy, A.M.; Amaro, M.I.; Paluch, K.J.; Tajber, L. Dry Powders for Oral Inhalation Free of Lactose Carrier Particles. *Advanced Drug Delivery Reviews* **2014**, *75*, 32–52, doi:10.1016/j.addr.2014.04.005.
58. Son, Y.-J.; Miller, D.P.; Weers, J.G. Optimizing Spray-Dried Porous Particles for High Dose Delivery with a Portable Dry Powder Inhaler. *Pharmaceutics* **2021**, *13*, 1528, doi:10.3390/pharmaceutics13091528.
59. Ni, R.; Muenster, U.; Zhao, J.; Zhang, L.; Becker-Pelster, E.-M.; Rosenbruch, M.; Mao, S. Exploring Polyvinylpyrrolidone in the Engineering of Large Porous PLGA Microparticles via Single Emulsion Method with Tunable Sustained Release in the Lung: In Vitro and in Vivo Characterization. *Journal of Controlled Release* **2017**, *249*, 11–22, doi:10.1016/j.jconrel.2017.01.023.
60. Tsapis, N.; Bennett, D.; Jackson, B.; Weitz, D.A.; Edwards, D.A. Trojan Particles: Large Porous Carriers of Nanoparticles for Drug Delivery. *Proc. Natl. Acad. Sci. U.S.A.* **2002**, *99*, 12001–12005, doi:10.1073/pnas.182233999.
61. Eslamian, M.; Ashgriz, N. Effect of Atomization Method on the Morphology of Spray-Generated Particles. *Journal of Engineering Materials and Technology* **2007**, *129*, 130–142, doi:10.1115/1.2400270.
62. Cui, Y.; Zhang, X.; Wang, W.; Huang, Z.; Zhao, Z.; Wang, G.; Cai, S.; Jing, H.; Huang, Y.; Pan, X.; et al. Moisture-Resistant Co-Spray-Dried Netilmicin with l-Leucine as Dry Powder Inhalation for the Treatment of Respiratory Infections. *Pharmaceutics* **2018**, *10*, 252, doi:10.3390/pharmaceutics10040252.
63. Karimi, K.; Pallagi, E.; Szabó-Révész, P.; Csóka, I.; Ambrus, R. Development of a Microparticle-Based Dry Powder Inhalation Formulation of Ciprofloxacin Hydrochloride Applying the Quality by Design Approach. *Drug Design, Development and Therapy* **2016**, *10*, 3331–3343, doi:10.2147/DDDT.S116443.
64. Shetty, N.; Zeng, L.; Mangal, S.; Nie, H.; Rowles, M.R.; Guo, R.; Han, Y.; Park, J.H.; Zhou, Q. Effects of Moisture-Induced Crystallization on the Aerosol Performance of Spray Dried Amorphous Ciprofloxacin Powder Formulations. *Pharmaceutical Research* **2018**, *35*, doi:10.1007/s11095-017-2281-5.
65. Yang, X.-F.; Xu, Y.; Qu, D.-S.; Zhu, J.; Li, H.-Y. Excipient-Free, Spray-Dried Powders for Pulmonary Aztreonam Delivery. *Journal of Drug Delivery Science and Technology* **2015**, *28*, 7–10, doi:10.1016/j.jddst.2015.04.005.
66. Adi, H.; Young, P.M.; Chan, H.-K.; Stewart, P.; Agus, H.; Traini, D. Cospray Dried Antibiotics for Dry Powder Lung Delivery. *Journal of Pharmaceutical Sciences* **2008**, *97*, 3356–3366, doi:10.1002/jps.21239.
67. Pilcer, G.; Sebti, T.; Amighi, K. Formulation and Characterization of Lipid-Coated Tobramycin Particles for Dry Powder Inhalation. *Pharm Res* **2006**, *23*, 931–940, doi:10.1007/s11095-006-9789-4.
68. Aquino, R.P.; Prota, L.; Auriemma, G.; Santoro, A.; Mencherini, T.; Colombo, G.; Russo, P. Dry Powder Inhalers of Gentamicin and Leucine: Formulation Parameters, Aerosol Performance and in Vitro Toxicity on CuFi1 Cells. *International Journal of Pharmaceutics* **2012**, *426*, 100–107, doi:10.1016/j.ijpharm.2012.01.026.
69. Yu, H.; Teo, J.; Chew, J.W.; Hadinoto, K. Dry Powder Inhaler Formulation of High-Payload Antibiotic Nanoparticle Complex Intended for Bronchiectasis Therapy: Spray Drying versus Spray Freeze Drying Preparation. *International Journal of Pharmaceutics* **2016**, *499*, 38–46, doi:10.1016/j.ijpharm.2015.12.072.
70. Du, J.; El-Sherbiny, I.M.; Smyth, H.D. Swellable Ciprofloxacin-Loaded Nano-in-Micro Hydrogel Particles for Local Lung Drug Delivery. *AAPS PharmSciTech* **2014**, *15*, 1535–1544, doi:10.1208/s12249-014-0176-x.
71. Ungaro, F.; d'Angelo, I.; Coletta, C.; d'Emmanuele di Villa Bianca, R.; Sorrentino, R.; Perfetto, B.; Tufano, M.A.; Miro, A.; La Rotonda, M.I.; Quaglia, F. Dry Powders Based on PLGA Nanoparticles for Pulmonary Delivery of Antibiotics: Modulation of Encapsulation Efficiency, Release Rate and Lung Deposition Pattern by Hydrophilic Polymers. *Journal of Controlled Release* **2012**, *157*, 149–159, doi:10.1016/j.jconrel.2011.08.010.
72. Garcia-Contreras, L.; Fiegel, J.; Telko, M.J.; Elbert, K.; Hawi, A.; Thomas, M.; VerBerkmoes, J.; Germishuizen, W.A.; Fourie, P.B.; Hickey, A.J.; et al. Inhaled Large Porous Particles of Capreomycin for Treatment of Tuberculosis in a Guinea Pig Model. *Antimicrob Agents Chemother* **2007**, *51*, 2830–2836, doi:10.1128/AAC.01164-06.
73. Weers, J. Comparison of Phospholipid-Based Particles for Sustained Release of Ciprofloxacin Following Pulmonary Administration to Bronchiectasis Patients. *Pulm Ther* **2019**, *5*, 127–150, doi:10.1007/s41030-019-00104-6.
74. Geller, D.E.; Weers, J.; Heuerding, S. Development of an Inhaled Dry-Powder Formulation of Tobramycin Using PulmoSphere™ Technology. *Journal of Aerosol Medicine and Pulmonary Drug Delivery* **2011**, *24*, 175–182, doi:10.1089/jamp.2010.0855.
75. Smith, D.J.; Gambone, L.M.; Tarara, T.; Meays, D.R.; Dellamary, L.A.; Woods, C.M.; Weers, J. Liquid Dose Pulmonary Instillation of Gentamicin PulmoSpheres Formulations: Tissue Distribution and Pharmacokinetics in Rabbits. *Pharmaceutical Research* **2001**, *18*, 1556–1561, doi:10.1023/A:1013078330485.
76. Eedara, B.B.; Rangnekar, B.; Doyle, C.; Cavallaro, A.; Das, S.C. The Influence of Surface Active L-Leucine and 1,2-Dipalmitoyl-Sn-Glycero-3-Phosphatidylcholine (DPPC) in the Improvement of Aerosolization of Pyrazinamide and Moxifloxacin Co-Spray Dried Powders. *International Journal of Pharmaceutics* **2018**, *542*, 72–81, doi:10.1016/j.ijpharm.2018.03.005.

77. Sung, J.C.; Padilla, D.J.; Garcia-Contreras, L.; VerBerkmoes, J.L.; Durbin, D.; Peloquin, C.A.; Elbert, K.J.; Hickey, A.J.; Edwards, D.A. Formulation and Pharmacokinetics of Self-Assembled Rifampicin Nanoparticle Systems for Pulmonary Delivery. *Pharm Res* **2009**, *26*, 1847–1855, doi:10.1007/s11095-009-9894-2.
78. Adi, H.; Traini, D.; Chan, H.-K.; Young, P.M. The Influence of Drug Morphology on Aerosolisation Efficiency of Dry Powder Inhaler Formulations. *Journal of Pharmaceutical Sciences* **2008**, *97*, 2780–2788, doi:10.1002/jps.21195.
79. Hazare, S.; Menon, M. Improvement of Inhalation Profile of DPI Formulations by Carrier Treatment with Magnesium Stearate. *Indian J Pharm Sci* **2009**, *71*, 725–727.
80. Faulhammer, E.; Zellnitz, S.; Wutscher, T.; Stranzinger, S.; Zimmer, A.; Paudel, A. Performance Indicators for Carrier-Based DPIs: Carrier Surface Properties for Capsule Filling and API Properties for in Vitro Aerosolisation. *International Journal of Pharmaceutics* **2018**, *536*, 326–335, doi:10.1016/j.ijpharm.2017.12.004.
81. Mönckedieck, M.; Kamplade, J.; Fakner, P.; Urbanetz, N.A.; Walzel, P.; Steckel, H.; Scherließ, R. Dry Powder Inhaler Performance of Spray Dried Mannitol with Tailored Surface Morphologies as Carrier and Salbutamol Sulphate. *International Journal of Pharmaceutics* **2017**, *524*, 351–363, doi:10.1016/j.ijpharm.2017.03.055.
82. Dal Negro, R.W. Dry Powder Inhalers and the Right Things to Remember: A Concept Review. *Multidisciplinary Respiratory Medicine* **2015**, *10*, 13, doi:10.1186/s40248-015-0012-5.
83. Benke E.; Hopp B.; Farkas Á.; Balásházy I.; Szabóné Révész P.; Ambrus R. Szárazporinhalációs készítmények bevitelére alkalmas eszközök és modern szerelékek aktualitásai II. *Gyógyszerészet* **2018**, *62*, 195–201.
84. Benke, E.; Varga, P.; Szabó-Révész, P.; Ambrus, R. Stability and In Vitro Aerodynamic Studies of Inhalation Powders Containing Ciprofloxacin Hydrochloride Applying Different DPI Capsule Types. *Pharmaceutics* **2021**, *13*, 689, doi:10.3390/pharmaceutics13050689.
85. Wauthoz, N.; Hennia, I.; Ecenarro, S.; Amighi, K. Impact of Capsule Type on Aerodynamic Performance of Inhalation Products: A Case Study Using a Formoterol-Lactose Binary or Ternary Blend. *International Journal of Pharmaceutics* **2018**, *553*, 47–56, doi:10.1016/j.ijpharm.2018.10.034.
86. Farkas, Á.; Tomisa, G.; Kugler, S.; Nagy, A.; Vaskó, A.; Kis, E.; Szénási, G.; Gálffy, G.; Horváth, A. The Effect of Exhalation before the Inhalation of Dry Powder Aerosol Drugs on the Breathing Parameters, Emitted Doses and Aerosol Size Distributions. *International Journal of Pharmaceutics: X* **2023**, *5*, 100167, doi:10.1016/j.ijpx.2023.100167.
87. Stockmann, C.; Sherwin, C.M.T.; Zobell, J.T.; Young, D.C.; Waters, C.D.; Spigarelli, M.G.; Ampofo, K. Optimization of Anti-pseudomonal Antibiotics for Cystic Fibrosis Pulmonary Exacerbations: III. Fluoroquinolones. *Pediatric Pulmonology* **2012**, *48*, 211–220, doi:10.1002/ppul.22667.
88. Elborn, J.S. Ciprofloxacin Dry Powder Inhaler in Cystic Fibrosis. *BMJ Open Respiratory Research* **2016**, *3*, 1–2, doi:10.1136/bmjresp-2015-000125.
89. Bosso, J.A. Use of Ciprofloxacin in Cystic Fibrosis Patients. *The American Journal of Medicine* **1989**, *87*, S123–S127, doi:10.1016/0002-9343(89)90040-5.
90. Akdag Cayli, Y.; Sahin, S.; Buttini, F.; Balducci, A.G.; Montanari, S.; Vural, I.; Oner, L. Dry Powders for the Inhalation of Ciprofloxacin or Levofloxacin Combined with a Mucolytic Agent for Cystic Fibrosis Patients. *Drug Development and Industrial Pharmacy* **2017**, *43*, 1378–1389, doi:10.1080/03639045.2017.1318902.
91. Razuc, M.; Piña, J.; Ramírez-Rigo, M.V. Optimization of Ciprofloxacin Hydrochloride Spray-Dried Microparticles for Pulmonary Delivery Using Design of Experiments. *AAPS PharmSciTech* **2018**, *19*, 3085–3096, doi:10.1208/s12249-018-1137-6.
92. Shrinivas, S.; Revanasiddappa, M. Analytical Stability Indicative Method Development and Validation by High Pressure Liquid Chromatography for Assay in Ciprofloxacin Hydrochloride Drug Substances. *AJAC* **2015**, *06*, 719–730, doi:10.4236/ajac.2015.69069.
93. PubChem Ciprofloxacin Hydrochloride Available online: https://pubchem.ncbi.nlm.nih.gov/compound/62999 (accessed on 16 October 2022).
94. Hamishehkar, H.; Rahimpour, Y.; Javadzadeh, Y. The Role of Carrier in Dry Powder Inhaler. In *Recent Advances in Novel Drug Carrier Systems*; Sezer, A.D., Ed.; InTech, 2012 ISBN 978-953-51-0810-8.
95. Hebbink, G.A.; Jaspers, M.; Peters, H.J.W.; Dickhoff, B.H.J. Recent Developments in Lactose Blend Formulations for Carrier-Based Dry Powder Inhalation. *Advanced Drug Delivery Reviews* **2022**, *189*, 114527, doi:10.1016/j.addr.2022.114527.
96. Wu, L.; Miao, X.; Shan, Z.; Huang, Y.; Li, L.; Pan, X.; Yao, Q.; Li, G.; Wu, C. Studies on the Spray Dried Lactose as Carrier for Dry Powder Inhalation. *Asian Journal of Pharmaceutical Sciences* **2014**, *9*, 336–341, doi:10.1016/j.ajps.2014.07.006.
97. Pilcer, G.; Wauthoz, N.; Amighi, K. Lactose Characteristics and the Generation of the Aerosol. *Advanced Drug Delivery Reviews* **2012**, *64*, 233–256, doi:10.1016/j.addr.2011.05.003.
98. Plastira, M. The Influence of Magnesium Stearate and Carrier Surface on the Deposition Performace of Carrier Based Dry Powder Inhaler Formulations.; 2008.
99. Islam, N.; Rashid, A.; Camm, G. Effects of Magnesium Stearate on the Efficient Dispersion of Salbutamol Sulphate from Carrier-Based Dry Powder Inhaler Formulations. In *Proceedings of RDD Europe 2011, Volume II*; Dalby, R.N., Byron, P.R., Suman, J.D., Young, P.M., Peart J, J., Eds.; Respiratory Drug Delivery (RDD) Online / Virginia Commonwealth University: United States, 2011; pp. 415–418 ISBN 978-1-933722-51-1.

100. Mehta, P. Imagine the Superiority of Dry Powder Inhalers from Carrier Engineering. *Journal of Drug Delivery* **2018**, *2018*, 1–19, doi:10.1155/2018/5635010.
101. Gyógyszerkereső Available online: https://www.pharmindex-online.hu/gyogyszerkereso/kereses (accessed on 30 March 2019).
102. Frank Alkanes India Pvt Ltd Available online: https://www.frankalkanes.com/frank-sodium-stearate.php (accessed on 16 October 2022).
103. Zhu, B.; Haghi, M.; Nguyen, A.; Goud, M.; Yeung, S.; Young, P.M.; Traini, D. Delivery of Theophylline as Dry Powder for Inhalation. *Asian Journal of Pharmaceutical Sciences* **2015**, *10*, 520–527, doi:10.1016/j.ajps.2015.08.005.
104. Parlati, C.; Colombo, P.; Buttini, F.; Young, P.M.; Adi, H.; Ammit, A.J.; Traini, D. Pulmonary Spray Dried Powders of Tobramycin Containing Sodium Stearate to Improve Aerosolization Efficiency. *Pharmaceutical Research* **2009**, *26*, 1084–1092, doi:10.1007/s11095-009-9825-2.
105. ICH Q3C (R6) Residual Solvents. European Medicines Agency 2018. Available online: https://www.ich.org/page/quality-guidelines#3-3 (accessed on 28 March 2021).
106. Spray Process - Buchi B-191 Manual [Page 14] Available online: https://www.manualslib.com/manual/1608571/Buchi-B-191.html (accessed on 16 October 2022).
107. Ji, S.; Thulstrup, P.W.; Mu, H.; Hansen, S.H.; van de Weert, M.; Rantanen, J.; Yang, M. Effect of Ethanol as a Co-Solvent on the Aerosol Performance and Stability of Spray-Dried Lysozyme. *International Journal of Pharmaceutics* **2016**, *513*, 175–182, doi:10.1016/j.ijpharm.2016.09.025.
108. Boraey, M.A.; Hoe, S.; Sharif, H.; Miller, D.P.; Lechuga-Ballesteros, D.; Vehring, R. Improvement of the Dispersibility of Spray-Dried Budesonide Powders Using Leucine in an Ethanol–Water Cosolvent System. *Powder Technology* **2013**, *236*, 171–178, doi:10.1016/j.powtec.2012.02.047.
109. Yang, J.-J.; Liu, C.-Y.; Quan, L.-H.; Liao, Y.-H. Preparation and In Vitro Aerosol Performance of Spray-Dried Shuang-Huang-Lian Corrugated Particles in Carrier-Based Dry Powder Inhalers. *AAPS PharmSciTech* **2012**, *13*, 816–825, doi:10.1208/s12249-012-9806-3.
110. Buttini, F.; Cuoghi, E.; Miozzi, M.; Rossi, A.; Sonvico, F.; Colombo, P. Insulin Spray-Dried Powder and Smoothed Lactose: A New Formulation Strategy for Nasal and Pulmonary Delivery Available online: https://www.researchgate.net/publication/284045495_Insulin_spray-dried_powder_and_smoothed_lactose_a_new_formulation_strategy_for_nasal_and_pulmonary_delivery (accessed on 11 April 2018).
111. Benke, E.; Szabó-Révész, P.; Ambrus, R. Development of Ciprofloxacin Hydrochloride Containing Dry Powder Inhalation System with an Innovative Technology. *Acta Pharmaceutica Hungarica* **2017**, *87*, 49–58.
112. Ambrus, R.; Benke, E.; Farkas, Á.; Balásházy, I.; Szabó-Révész, P. Novel Dry Powder Inhaler Formulation Containing Antibiotic Using Combined Technology to Improve Aerodynamic Properties. *Eur J Pharm Sci.* **2018**, *123*, 20–27, doi:10.1016/j.ejps.2018.07.030.
113. Benke, E.; Farkas, Á.; Balásházy, I.; Szabó-Révész, P.; Ambrus, R. Stability Test of Novel Combined Formulated Dry Powder Inhalation System Containing Antibiotic: Physical Characterization and *in Vitro – in Silico* Lung Deposition Results. *Drug Development and Industrial Pharmacy* **2019**, *45*, 1369–1378, doi:10.1080/03639045.2019.1620268.
114. Cocconi, D.; Alberi, M.D.; Busca, A.; Schiaretti, F. Use of Magnesium Stearate in Dry Powder Formulations for Inhalation 2012, US20120082727A1.
115. *Pharmaceutical Inhalation Aerosol Technology*; Hickey, A.J., Rocha, S.R.P. da, Eds.; Drugs and the pharmaceutical sciences; Third edition.; CRC Press, Taylor & Francis Group: Boca Raton, 2019; ISBN 978-1-138-06307-5.
116. Kaialy, W.; Nokhodchi, A. Engineered Mannitol Ternary Additives Improve Dispersion of Lactose–Salbutamol Sulphate Dry Powder Inhalations. *AAPS J* **2013**, *15*, 728–743, doi:10.1208/s12248-013-9476-4.
117. Schuster, J.M.; Schvezov, C.E.; Rosenberger, M.R. Analysis of the Results of Surface Free Energy Measurement of Ti6Al4V by Different Methods. *Procedia Materials Science* **2015**, *8*, 732–741, doi:10.1016/j.mspro.2015.04.130.
118. Farkas, B.; Révész, P. *Kristályosítástól a tablettázásig*; Universitas Szeged, 2007; ISBN 9630619141.
119. Tüske, Z. Influence of the Surface Free Energy on the Parameters of Pellets.; 2005.
120. Inhaler Testing Brochure 2021 Available online: https://www.copleyscientific.com/downloads/inhaler-testing-brochure-2021/ (accessed on 18 March 2021).
121. Li, X.; Vogt, F.G.; Hayes, D.; Mansour, H.M. Physicochemical Characterization and Aerosol Dispersion Performance of Organic Solution Advanced Spray-Dried Microparticulate/Nanoparticulate Antibiotic Dry Powders of Tobramycin and Azithromycin for Pulmonary Inhalation Aerosol Delivery. *European Journal of Pharmaceutical Sciences* **2014**, *52*, 191–205, doi:10.1016/j.ejps.2013.10.016.
122. Laube, B.L.; Janssens, H.M.; de Jongh, F.H.C.; Devadason, S.G.; Dhand, R.; Diot, P.; Everard, M.L.; Horvath, I.; Navalesi, P.; Voshaar, T.; et al. What the Pulmonary Specialist Should Know about the New Inhalation Therapies. *European Respiratory Journal* **2011**, *37*, 1308–1417, doi:10.1183/09031936.00166410.
123. Koblinger, L.; Hofmann, W. Monte Carlo Modeling of Aerosol Deposition in Human Lungs. Part I: Simulation of Particle Transport in a Stochastic Lung Structure. *Journal of Aerosol Science* **1990**, *21*, 661–674, doi:10.1016/0021-8502(90)90121-D.

124. Cheng, Y.S. Aerosol Deposition in the Extrathoracic Region. *Aerosol Science and Technology* **2003**, *37*, 659–671, doi:10.1080/02786820300906.
125. Otto G., R.; Yeh, H.; Schum, G.M.; Phalen, R.F. Tracheobronchial Geometry: Human, Dog, Rat, Hamster - A Compilation of Selected Data from the Project Respiratory Tract Deposition Models. *U.S. Government Printing Office* **1976**.
126. Haefeli-Bleuer, B.; Weibel, E.R. Morphometry of the Human Pulmonary Acinus. *The Anatomical Record* **1988**, *220*, 401–414, doi:10.1002/ar.1092200410.
127. Colthorpe, P.; Voshaar, T.; Kieckbusch, T.; Cuoghi, E.; Jauernig, J. Delivery Characteristics of a Low-Resistance Dry-Powder Inhaler Used to Deliver the Long-Acting Muscarinic Antagonist Glycopyrronium. *Journal of Drug Assessment* **2013**, *2*, 11–16, doi:10.3109/21556660.2013.766197.
128. Social Science Statistic Online: Available online: https://www.socscistatistics.com/tests/studentttest/default2.aspx (accessed on 6 April 2020).
129. Lechanteur, A.; Evrard, B. Influence of Composition and Spray-Drying Process Parameters on Carrier-Free DPI Properties and Behaviors in the Lung: A Review. *Pharmaceutics* **2020**, *12*, 55, doi:10.3390/pharmaceutics12010055.
130. Belotti, S.; Rossi, A.; Colombo, P.; Bettini, R.; Rekkas, D.; Politis, S.; Colombo, G.; Balducci, A.G.; Buttini, F. Spray-Dried Amikacin Sulphate Powder for Inhalation in Cystic Fibrosis Patients: The Role of Ethanol in Particle Formation. *European Journal of Pharmaceutics and Biopharmaceutics* **2015**, *93*, 165–172, doi:10.1016/j.ejpb.2015.03.023.
131. *Inhalation Drug Delivery: Techniques and Products*; Colombo, P., Traini, D., Buttini, F., Eds.; John Wiley & Sons, Ltd: Chichester, UK, 2013; ISBN 978-1-118-39714-5.
132. Lewis, D.; Rouse, T.; Singh, D.; Edge, S. Defining the 'Dose' for Dry Powder Inhalers: The Challenge of Correlating In-Vitro Dose Delivery Results with Clinical Efficacy. *Am. Pharm. Rev.* **2017**, *20*, 54–62.
133. Benke, E.; Szabó-Révész, P.; Ambrus, R. Development of Meloxicam Potassium-Containing Co-Spray-Dried Inhalation Powder with Sodium Stearate. *Acta Pharmaceutica Hungarica* **2021**, *91*, 75–82, doi:10.33892/aph.2021.91.75-82.
134. Hohenheim, U. Determination of water content in lactose by Karl Fischer titration - Interlaboratory collaborative study Available online: https://www.uni-hohenheim.de/organisation/publikation/determination-of-water-content-in-lactose-by-karl-fischer-titration-interlaboratory-collaborative-study (accessed on 18 March 2021).
135. Guchardi, R.; Frei, M.; John, E.; Kaerger, J. Influence of Fine Lactose and Magnesium Stearate on Low Dose Dry Powder Inhaler Formulations. *International Journal of Pharmaceutics* **2008**, *348*, 10–17, doi:10.1016/j.ijpharm.2007.06.041.
136. Ding, L.; Brunaugh, A.D.; Stegemann, S.; Jermain, S.V.; Herpin, M.J.; Kalafat, J.; Smyth, H.D.C. A Quality by Design Framework for Capsule-Based Dry Powder Inhalers. *Pharmaceutics* **2021**, *13*, 1213, doi:10.3390/pharmaceutics13081213.
137. Buttini, F.; Quarta, E.; Allegrini, C.; Lavorini, F. Understanding the Importance of Capsules in Dry Powder Inhalers. *Pharmaceutics* **2021**, *13*, 1936, doi:10.3390/pharmaceutics13111936.
138. Ramezani Kalmer, R.; Karimi, A.; Golizadeh, M.; Mohammadi Haddadan, M.; Azizi, M.; Ramezanalizadeh, H.; Ghanbari, M. Effect of Different Molecular Weights of Polyethylene Glycol as a Plasticizer on the Formulation of Dry Powder Inhaler Capsules: Investigation of Puncturing Size, Morphologies, and Surface Properties. *Arabian Journal of Chemistry* **2022**, *15*, 104239, doi:10.1016/j.arabjc.2022.104239.

ACKNOWLEDGEMENTS

I am grateful to my supervisor ***Dr. habil. Rita Ambrus*** for her scientific guidance, encouragement and support throughout my Ph.D. studies. I especially want to thank ***Prof. Dr. Piroska Szabó-Révész,*** who also provided me with a lot of professional guidance. I am also thankful to ***Prof. Dr. Ildikó Csóka*** for ensuring the conditions for me to work as a Ph. D. student at the Institute of Pharmaceutical Technology and Regulatory Affairs, University of Szeged. Special acknowledgements to ***Dr. Patrícia Varga*** for her contribution. I would like to thank ***Erika Feczkóné Boda, Piroska Ágnes Lakatos-Fekete*** for excellent technical assistance and to all the members of the Institute of Pharmaceutical Technology and Regulatory Affairs for their support and kindness.

I am indebted to my co-authors for their scientific support during my Ph.D. studies:

- ***Dr. Árpád Farkas Ph.D.*** – Centre for Energy Research Hungarian Academy of Sciences, Budapest (Hungary)
- ***Dr. Christina Winter Ph.D.*** *and* ***Prof. Dr. Eva Roblegg*** – Institute of Pharmaceutical Sciences, Pharmaceutical Technology and Biopharmacy, University of Graz, Graz (Austria); Research Center Pharmaceutical Engineering GmbH, Graz (Austria)

This work was supported by:

- *UNKP-16-2-SZTE: New National Excellence Program of the Ministry of Human Capacities*
- *UNKP-17-4-SZTE: New National Excellence Program of the Ministry of Human Capacities*
- *UNKP-18-3-SZTE New National Excellence Program of the Ministry of Human Capacities*
- *UNKP-19–3-SZTE New National Excellence Program of the Ministry for Innovation and Technology*
- *UNKP-20-3-SZTE New National Excellence Program of the Ministry for Innovation and Technology*
- *EFOP-3.6.2-16-2017-00006 'LIVE LONGER—Development of Modern Medical Diagnostic Procedures and Therapies in a Translational Approach: from a Laboratory to a Patient Bed' project*
- *EFOP 3.6.3- VEKOP-16-2017-00009 project*
- *The Ministry of Human Capacities, Hungary grant 20391-3/2018/FEKUSTRAT*
- *CEEPUS CIII-RS-1113 short-term student mobility scholarship at the University of Graz, Austria*
- *University of Szeged Open Access Fund grant*
- *Gedeon Richter's Centenary Foundation*
- *TUDFO/47138-1/2019-ITM*
- *SimInhale COST Action MP1404*

I am grateful to **my parents** and **my friends** for their love, support and understanding throughout my Ph.D. studies.

ANNEXES

I.) **Benke E.**, Szabóné Révész P., Hopp B., Ambrus R.: Hordozó alapú száraz porinhalációs rendszerek jellemzése és fejlesztési lehetőségei. Acta Pharmaceutica Hungarica, 87, 59-68 (2017).

II.) **Benke, E.**, Szabóné Révész, P., Ambrus, R.: Innovatív technológiájú ciprofloxacin-hidroklorid tartalmú száraz porinhalációs rendszer fejlesztése. Acta Pharmaceutica Hungarica, 87, 49-58 (2017).

III.) **Benke, E.**, Farkas, Á., Balásházy, I., Szabó-Révész, P., Ambrus, R.: Szárazporinhalációs készítmények bevitelére alkalmas eszközök és modern szerelékek aktualitásai I. Gyógyszerészet/Pharmacy, 62, 131-139 (2018).

IV.) **Benke, E.**, Hopp, B., Farkas, Á., Balásházy, I., Szabó-Révész, P., Ambrus, R.: Szárazporinhalációs készítmények bevitelére alkalmas eszközök és modern szerelékek aktualitásai II. Gyógyszerészet/Pharmacy, 62, 195-201 (2018).

V.) R. Ambrus, **E. Benke**, Á. Farkas, I. Balásházy, P. Szabó-Révész: Novel dry powder inhaler formulation containing antibiotic using combined technology to improve aerodynamic properties, European Journal of Pharmaceutical Sciences, 123, 20-27 (2018). (https://doi.org/10.1016/j.ejps.2018.07.030)

VI.) **E. Benke**, Á. Farkas, I. Balásházy, P. Szabó-Révész, R. Ambrus: Stability test of novel combined formulated dry powder inhalation system containing antibiotic: Physical characterization and *in vitro-in silico* lung deposition results, Drug Development and Industrial Pharmacy, 45, 1369-1378 (2019). (https://doi.org/10.1080/03639045.2019.1620268)

VII.) **E. Benke**, Á. Farkas, P. Szabó-Révész, R. Ambrus: Development of an Innovative, Carrier-Based Dry Powder Inhalation Formulation Containing Spray-Dried Meloxicam Potassium to Improve the *In Vitro* and *In Silico* Aerodynamic Properties. Pharmaceutics, 12, 535 (2020). (https://doi.org/10.3390/pharmaceutics12060535)

VIII.) **E. Benke**, P. Varga, P. Szabó-Révész, R. Ambrus: Stability and *in vitro* aerodynamic studies of inhalation powders containing ciprofloxacin hydrochloride applying different DPI capsule types. Pharmaceutics, 13, 689 (2021).

IX.) **E. Benke**, C. Winter, P. Szabó-Révész, E. Roblegg, R. Ambrus: The effect of ethanol on the habit and *in vitro* aerodynamic results of dry powder inhalation formulations containing ciprofloxacin hydrochloride. Asian Journal of Pharmaceutical Sciences, 16, 471-482 (2021). (https://doi.org/10.1016/j.ajps.2021.04.003)

X.) **E. Benke**, P. Szabó-Révész, R. Ambrus: Development of meloxicam potassium-containing co-spray-dried inhalation powder with sodium stearate. Acta Pharmaceutica Hungarica, 91, 75-82 (2021). (https://doi.org/10.33892/aph.2021.91.75-82)

Nyilatkozat saját munkáról

Név: **Dr. Benke Edit**

A doktori értekezés címe:

DEVELOPMENT OF NOVEL FORMULATED CIPROFLOXACIN HYDROCHLORIDE CONTAINING DRY POWDER INHALATION SYSTEM /

ÚJ FORMULÁLÁSÚ CIPROFLOXACIN-HIDROKLORIDOT TARTALMAZÓ SZÁRAZ PORINHALÁCIÓS RENDSZER FEJLESZTÉSE

Én, **Dr. Benke Edit** teljes felelősségem tudatában kijelentem, hogy a Szegedi Tudományegyetem Gyógyszertudományok Doktori Iskolában elkészített doktori (PhD) disszertációm saját kutatási eredményeimre alapulnak. Kutatómunkám, eredményeim publikálása, valamint disszertációm megírása során a Magyar Tudományos Akadémia Tudományetikai Kódexében lefektetett alapelvek és ajánlások szerint jártam el.

Szeged, 2023.06.05.

.....

Dr. Benke Edit
doktorjelölt